JAROSŁAW GÓRSKI

NON-LINEAR MODELS OF STRUCTURES WITH RANDOM GEOMETRIC AND MATERIAL IMPERFECTIONS SIMULATION-BASED APPROACH

POLITECHNIKA GDAŃSKA

monografie
68

GDANSK UNIVERSITY OF TECHNOLOGY

JAROSŁAW GÓRSKI

NON-LINEAR MODELS OF STRUCTURES WITH RANDOM GEOMETRIC AND MATERIAL IMPERFECTIONS SIMULATION-BASED APPROACH

GDAŃSK 2006

PRZEWODNICZĄCY KOMITETU REDAKCYJNEGO
WYDAWNICTWA POLITECHNIKI GDAŃSKIEJ
Romuald Szymkiewicz

REDAKTOR PUBLIKACJI NAUKOWYCH
Janusz T. Cieśliński

REDAKTOR SERII
Andrzej Małasiewicz

RECENZENCI
Eugeniusz Bielewicz
Tadeusz Burczyński

PROJEKT OKŁADKI
Jolanta Cieślawska

Wydano za zgodą
Rektora Politechniki Gdańskiej

Oferta wydawnicza Politechniki Gdańskiej jest dostępna pod adresem
http://www.pg.edu.pl/wydawnictwo/katalog
zamówienia prosimy kierować na adres wydaw@pg.gda.pl

ISBN 83-7348-142-7

WYDAWNICTWO POLITECHNIKI GDAŃSKIEJ

Wydanie I. Ark. wyd. 8,6. Ark. druku 8,5.
Nr 68/426. Zamówienie nr 38/2006

Druk: Zakład Poligrafii Politechniki Gdańskiej
ul. G. Narutowicza 11/12, 80-952 Gdańsk, tel. 058 347 23 56

CONTENTS

LIST OF SYMBOL AND ABBREVIATIONS

Symbols

D_w – standard deviation of the normal or uniform random variables
$\hat{D}_N$ – standard deviation of the critical load force N_{cr}
$\mathrm{D}(\cdot)$ – variance errors
E – Young modulus
$E(\cdot)$ – expectation operator
$E(V_{er})$ – error of variances
$E(L_{er})$ – single element error
E_0 – Young modulus expected value
$E(G_{er})$ – global errors of covariance matrix
$f(\mathbf{X})$ – joint normal probability density
$f(\mathbf{X}_u / \mathbf{X}_k)$ – conditional distribution
$f_t(x)$ – truncated t normal probability density
$f_t(\mathbf{X}_u / \mathbf{X}_k)$ – conditional distribution
$f_S(s)$ – probability density function of S
$F(x)$ – cumulative distributions of x variable
F_P – cumulative distributions of the external load
$F_P(s)$ – cumulative distribution function of load P
K – correlation function
$\mathbf{K}$ – theoretical covariance matrix
$\hat{\mathbf{K}}$ – estimator of covariance matrix
$\|\hat{\mathbf{K}}\|$ – the norm of covariance matrix $\hat{\mathbf{K}}$
$K_B(\mathbf{r}_1, \mathbf{r}_2)$ – Brown field
$\mathbf{K}_c$ – conditional covariance matrix
$\hat{m}_N$ – expected values of the critical load force N_{cr}
m_w – mean value of the normal or uniform random variables
$N(\mathbf{r}, \omega)$ – White noise field
N_{cr} – critical load
NR – number of realizations
p – probability
p_f – probability of failure
P – external load
$\mathbf{r}$ – position vector
R – structural reliability
$S(\mathbf{r}, \omega)$ – Homogeneous (Shinozuka) field
$\mathbf{X}(\mathbf{r}, \omega)$ – vector of random field
$\bar{\mathbf{X}}_c$ – conditional expected value vector
$\bar{w}$ – expected value
$\hat{w}$ – estimator of the expected value
$\mathbf{w}$ – mean value
$\hat{\mathbf{w}}$ – estimators of mean value
$W(\mathbf{r}, \omega)$ – Wiener field
α – coefficient of variations

α_i – limit state histogram multiplier
β – reliability index
$\beta(x, y)$ – normalized homogeneous random field
γ_1 – coefficient of variation
γ_2 – coefficient of asymmetry
γ_3 – coefficient of kurtosis
δ – Dirac delta
λ – load parameter
λ_x, λ_y – decay coefficients
ν – Poissson coefficient
σ_w – standard deviation
$\hat{\sigma}_w$ – estimator of the standard deviation
σ_y – material yield stress value
σ_{y0} – expected value of material yield stress value

Abbreviations

CDF – cumulative distribution function
FEM – finite element methods
FFT – fast Fourier transform technique
FORM – first-order reliability methods
PDF – probability density function
SFEM – stochastic finite element methods
SORM – second-order reliability methods
SBEM – stochastic boundary element methods

Chapter 1

INTRODUCTION

1.1. General remarks

In contemporary mechanics the problem of understanding the structural responses to the initial data, such as loads, material and geometric properties has become one of the major concerns of engineers and scientists. It is now generally accepted that initial discrepancies and random loadings should be considered in engineering design. For example, Arbocz (1998) wrote: *It is felt that quantifying and understanding the "problem of uncertainties" and their influence on the design variables provides an approach which will ultimately lead to a better engineered, better designed, and safer structure*.

The main purpose of structural mechanics is creation and analysis of theoretical models of real engineering structures. The response of a large class of imperfection-sensitive structures (thin shells, thin-walled beams, arches, trusses, frames and others) exhibit some features of chaotic systems. It is also known that the effect of structural imperfections can evidently decrease their nominal load carrying capacity (Arbocz and Starnes 2002**,** Khamlichi et al. 2004, Papadopoulos and Papadrakakis 2004). For that reason the stability of one-, and two-dimensional structure models with some imperfection has been of great concern to researchers (Huseyin 1975, Kleiber and Woźniak 1991, Thompson and Hunt 1973, Tylikowski 1991, Waszczyszyn et al. 1990). These models deal mainly with elastic stability, and deterministic imperfections. Alternative methods are also implemented. The random nature of the structure behaviour has initiated the use of probabilistic methods (see Augusti et al. 1984). Random vibrations and stochastic processes are the most explored subjects (Śniady 2001, Skalmierski and Tylikowski 1982, Sólnes 1997). On the basis of measured and experimental data the initial structure discrepancies can be realistically described by random variables or random fields (Arbocz and Starnes 2002). The developed methods of the structural data identification are related mainly to dynamic problems (Brandt 1998, Bendat and Piersol 1971 and 1993, Devroye et al. 1996, and Bendat 1990), and their application to the static analysis needs further investigation. Theoretical considerations (see Zubrzycki 1966, Bołotin 1968, Borowkow 1977, Elishakoff 1983, Srivastava and Carter 1983, Bethea et al. 1984, or Doob 1994) form the basis for the engineering solutions. It should be mentioned that the probabilistic analysis should be used cautiously. For example, Ferson and Ginzburg (1996) demonstrated what spurious results could be obtained by an inappropriately applied stochastic method.

Within the range of the probabilistic analysis the most common analytical method in the assessment of uncertainty of structures and loads is the *Perturbation Technique* (Kleiber and Hien 1992, Augusti et al. 1984). A great variety of *Stochastic Finite Element Methods* and *Stochastic Boundary Element Methods* have been developed to describe the safety of structures and the sensitivity problems (see Anders and Hori 1999 and 2000, Kleiber and Hien 1992, Kleiber and Woźniak 1991, Burczyński and Skrzypczyk 1999, Burczyński 1995). Statistical models for the description of material failures have also been implemented (see, for example, Krajcinovic 1996).

A more general approach to assess the random nature of the engineering structures is the estimation of their *reliability* (Cederbaum and Arbocz 1996b, Ditlevsen and Madsen 1996, Murzewski 1989, Raizer 2004, Thoft-Christensen and Murotsu 1986, Simonnet 1996, Biegus 1999, Beniamin and Cornell, and many others). The following techniques are in use: the *Monte Carlo* methods, *First* and *Second Order Reliability Methods* , *Response Surface* methods, and *Artificial Neural Networks*. An important part of the finite element modelling in a reliability context is the representation of random fields describing the statistical variation of properties or structure parameters. Various ways have been suggested for doing this (e.g. Vanmarcke et al. 1986, Li and Der Kiureghian 1993, Zhang and Elingwood 1995, Matthies et al. 1997).

The probabilistic methods have a great influence on the engineering design (see Haugen 1968, and Lind (Ed.) 1970). A short review of the theory of reliability and its use for design codes can be found in Raizer (2004). A relatively new concept, known as *Simulation Based Reliability Assessment*, takes advantage of the simulation of random variables describing loads and material properties, and of the Monte Carlo method (Marek et al. 1996, 1998, 1999a, and 1999b). The random sampling approaches are not new (see, for example, Bucher 1997, Augusti et al. 1984, Elishakoff 1978, and Hurtado and Barbat 1998), but the idea of applying these methods to practical design procedures deserves attention. The performed stochastic analysis of real engineering structures also allows for finding the shortcomings in the existing codes. To illustrate this the numerical calculation of reinforced columns carried out by Hong and Zhou (1999) suggests that the code of the Canadian Standard Association may not be reliability consistent by ignoring the correlation between variability of eccentric loads and the bending moments. The inconsistency of the reliability/redundancy factor in the current code is pointed out by Went (2001). Some computer commercial programs based on the probabilistic methods have also been prepared, e.g. MCREL (Frangopol et al. 1996), @RISK (Low and Tang 2004), COSSAN (Bucher and Schuëller 1994), and others.

It should be stressed that the assessment of reliability, safety and also stability of structures with initial imperfection and random loading belong to the most complex problems in applied mechanics. The probabilistic calculation procedures can be carried out with varying degrees of complexity. The analytical description of stochastic problems can be presented in the following form

$$L_{\omega}(\omega)\left[\mathbf{u}(\mathbf{r}, \omega)\right] = \mathbf{P}(\mathbf{r}, \omega) \tag{1.1}$$

where ω is an elementary event, $L_{\omega}(\omega)$ is a nonlinear stochastic operator depending on random variables, $\mathbf{u}(\mathbf{r}, \omega)$ and $\mathbf{P}(\mathbf{r}, \omega)$ are vector random fields of displacements and loading, and $\mathbf{r}$ is a position vector. To complete the above equation boundary and/or initial random conditions should be known.

Using Eq. (1.1) a general classification of theoretical models of structures can be specified:

— linear stochastic models (operator $L_{\omega}(\omega)$ is linear and deterministic; the loadings are random only),
— stochastically nonlinear models (operator $L_{\omega}(\omega)$ is linear but some parameters or functions of this operator are random),
— general nonlinear stochastic models.

It is worth noting that exact analytical solutions of the stochastic problems exist only for very simple models of structures and uncomplicated cases of loading. For more complex two- and three-dimensional structures the solution of Eq. (1.1) is not explicitly

available. Moreover, in many cases nonlinear geometric effects are combined with plastic deformations. In such circumstances, Eq. (1.1) can be evaluated only numerically.

In this work some general nonlinear stochastic models for static analysis of physically and geometrically nonlinear models of structures with random geometric and material imperfections are implemented. The load action is considered random but the modelling of the loading is not discussed here. It is assumed that the limit state of the structure is known as a function of a number of random variables. The Monte Carlo simulation seems to be the only method to solve such a class of nonlinear problems. Thus, digital simulations of random variables and random fields on regular or irregular two-dimensional meshes in conjunction with the probabilistic methods are applied. The simulation process is based on the *original conditional, rejection method of generation* proposed by Bielewicz et al. (1985a) and modified by Bielewicz et al. (1994b) and Walukiewicz et al. (1997).

Structural initial imperfections are assumed as random fields described in terms of a set of generated realizations and the resulting statistic estimators. This leads to solutions of a set of deterministic problems for the assessment of the response of the structural models. Therefore, the simulation methods of random variables and random fields are of primary significance. The proposed methodology to solve the random problems can be described as a random sampling method or *a simulation-based approach*. This method allows for a complex analysis of liner or non-linear models of imperfect structures.

The Monte Carlo method combined with a finite element program analysis is employed. The numerically obtained critical load histograms make it possible to estimate the structure reliability. The exact approach, the so-called *level-3 reliability method* (see, for example, Thoft-Christensen and Murotsu 1986) is applied.

An alternative procedure for the reliability estimation is also proposed. Random imperfections of the structure and the applied loads are simultaneously generated and an appropriate loading multiplier responsible for the structure failure is calculated. A set of the loading multipliers defines *the histogram of the limit state of the structure*. And on its basis the multiplier describing the structures reliability is calculated. This approach in the solutions of the non-liner problems seems to have evident advantages.

Special attention is paid to the discussion of the *reduction methods of the initial sets of data* in the Monte Carlo approach, and to *accuracy analysis of the output results*. An assessment of an *interval of the structure reliability* is also proposed.

Various civil engineering problems are presented and solved using the simulation-based approach. A *comprehensive analysis of simple models* – rigid bars with inclined springs – allow for an examination of various versions of the Monte Carlo method. But, most of examples presented here concern shell structures. It is frequently stated that the scatter buckling loads of shells can only be approximated through including randomness in imperfect geometries, the effect of thickness variation, the modulus of elasticity and the boundary condition (see Papadopoulos and Papadrakakis 2004). This can only be achieved by stochastic analysis of structures in conjunction with the nonlinear analysis of shells. Despite some achievements in accurate prediction of the load carrying capacity of an imperfect shell, the problem is still an open question (Chryssanthopoulos and Poggi 1995, Deml and Wunderlich 1997, Papadopoulos and Papadrakakis 2004).

At last, two examples of *identifications and simulations of initial, measured geometric discrepancies of real engineering structures* are presented. The first case concerns the numerical analysis of the measurement results obtained for a petrol tank of 5000 m^3 capacity (Orlik 1976, and Wilde 1981) and the second deals with longitudinally stiffened

ship hull panels (Kmiecik 1970). The examples illustrate the application of the simulation method to specific engineering problems. The numerical analysis of the petrol tank indicates that the initial geometric imperfections strongly influence the solution.

Using the simulation-based approach to solving the nonlinear problems of a structure with geometric and material imperfections the following questions should be answered:

— What type of random field describing the initial geometrical imperfections should be assumed?
— What estimators are necessary to describe the initial set of realizations; especially in a two dimensional case?
— How many of these realizations should be taken into account in the calculation?
— Is it possible to reduce the initial set of realizations to a smaller one without diminishing the accuracy of the solution?
— What type of the Monte Carlo method should be applied to the calculations?
— What estimators should be assumed to describe the probability distribution of the outcomes?
— Is it possible to estimate the influence of the number of the realizations on the probability distribution?
— What is the effect of the assumed types of random geometrical imperfections on the structure response?
— In what way can the real, measured structure or material imperfections be identified?

The work is an attempt at answering at least some of these questions.

1.2. Scope of the work

The work is organized as follows.

Chapter 2 deals with the stochastic mechanics methods. The state of the knowledge to analyse the effect of uncertainties in structural mechanics has been outlined. The following topics are briefly discussed including random fields discretization methods, generation of random variates, perturbation techniques, stochastic finite element methods, structural reliability calculations, first and second order reliability methods, and response surface techniques.

Special attention is given to various versions of the Monte Carlo method, i.e. direct, stratified, importance and directional sampling. A short review of numerous papers makes it possible to assert that most of them concern a numerically difficult problem of reliability assessment, and few are devoted to the research of the stochastic spatial variability of the structural parameters. The use of the methods has undoubtedly been affected by the rapid development of the computational resources enabling to perform the Monte Carlo analyses (see Melchers 1999, Hurtado et al. 1998).

Chapter 3 presents a modified generation method of two-dimensional, discretized homogeneous and nonhomogeneous random fields proposed by Bielewicz et al. (1985a and 1994b) and Walukiewicz et al. (1997). The algorithm is based on an effective version of the rejection method, and on conditional probability distribution formula. An important role in the calculations is played by a propagation base scheme covering sequentially the field points. In order to fulfil the geometric and boundary conditions of the structure model, the realisations of random fields are bounded by appropriate envelopes. The use of these field envelopes is an original feature of this method. Any irregularity of the meshes and any shapes of the domains are allowed.

The accuracy of the random field generations is analysed. The results of numerical experiments for the two-dimensional homogeneous and non-homogeneous fields are presented. The results have proved that the adopted algorithm is correct.

The generation method has already been successfully implemented not only in structure analysis (see, for example, Bielewicz et al. 1994a) but also in an examination of environmental pollutions (Jankowski and Walukiewicz 1997, Bielewicz et al. 1995a, and Walukiewicz et al. 1998), and soil random problems (Przewłócki and Górski 2001).

In **Chapter 4** attention is focused on preliminary analysis of the limit states of spatial nonlinear models of rigid bars supported by elastic and elastic-plastic springs with one and two degrees of freedoms. The angles of the initial bar inclinations are described using random variables. Simulation-based approach is implemented. Geometric and material imperfections are taken into account in the form of random variables.

A transformation of random input data (imperfections) into random output results is discussed. A statistical analysis of the output results leads to limit load or limit state histograms. In the transformation procedure the nonlinear operator of the structure model plays the most important role. The effects of stable and unstable operators are considered.

The output results allow for the assessment of the reliability of the structure models. Two methods of the reliability calculations are presented.

The first method is a standard one. The final results of the proposed simulation-based approach present the numerically obtained probability distribution of the critical load. Assuming that the probability distribution of the applied load is known, an exact formula for the reliability of the structure can be used (see, for example, Thoft-Christensen and Baker 1982). The reliability theory based on the knowledge of the probability distributions of all basic variables is called the level-3 method. The simulation-based approach makes it possible to use the exact reliability calculation.

The second reliability calculation method is more general. The aim of this approach is an adequate description of the behaviour of a random model of the structure under random loading. The probability distribution of the applied loads is taken into account and the idea of the probability distribution of the limit state of the structure is implemented. Random imperfections of the structure and the applied loads are simultaneously generated at every Monte Carlo step. Making imperfections constant at every step the loading multiplier responsible for the structure failure is calculated. A set of the loading multipliers obtained in this way defines the histogram of the limit state of the structure. The histogram has a nondimensional form and is a numerical estimate of the probability distribution of the limit state.

The direct Monte Carlo calculations are compared with various stratified sampling methods. The influence of the chosen method on the structure reliability estimation is analysed. Additionally a simple sensitivity analysis of random variables is given.

In **Chapter 5** the simulation-based approach is applied to solving two-dimensional nonlinear structural random problems. The main subject of this section is a description of the reduction of a number of initial imperfection field sets and a convergence analysis of the output results.

Applying the non-linear theory to two-dimensional models of structures the limit state description can be obtained only by the numerical way. The proposed generation algorithm together with the Monte Carlo method and the finite element procedures are applied. The numerically obtained results of the proposed approach are in the form of the probability distribution of the critical load. On the assumption that the probability distribution of the applied load is known the reliability of the structure can be estimated. The simulation-based approach allows using the level-3 exact reliability method.

During the numerical calculation each realization is solved by a finite element program and the incremental operations. These procedures, in the case of geometrically and/or materially nonlinear problem, are time-consuming even for powerful computers. It is obvious that the accuracy of calculations depends on the number of the realisations considered. Therefore, it is important to know how many realizations ought to be simulated in order to obtain satisfactory results. The accuracy of the simulation-based approach can be analysed:

— at the input data level (a statistical description of the initial random structure parameters),
— at the level of the output results (an analysis of the structure response obtained in a numerical way).

The first method of the accuracy analysis is relatively easy. When the theoretical form of the imperfection fields has been assumed, the simulation process is applied, and the results can be compared with the theoretical fields. The well known statistical formulas are the best and adequate for this comparison.

It should be pointed out that the applications of this methodology to the structure random analysis have occurred to be difficult. Simulation and convergence analysis of two–dimensional random fields shows that with respect to meshes of $100 \div 200$ points a sufficient number of realizations must be at least of the order 1000 (Bielewicz et al. 1994b). From the point of view of the efficiency of non-linear numerical calculations such a numerous set of realizations is too big.

It is possible to reduce the number of the input realizations. The following two methods of reducing the generated input realizations are applied to:

— a number of representative realizations with prescribed probability,
— some specific input realizations, chosen from the generated set, which are supposed to give an extreme mechanical answer of a structure model.

The above methods are employed in analysing the effect of the initial imperfections on the response of non-linear model of shallow cylindrical shell.

The statistical analysis of the random output results differs significantly from the analysis of the random input data. The analytical solutions of the discussed stochastical non-linear problems are unknown. A comparative analysis of the output results obtained from different numbers of realizations seems to be the best way to assess convergence. The choice of the convergence description of the numerical results is crucial in the analysis. When the fluctuation of the estimated values is meaningless one can assume that the analysed set of sampling is sufficient. Thus, the maximal number of realizations depends on the progress of the non-linear calculation of the structure under consideration. This form of the assessment of the accuracy of sampling can also be verified by a comparison of the limit load histograms for a chosen number of realizations. It seems rational to assume that for engineering purposes the analysis can be limited only to the output results.

On the basis of the simulation-based approach an interval of the structure reliability can be assessed. A concept of choosing a specific type of favourable and unfavourable probability distributions of random variables defined for the same interval is proposed. The structure imperfections are described as the minimum or the maximum values of a set of n random variables. It is easy to apply the imperfection sets to the Monte Carlo analysis and to calculate two histograms of the limit loads. Following this procedure an analysis based on the level-3 method leads to the estimation of two reliability values of the structure. These values assess the structure reliability interval.

In **Chapter 6** two examples of identifications and simulation of initial geometric discrepancies of real engineering structures are provided.

The first case concerns the numerical analysis of the measurement results obtained for a petrol tanks of $5000 \div 50000$ m^3 capacity (Orlik 1976, and Wilde 1981). The achieved results, aided by the statistical analysis, have demonstrated the method's capability of simulating a large random nonhomogeneous field. An envelope of the tank extreme initial imperfections is also proposed. The results of the nonlinear calculations indicate that the tank initial discrepancies can cause significant variations in the stress fields in comparison with the solution of an ideal surface.

The second example deals with longitudinally stiffened ship's hull panels (Kmiecik 1970). The example presents the application of the simulation method adopted for specific engineering problems. It is shown that the computer program makes it possible to generate a unique random field of imperfections, bounded by an envelope which determines the structure shape and the boundary conditions. The stiffened plate with ribs is an illustration of the complicated boundary conditions.

In both cases the estimators of the obtained realizations of the geometric field imperfections are compared with the test data.

In **Chapter 7** some conclusions are formulated. It should be pointed out that the application of the simulation-based approach can results in a reduction of the laborious and expensive experiments. However, it should also be stressed that engineering knowledge and experience play an essential role in the analysis.

The idea of this work and some of the presented results are based on analyses performed mainly by prof. dr hab. E. Bielewicz, dr hab. H. Walukiewicz and the author of the work, published in the form of projects (Central Research and Development Problems of Polish Ministry of Science and Higher Education, *Nonlinear problems in stochastic theory of shells* (Bielewicz et al. 1980, 1982 1984, 1985b, and 1988), and Polish State Committee for Scientific Research Problem, *Random fields and their applications in structural mechanics*. No. 304259101 (Bielewicz et al. 1993), and No. 3 P40405505 (Bielewicz et al. 1995c), and papers (see References).

The original elements – the results of the author's scientific research – which have not been published in the joint papers and project reports are: the improvements of the generation algorithm which allow for the generation of practically unlimited size fields (Chapter 3), verification of the Monte Carlo method efficiency in solving stochastic nonlinear problems (Chapter 4.1), and identification and generation of geometric imperfections on the basis of measured discrepancies of vertical cylindrical tanks (Chapter 6.2). The new element in comparison with the joint works is also the review of literature presented in Chapter 2.

Chapter 2

STOCHASTIC MECHANICS METHODS

The mathematical description of uncertainty is usually given within the framework of probability theory, although this is not the only possible approach. The problem can be solved using for example fuzzy sets (Zadeh 1983, De Lima and Ebecken 2000, Niczyj 2003), rough sets (Bargiela and Pedrycz 2001), convex model (Ben Haim 1995 and 1999, and Elseifi et al. 1999) or interval arithmetic (Moore 1979). The purpose of this chapter is to review the methods of calculations that require a knowledge of the probability distribution of uncertain systems to uncertain inputs. The existing theories for stochastic mechanics approaches can be classified with respect to the type of the obtained results (see, for example, Surdet and Der Kiureghian 2000):

— Perturbation Method – calculating the first two statistic moments of the response quantities, i.e. the mean, variance and correlation coefficient,
— Stochastic Finite Element Methods (SFEM) – evaluating the global response quantities considered as random processes,
— Reliability Methods – estimating the probability of failure of the system.

To estimate the structure reliability the following dominant approaches have been explored in the literature:

a) Monte Carlo methods,
b) First- and Second-order Reliability Methods (FORM and SORM methods),
c) Response Surface method,
d) Neural-network based reliability.

In this chapter some of the above methods are briefly described. A special consideration is given to the Monte Carlo techniques as this method is applied in the present work. The following contributions, among other, are used as a basis for the description: Melchers (1999), Hurtado et al. (1998), Surdet and Der Kiureghian (2000) and (2002), Matthies et al. (1997), Schuëller (1997) and (2001), Liu (2001).

A common feature in most of the stochastic mechanics approaches is the need to represent the spatial variability of the input parameters. Thus the methods of random fields discretization (see Vanmarcke 1983, or Surdet and Der Kiureghian 2000) are dealt with first.

2.1. Random fields discretization methods

A real random variable X is a mapping $X:(\Theta, \mathcal{F}, P)\rightarrow\mathbb{R}$, where Θ is sample space, $\mathcal{F}$ denotes the collection of possible events having well-defined probabilities, and P is probability measure (Surdet and Der Kiureghian 2000). In continuous random variables the probability density function (PDF) and the cumulative distribution function (CDF) are denoted by $f_X(x)$ and $F_X(x)$, respectively. The random nature of X (dependence on the outcomes θ) may be described as $X(\theta)$. Random vector $\boldsymbol{\chi}$ is a collection of random variables.

The mathematical expectation will be denoted by $E(\cdot)$. The mean, the variance and the n-th moment of variable X are:

$$\mu \equiv E(X) = \int_{-\infty}^{\infty} x f_X(x)\,dx \tag{2.1}$$

$$\sigma^2 = E\left[(X-\mu)^2\right] = \int_{-\infty}^{\infty} (x-\mu)^2 f_X(x)\,dx \tag{2.2}$$

$$E\left[X^n\right] = \int_{-\infty}^{\infty} x^n f_X(x)\,dx \tag{2.3}$$

The covariance of two random variables X and Y is

$$\mathrm{Cov}[X,Y] = E\left[(X-\mu_X)(Y-\mu_Y)\right] \tag{2.4}$$

Introducing the joint distribution $f_{X,Y}(x,y)$ of the variables Eq. (2.4) can be rewritten as

$$\mathrm{Cov}[X,Y] = \int_{-\infty}^{\infty}\int_{-\infty}^{\infty} (x-\mu_X)(y-\mu_Y) f_{X,Y}(x,y)\,dxdy \tag{2.5}$$

The vectorial space of the real random variables with finite second moment ($E[X^2]<\infty$) is denoted by $\mathcal{L}^2(\Theta, \mathcal{F}, P)$. The space $\mathcal{L}^2(\Theta, \mathcal{F}, P)$ is usually described as the Hilbert space which has convenient properties to develop approximate solutions of boundary value problems (Sobczyk 1991). Then, a random field $H(\mathbf{x},\theta)$ can be defined as a curve in $\mathcal{L}^2(\Theta, \mathcal{F}, P)$, which is a collection of random variables indexed by a continuous parameter $\mathbf{x} \in \Omega$, where Ω is an open set of $\mathbb{R}^d$ describing the system geometry. This means that for a given $\mathbf{x}_o$, $H(\mathbf{x}_o,\theta)$ is a random variable, and reversely, for a given outcome θ_o, $H(\mathbf{x},\theta_o)$ is a realization of the field.

A random field is called univariate or multivariate depending on whether the quantity $H(\mathbf{x})$ attached to point $\mathbf{x}$ is a random variable or a random vector.

The random field is Gaussian if any vector $\{H(\mathbf{x}_1),\ldots H(\mathbf{x}_n)\}$ is Gaussian. A Gaussian field is completely defined by its mean $\mu(\mathbf{x})$, variance $\sigma^2(\mathbf{x})$ and autocorrelation coefficient $\rho(\mathbf{x},\mathbf{x}')$ functions. Moreover, it is homogeneous if the mean and the variance are constant and ρ is a function of the difference $\mathbf{x}-\mathbf{x}'$ only.

A discretization procedure is approximation of a random field $H(\cdot)$ by $\hat{H}(\cdot)$ defined by means of a finite set of random variables $\{\chi_i,\ i=1,\ldots n\}$ grouped in a random vector $\boldsymbol{\chi}$ (Surdet and Der Kiureghian 2000)

$$H(\mathbf{x}) \xrightarrow{\text{Discretization}} \hat{H}(\mathbf{x}) = \mathrm{F}\left[\mathbf{x},\boldsymbol{\chi}\right] \tag{2.6}$$

The best approximation with respect to some error estimator is the one using the minimum number of random variables. The discretization methods can be divided into the following groups:

— point discretization methods,
— average discretization methods,
— series expansion methods.

The discretization methods will be described with special attention given to the Finite Element Method application. The review work by Surdet and Der Kiureghian (2000) is used as a basis for the description.

Point discretization methods

The midpoint method (Der Kiureghian and Ke 1988) is founded on approximating the random field in each element Ω_e by a single random variable defined as the value of the field at the centre $\mathbf{x}_c$ of this element

$$\hat{H}(\mathbf{x}) = H(\mathbf{x}_c), \qquad \mathbf{x} \in \Omega_e \tag{2.7}$$

The approximated field $\hat{H}(\cdot)$ is then entirely defined by the random vector $\boldsymbol{\chi} = \{H(\mathbf{x}_c^1), \ldots H(\mathbf{x}_c^{N_e})\}$ (N_e stands for the number of elements in the mesh). It has been shown (Der Kiureghian and Ke 1988) that the midpoint method tends to over-represent the variability of the random field within each element.

The shape function method (Liu et al. 1986) approximates $\hat{H}(\cdot)$ in each element using the nodal values $\mathbf{x}_i$ and the shape function as follows

$$\hat{H}(\mathbf{x}) = \sum_{i=1}^{q} N_i(\mathbf{x}) H(\mathbf{x}_i), \qquad \mathbf{x} \in \Omega_e \tag{2.8}$$

where q is the number of element nodes, $\mathbf{x}_i$ the coordinates of the i-th node and N_i polynomial shape functions associated with the element. The approximated field $\hat{H}(\cdot)$ is obtained in this case from $\boldsymbol{\chi} = \{H(\mathbf{x}_1), \ldots H(\mathbf{x}_N)\}$, where $\{\mathbf{x}_i, i = 1, \ldots N\}$ is the set of the nodal coordinate of the mesh. Each realization of $\hat{H}(\cdot)$ is a continuous function over Ω, which is an advantage over the midpoint method.

The integration point method (Brenner and Bucher 1995, and Matthies et al. 1997) discretizes the random field by associating a single random variable with each of the Gauss points. This gives accurate results for a short correlation length. However, the total number of random variables involved increases enormously with the size of the problem.

The optimal linear estimation method (Li and Der Kiureghian 1993) defines the field $\hat{H}(\cdot)$ by a linear function of nodal values $\boldsymbol{\chi} = \{H(\mathbf{x}_1), \ldots H(\mathbf{x}_q)\}$ in the follows way

$$\hat{H}(\mathbf{x}) = a(\mathbf{x}) + b^T(\mathbf{x}) \cdot \boldsymbol{\chi} \tag{2.9}$$

where q is the number of nodal points involved in the approximation. The functions $a(\mathbf{x})$ and $b(\mathbf{x})$ are determined by minimazing in each point $\mathbf{x}$ the variance of the error $\mathrm{Var}\{H(\mathbf{x}) - \hat{H}(\mathbf{x})\}$.

Average discretization methods

The spatial average method (Vanmarcke and Grigoriu 1983, Vanmarcke 1983, and Knabe et al. 1998) approximates the field in each element Ω_e by a constant computed as the average of the original field over the element

$$\hat{H}(\mathbf{x}) = \frac{1}{|\Omega_e|} \int_{\Omega_e} H(\mathbf{x}) d\Omega_e \equiv \hat{H}_e \tag{2.10}$$

Vector $\boldsymbol{\chi}$ is then defined as the collection of these random variables $\chi^T = \{\hat{H}_e, e = 1, \ldots N_e\}$. As indicated by Fig. 2.1, the randomness of the average process $\hat{H}(\mathbf{x})$ will be less than that of $H(\mathbf{x})$.

Vanmarcke (1983) and Knabe et al. (1998) give the results for homogeneous fields and rectangular domains. It has been shown that the variance of the spatial average over an

element, under-represents the local variance of the random field (Der Kiureghian and Ke 1988).

The weighted *integral method* (Deodatis 1990 and 1991), Deodatis and Shinozuka 1991, Takeda 1990a and 1990b) does not require any discretization of the random field. In the case of linear elasticity, the element stiffness matrices are considered as the basic random quantities

$$k^e = \int_{\Omega_e} \mathbf{B}^T \cdot \mathbf{D} \cdot \mathbf{B} d\Omega_e \qquad (2.11)$$

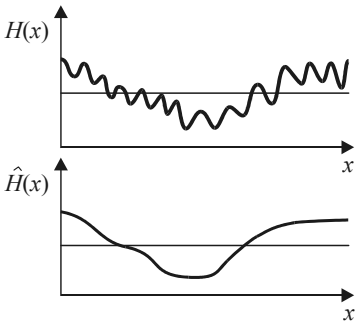

Fig. 2.1. Local averages of random field

In Eq. (2.11) **B** denotes a matrix that relates components of strains to the nodal displacements and **D** is the elasticity matrix obtained as a product of a deterministic matrix by a univariate field

$$\mathbf{D}(\mathbf{x},\theta) = \mathbf{D}_o \left[1 + H(\mathbf{x},\theta)\right] \qquad (2.12)$$

where $\mathbf{D}_o$ is the mean value and $H(\mathbf{x},\theta)$ is a zero mean process.

The weighted integral method is mesh-dependent (Matthies et al. 1997).

Series expansion methods

The Karhunen-Loève expansion of a random field $H(\cdot)$ is based on the spectral decomposition of its autocovariance function $C_{HH}(\mathbf{x},\mathbf{x}') = \sigma(\mathbf{x})\sigma(\mathbf{x}')\rho(\mathbf{x},\mathbf{x}')$. The set of the deterministic functions over which any realization of the field $H(x,\theta_o)$ is expanded is defined by the eigenvalue problem (Fredholm integral equation)

$$\forall i = 1,... \qquad \int_{\Omega} C_{HH}(\mathbf{x},\mathbf{x}')\varphi_i(\mathbf{x}')d\Omega_{x'} = \lambda_i \varphi_i(\mathbf{x}) \qquad (2.13)$$

The set of $\{\varphi_i\}$ forms a complete orthogonal basis of $\mathcal{L}^2(\Omega)$. Any realization of $H(\cdot)$ can be expanded over this basis as follows

$$H(\mathbf{x},\theta) = \mu(\mathbf{x}) + \sum_{i=1}^{\infty} \sqrt{\lambda_i}\,\xi_i(\theta)\varphi_i(\mathbf{x}) \qquad (2.14)$$

where $\{\xi_i(\theta),\ i = 1,...\}$ denotes the coordinates of the realizations of the random field with respect to the set of deterministic functions $\{\varphi_i\}$.

Taking into account all possible realizations of the field $\{\xi_i, i = 1,...\}$ becomes a numerable set of random variables. When no analytical solution of integral eigenvalue problem (2.13) is available, the set of orthogonal functions $\{\varphi_i,\ i = 1,...\}$ has to be computed numerically.

The orthogonal series expansion method (Zhang and Ellingwood 1994) avoids solving the eigenvalue problem (2.13) by selecting a complete set of orthogonal functions $\{h_i(\mathbf{x})\}_{i=1}^{\infty}$, forming an orthonormal basis of $\mathrm{L}^2(\Omega)$

$$\int_{\Omega} h_i(\mathbf{x})h_j(\mathbf{x}')d\Omega = \delta_{ij} \qquad (2.15)$$

where δ_{ij} is Kronecker symbol.

Any realization of the random field $H(\mathbf{x},\theta)$ is a function of $\mathcal{L}^2(\Omega)$, which can be expanded by means of orthogonal function $\{h_i(\mathbf{x})\}_{i=1}^{\infty}$. Considering all possible outcomes of the field, the following expansion holds

$$H(\mathbf{x},\theta) = \mu(\mathbf{x}) + \sum_{i=1}^{\infty} \chi_i(\theta) h_i(\mathbf{x}) \tag{2.16}$$

where $\mu(\mathbf{x})$ is mean function, and $\chi_i(\theta)$ are zero-mean random variables.

It can be shown that:

$$\chi_i(\theta) = \int_{\Omega} \left[H(\mathbf{x},\theta) - \mu(\mathbf{x}) \right] h_i(\mathbf{x}) d\Omega \tag{2.17}$$

$$E[\chi_k \chi_l] = \int_{\Omega}\int_{\Omega} C_{HH}(\mathbf{x},\mathbf{x}') h_k(\mathbf{x}) h_l(\mathbf{x}') d\Omega_x d\Omega_{x'} \tag{2.18}$$

where $C_{HH}(\mathbf{x},\mathbf{x}')$ is the autocovariance function of the random field $H(x,\theta)$.

The expansion optimal linear estimation method (Li and Der Kiureghian 1993) is an extension of the optimal linear estimation using a spectral representation of the random nodal variables $\boldsymbol{\chi}$. Assuming that $H(\cdot)$ is Gaussian, the spectral decomposition of the covariance matrix $\boldsymbol{\Sigma}_{\chi\chi}$ of $\boldsymbol{\chi} = \{H(\mathbf{x}_1),...H(\mathbf{x}_N)\}$ is

$$\boldsymbol{\chi}(\theta) = \boldsymbol{\mu}_{\chi} + \sum_{i=1}^{N} \sqrt{\lambda_i} \xi_i(\theta) \boldsymbol{\phi}_i \tag{2.19}$$

where $\{\xi_i, i = 1,...N\}$ are independent standard normal variables, and $(\lambda_i, \boldsymbol{\phi}_i)$ are the eigenvalues and eigenvectors of the covariance matrix $\boldsymbol{\Sigma}_{\chi\chi}$ fulfilling $\boldsymbol{\Sigma}_{\chi\chi}\boldsymbol{\phi}_i = \lambda_i \boldsymbol{\phi}_i$. Substituting (2.19) to (2.9) and solving the optimal linear estimation problems yields

$$\hat{H}(\mathbf{x},\theta) = \mu(\mathbf{x}) + \sum_{i=1}^{N} \frac{\xi_i(\theta)}{\sqrt{\lambda_i}} \boldsymbol{\phi}_i^T \boldsymbol{\Sigma}_{H(\mathbf{x})\chi} \tag{2.20}$$

Selection of the random field mesh

It should be pointed out that the finite element mesh and the random field mesh have to be designed on the basis of different criteria (see Der Kiureghian and Ke 1988, and Mahadevan and Halder 1991):

— the design of the finite element mesh is governed by stress gradients of the response,
— the typical element size L_{RF} in random field mesh is related to the correlation length of the autocorrelation function.

Depending on the discretization method different recommendations relating to the element size and mesh construction can be found in the literature. For example:

— Der Kiureghian and Ke (1988), and Li and Der Kiureghian (1993) proposed the value

$$L_{RF} \approx \frac{a}{4} \text{ to } \frac{a}{2} \tag{2.21}$$

— Der Kiureghian and Ke (1988) and Mahadevan and Haldar (1991) reported numerical difficulties when L_{RF} was too small. In this case the random variables appearing in the discretization are highly correlated leading to numerical instabilities.

— As the correlation length is usually constant over Ω the associated mesh can be constructed on a regular pattern.
— Some authors simply construct the random field mesh by grouping several elements of the finite element mesh in a single one (Liu and Der Kiureghian 1991). This makes it possible to reduce the size of the random vector χ.
— In the context of reliability analysis Liu and Liu (1993) showed that the refinement of the random field mesh should be connected to the gradient of the limit state function.

2.2. Generation of random variates

Generation of random numbers is usually carried out with the help of computer programs. Although the obtained in this way sequence of the "pseudo numbers" repeats itself after a long cycle interval, for many practical purposes it is indistinguishable from a population of strictly true random numbers. It should be mentioned that the reproducible sequence has an advantage in some types of research work.

Basic variables are seldom uniformly distributed and only such set can be obtained by the "pseudo-generators". A sample value for a basic variable with a given nonuniform distribution is called a "random variate". There are two general techniques in generating random variables: inversion and rejection method.

The *inversion method* starts with generation of uniformly distributed random numbers r_i $(0 \le r_i \le 1)$ followed by the calculation of the corresponding variables by inversion of the cumulative distribution function $F_{X_i}(x_i)$ (see Fig. 2.2)

$$F_{X_i}(x_i) = r_i \qquad \Rightarrow \qquad x_i = F_{X_i}^{-1}(r_i) \tag{2.22}$$

This uniquely fixes the sample value $x_i = \hat{x}_i$ when an analytic expression for the inverse $F_{X_i}^{-1}(r_i)$ exists (for example, the normal, Weibull, exponential, Gumbell and other distributions). The technique can also be applied to basic variables with cumulative distribution function obtained from direct observation.

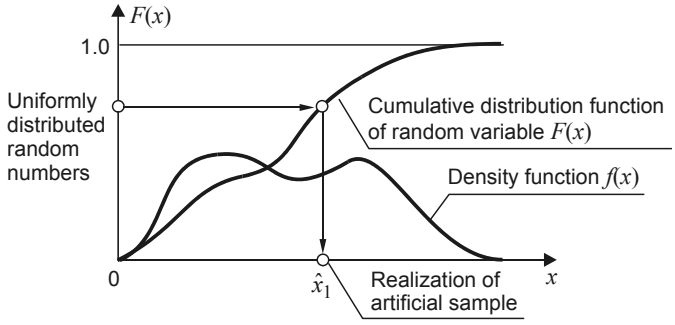

Fig. 2.2. Inversion method of generating random variates

The *rejection method* is based on the idea shown in Fig. 2.3 (Hurtado and Bardat 1998, Brandt 1998). A random variable x_i is generated using a fictitious probability density $f(x_i)$ that envelopes the target one $p(x_i)$. The generated variable x_i is accepted with specified probability that depends on the ratio of the true and fictitious densities. The theoretical basis of the rejection method is described in detail in Chapter 3.

One of the most frequently applied technique to estimate the required joint density is the *Nataf's method* (see, for example, Rozmarynowski 1997) in which use is made of the multidimensional Gaussian distributions with correlation coefficient modified according to the nonlinear transformation linking the given marginal and Gaussian densities. The corresponding samples of the correlated variables can then be generated by means of the approximated distributions. It should be pointed out that in the stochastic analysis the joint density function of all the random variables is usually ignored, and the problems are commonly described solely by their marginal distribution and covariance functions (Der Kiureghian and Liu 1986).

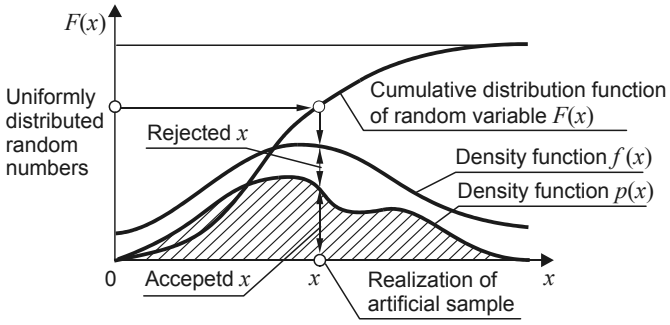

Fig. 2.3. Inversion and rejection methods of generating random variables

2.3. Stochastic finite element methods

The most common analytical method to assess statistical measures of responses to uncertainties of structures and loads is the *Perturbation Technique*. This method uses the Taylor expansion of the mathematical operator that relates the input and output variables (Kleiber and Hien 1992, Augusti et al. 1984, Liu et al. 1986, Bielewicz et al. 1983). The truncation of the series in the first two terms implies that the accuracy of the method is limited to such cases in which the random input variables have very low coefficients of variation of the order of 0.15 as a maximum (Hurtado and Barbat 1998). This condition is more restrictive in the case of nonlinear systems.

Another well known technique is the *Hierarchical Closure Approximation* (Adomian 1983) in which higher order moments of the system and the output are expressed as functions of lower order.

Various problems are solved by means of the S*tochastic Finite Element* modelling SFEM (see Hurtado and Alvarez 1999, Shinozuka 1994, Cheng and Young 1993). Papadrakakis and Papadopoulos (1996) and Papadopoulos and Papadrakakis (1998) proposed using an effective version of SFEM for the analysis of space frames. Chakraborty and Bhattacharyya (2002) generalized the local averaging 2D technique for 3D random fields.

In this group the most powerful analytical method developed in the last years seems to be the *Spectral Approach* (Spanos and Mignolet, 1992, Spanos and Zeldin, 1996). This technique consists of the following steps:

a) a description of the random field by truncated infinite series using the Karhunen-Loeve decomposition,
b) projection of the decomposed random field of the solution on a class of polynomials on nonlinear systems known as Homogeneous Chaos,

c) solution of the resulting system of equations.

Shinozuka and his co-workers have made a valuable contribution to the development of many techniques for analysing random fields (see, for example, Shinozuka 1987b, Shinozuka and Deodatis 1996). According to the method, in the one-dimensional application the spectral density function of a harmonic process can be presented as follows

$$x(s) = \sum_{i=1}^{N} A_i(\kappa_i)\cos(\kappa_i s + \phi_i) \tag{2.23}$$

in which the ϕ_i are random phases.

The harmonic process is convergent to the Gaussian one with a single-sided spectral density (i.e. defined only over positive wave number or frequencies) $G(\kappa) = 2S(\kappa)$. This takes place if the amplitudes of the waves $A_i(\kappa_i)$ are estimated as functions of the discretized spectral density intervals of the length $\Delta\kappa$

$$A_i(\kappa_i) = \sqrt{2G(\kappa_i)\Delta\kappa} \tag{2.24}$$

due to the fact that the variance of the process is equal to the area under the curve of the spectral density.

The extension of the formulation to the higher dimension processes has been done in Shinozuka and Lenoe (1976), Vanmarcke et al. (1986), Shinozuka (1987b), Yamazaki and Shinozuka (1988). In another version transformation of the above equations is used for complex space. The *Fast Fourier Transform* (FFT) technique is applied (Shinozuka and Lenoe 1976). The method is also extended to non-Gaussian fields (Yamazaki and Shinozuka 1988). It has been proved that greater accuracy is obtained if the simulation is accomplished by a statistical preconditioning (Yamazaki and Shinozuka 1990). A comparison with spectral stochastic finite element method can be found in (Surdet and Der Kiureghian 2002).

Fenton and Vanmarcke (1990) criticized the above FFT technique, and proposed a sampling method of random fields known as *Local Average Subdivision*. The main disadvantage of this method is that it is in itself a mesh generator of a specific nature (rectangular elements of equal size) that puts it in conflict with the particular FE discretization. Penmetsa and Grandhi (2003) suggested an efficiency solution of the convolution integral using the FFT technique.

Other methods for simulating random fields are those proposed in (Mignolet and Spanos 1992, Spanos and Mignolet 1992) in which use is made of the *Auto Regressive Moving Averages* (ARMA) procedures commonly employed in the field of time series analysis. Also the *Turning Bands Method* is applied. It generates two dimensional fields by simulating diagonal processes on arbitrary lines contained in the plane. Some methods devised in the earthquake engineering for simulating random fields upon the available information of a realization obtained by instrumentation (Kamada and Morikawa 1994; Lutes et al. 1996) can be useful in SFEM analysis. The application of the Krieging methods that are common in Geostatistics has also been proposed (Hoshiya 1994). It must be noted that measurement experience of random fields of material properties in structural engineering is quite limited as compared with other areas of research (Vanmarcke 1994).

Puig et al. (2002) have proposed various algorithm allowing for simulations of general non-Gaussian processes. The methods are based on the simulation of a Gaussian process, which can be simulated using a spectral or some Markovian approach. The results can estimate time- or space-dependent phenomena.

A classification approach for reliability analysis with SFEM modelling has been proposed by Hurtado and Alvarez (1999). Other analytical approaches that deserve consideration are those put forward by Li and Der Kiureghmiamm (1993) and Zhang and Ellingwood (1994). Stefanou and Papadrakakis (2004) presented a stochastic triangular shell element for the case of combined uncertain material and geometric properties. Stochastic element-free Galerkin method was also developed (Rahman and Rao 2001).

Stochastic Boundary Element Metchods (SBEM) are formulated (see, for example, Burczyński 1995, and Burczyński and Skrzypczyk 1999). In Burczyński (1995) application of SBEM to static and dynamic with random boundary conditions, stochastic media, stochastic sensitivity analysis and internal defects are presented.

2.4. Structural reliability

In general, reliability can be defined as the ability of a structure to fulfil its functions during an established time of service (see for example Melchers 1999, or Raizer 2004). Reliability analysis can also be understood as the calculation of the probability of failure of a random system subjected to random conditions (Hurtado and Barbat 1998). It should be pointed out that the "system failure" can be defined differentially in each case. For example, the failure of a structure usually means that its deformations or stresses are higher than the given critical values. Reliability is described in terms of probability measure, taking into consideration the fact that all strength, geometry, and deformation characteristics of a structure and all loads are random variables or random process.

In a basic structural reliability problem account is only taken of one effect S and one resistance R, usually described by known probability density functions $f_S(s)$ and $f_R(r)$ respectively. The probability of failure p_f can be defined as follows (Melchers 1999):

$$p_f = P\left(R \le S\right) = P\left(R - S \le 0\right) = P\left(\frac{R}{S} \le 1\right) = P\left(\ln R - \ln S \le 0\right) \tag{2.25}$$

or in a general form

$$p_f = P\left[G\left(R,S\right) \le 0\right] \tag{2.26}$$

where $G(R,S)$ is termed the "limit state function".

If the joint density function $f_{RS}(r,s)$ of R and S are known the failure probability becomes (see Fig. 2.4)

$$p_f = P\left(R - S \le 0\right) = \iint_D f_{RS}\left(r,s\right) drds \tag{2.27}$$

where D is the failure domain.

When R and S are independent, the failure probability is expressed by so-called convolution integral

$$p_f = P\left(R - S \le 0\right) = \int_{-\infty}^{\infty} \int_{-\infty}^{s \ge r} f_R\left(r\right) f_S\left(s\right) drds \tag{2.28}$$

or taking into account the cumulative distribution function $F_x(x) = P\left(X \le x\right)$ by

$$p_f = P\left(R - S \le 0\right) = \int_{-\infty}^{\infty} F_R\left(x\right) f_S\left(x\right) dx = \int_{\infty}^{\infty} \left[1 - F_S\left(x\right)\right] f_R\left(x\right) dx \tag{2.29}$$

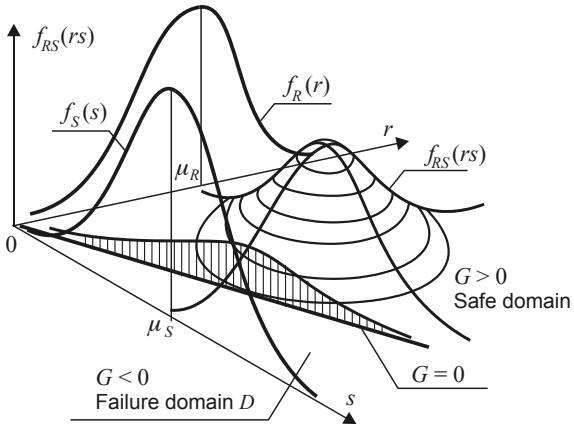

Fig. 2.4. Two random variable joint functions $f_{RS}(r,s)$, marginal density function $f_R(r)$ and $f_S(s)$ and failure domain D

A graphical interpretation of the Eqs. (2.29) is presented in Fig. 2.5.

If both distributions of R and S are normal variables defined by means μ_R and μ_S and variances σ_R^2 and σ_S^2 respectively, then the failure probability becomes

$$p_f = P(R - S \le 0) = \Phi\left(\frac{-(\mu_R - \mu_S)}{(\sigma_S^2 + \sigma_R^2)^{1/2}}\right) = \Phi(-\beta) \tag{2.30}$$

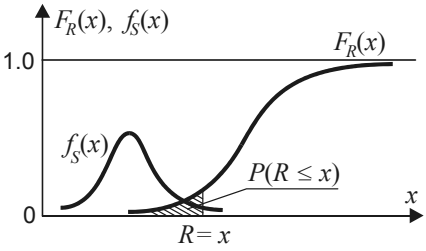

where $\Phi(\cdot)$ is the standard normal distribution function and $\beta = \mu_Z / \sigma_Z$ is defined as "safety index" (see Fig. 2.6). A review of the safety index methods can be found, for example, in Putresza and Jendo (1995).

In many problems it may not be possible to reduce the structural reliability to a simple R versus S formulation. In general, R is a function of material properties and element or structure dimensions, while S is a function of the applied loads, the material densities and the dimensions of the structure, each of which may be a random variable. The fundamental variables which define and characterize the behaviour of a structure are referred to as the "basic" variables. The description of these variables depends on the knowledge that is available. Observations and experience gained in the past with respect to similar structures can be used. Sometimes physical reasoning may suggest an appropriate probability distribution. It is very convenient to choose the basic variables so that they are independent but this cannot always be possible.

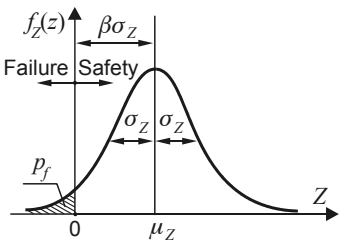

Fig. 2.6. Distribution of the safety margin $Z = R - S$

The simple form of the limit state function (2.27) can be replaced with a generalized version expressed directly in terms of basic variables and their probability distributions

$$p_f = P\left[G(\mathbf{X}) \le 0\right] = \int \ldots \int_{G(\mathbf{X})\le 0} f_{\mathbf{X}}(\mathbf{x})\, dx \tag{2.31}$$

where $G(\mathbf{X})$ describes the limit state function, $f_{\mathbf{X}}(\mathbf{x})$ is the joint probability density function for the n-dimensional vector $\mathbf{X}$ of basic variables. If the basic variables are independent, the formulation (2.31) can be simplified

$$f_{\mathbf{X}}(\mathbf{x}) = \prod_{i=1}^{n} f_{X_i}(x_i) = f_{X_1}(x_1) \cdot f_{X_2}(x_2) \cdot f_{X_3}(x_3) \ldots \tag{2.32}$$

where $f_{X_i}(x_i)$ is the marginal probability density function of the basic variable X_i.

Usually, the integration of (2.31) cannot be performed analytically. However, it can be solved using simplified formulas or numerical methods. The following dominant approaches have been explored (see for example Melchers, 1999) by:

a) numerical approximation such as simulation to perform the multidimensional integration required in (2.31) – the *Monte Carlo methods*.
b) transforming $f_{\mathbf{X}}(\mathbf{x})$ in (2.31) to a multi-normal probability density function and the use of some properties – the so called *First- and Second-order Reliability Methods* (FORM and SORM methods).
c) carefully planned numerical experiments to obtain a description of the influence of each variable and their possible combinations on the response of the system – the so called *Response Surface* methods.

The above techniques are described in the next sections. It should be pointed out that other reliability methods, not discussed here, are being developed. For example, Ben-Haim in (1996) summarizes a convex-set-model of uncertainty in a range of technological applications. Progress of the so-called *Robust Reliability* can be followed in the literature of the past few decades. Recently, the *artificial neural networks* have also been applied to evaluate the structural reliability (see Hurtado and Alvarez, 2001, Gomes and Awruch, 2004, Hurtado 2002, Papadrakakis et al. 1996, Papadrakakis and Lagaros 2002).

2.5. Monte Carlo methods

The Monte Carlo method has for long been recognized as the most exact method for all the calculations that require the knowledge of the probability distribution of response of uncertain systems to uncertain inputs. Applications of the Monte Carlo technique to a large variety of problems have been described (see, for example, Rubinstein 1981). Some typical early structural engineering applications have been proposed by Moses and Kinser (1967). Warner and Kabaila (1968) reported on various ways of applying the Monte Carlo technique to an idealized reinforced concrete member.

It should be pointed out that the Monte Carlo methods can successfully be used not merely to solve the reliability problems. For example, Wang (1999) generated random aggregate structure in which the shape, size and the distribution of the aggregate particles resemble real concrete in the statistical sense. Graham et al. (2003) created a series of local stress fields associated with the random material sample under uniaxial tension. Similar solution in ceramics is also available (Niezgoda 2001). Hou et al. (2004) used the Monte Carlo method to generate large-sized samples that have similar characteristics in time and frequency for structural dynamics applications. This method can also be of use in solving integral equations (Brandt 1998). Shia and Hui (2000) introduced a method called *walk on*

the boundary (WBM) to solve linear elasticity problems. The WBM method does not require any kind of meshing.

Theoretical basis and advance engineering application of the Monte Carlo method can be found for example in Hammersley and Handscomb (1964), Rubinstein (1981), Liu (2001), or Winkler (1995), and such areas as financial sector and statistical quality control are investigated in Fu and Hu (1997).

A general idea of the Monte Carlo method can be summarized as follows. Suppose that the following integral, the generalized form of (2.31), is evaluated (Liu 2001)

$$I = \int_D g(\mathbf{x})\, dx \tag{2.33}$$

where D is a region in high-dimensional space and $g(\mathbf{x})$ is the target function of interest. If independent and identically distributed random samples $\mathbf{x}_1, ..., \mathbf{x}_m$, uniformly simulated from D, an approximation of I can be obtained as

$$\hat{I}_m = \frac{1}{m}\left[g(\mathbf{x}_1) + ... + g(\mathbf{x}_m) \right] \tag{2.34}$$

According to the law of large numbers the average of many independent random variables with common mean and finite variances tends to stabilize at their common mean

$$\lim_{m\to\infty} \hat{I}_m = I, \quad \text{with probability} \quad 1 \tag{2.35}$$

Its convergence rate can be assessed by the central limit theorem

$$\sqrt{m}\left(\hat{I}_m - I \right) \to N\left(0, \sigma^2\right) \tag{2.36}$$

where $\sigma^2 = \text{var}[g(\mathbf{x})]$. Hence, the error term of the Monte Carlo approximation is $O(m^{-1/2})$, regardless of the dimensionality of $\mathbf{x}$. This basic setting underlines the potential role of the Monte Carlo methodology in science and statistics.

In the case of structural reliability analysis, this means, that each random variable vector $\mathbf{x}_i$ is randomly generated to obtain sample value $\hat{\mathbf{x}}_i$, and then the limit state function $G(\hat{\mathbf{x}}_i) = 0$ is checked. If the limit state is violated, i.e. $G(\hat{\mathbf{x}}_i) \le 0$, the structure or structural element has "failed" (Melchers, 1999). The experiment is repeated many times. If N trials are conducted, the probability of failure is given approximately by

$$p_f = \frac{n\left(G(\hat{\mathbf{x}}_i) \le 0\right)}{N} \tag{2.37}$$

where $n(G(\hat{\mathbf{x}}_i) \le 0)$ denotes the number of trials n for which $G(\hat{\mathbf{x}}_i) \le 0$. The number N of trials is related to the accuracy for p_f estimation.

To apply the Monte Carlo techniques to structural reliability it is necessary (Melchers 1999):

1) to develop simulation technique for numerical sampling of the basic variables $\hat{\mathbf{x}}_i$,
2) to consider the effect of the complexity of calculating the limit state function $G(\hat{\mathbf{x}}_i)$ and the number of basic variables on the simulation techniques used,
3) to determine the amount of sampling required to obtain a reasonable estimate of the structure probability of failure p_f.

In the next sections various Monte Carlo techniques for reliability estimation are outlined.

2.5.1. Direct Monte Carlo method

The *direct sampling* or *Simple Random Sampling* (Hurtado and Barbat 1998) is the simplest Monte Carlo approach in solving reliability problems. It can be graphically presented as so-called *ant-hill* (see Fig 2.7). It does not apply any reduction method to the generated set of variates, which allows for the statistical description of the structural behaviour without scarifying the description quality. Thus, this method can be fast enough for the reliability analysis of structures with a reduced number of degree of freedom (Marek et al. 1996) but it is too costly for any large structure analysis.

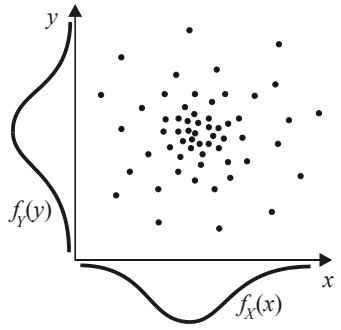

Fig. 2.7. Simple random sampling

In this case the probability of structure failure (2.31) may be expressed as (Melchers 1999)

$$p_f = J = \int \ldots \int I\left[G(\mathbf{X}) \le 0\right] f_{\mathbf{X}}(\mathbf{x})\, d\mathbf{x} \tag{2.38}$$

where $I[\cdot]$ is an indicator function which equals 1 if $[\cdot]$ is "true" and 0 if $[\cdot]$ is "false". Thus, the indicator function identifies the integration domain. The unbiased estimator of the expected value J and the estimator of standard deviation can be calculated as follows:

$$p_f \approx J_1 = \frac{1}{N}\sum_{i=1}^{N} I\left[G(\hat{\mathbf{x}}_i) \le 0\right] \tag{2.39}$$

$$\sigma_{J_1}^2 = \sum_{i=1}^{N} \frac{1}{N^2} \operatorname{var}\left[I(G \le 0)\right] = \frac{\sigma_{I(G\le 0)}^2}{N} \tag{2.40}$$

where $\hat{\mathbf{x}}_i$ represents the i-th vector of random observations from $f_{\mathbf{X}}(\cdot)$. The standard deviation of J_1 and hence of the Monte Carlo estimate p_f (2.39) varies inversely with $N^{1/2}$ (see also Eq. (2.36)) These observations are important in determining the number of simulations required for a particular level of confidence.

On the basis of the central limit theorem, the following confidence statement can be made concerning the number of J_1 trails in which failure are possible (see Melchers 1999)

$$P\left(-k\sigma < J_1 - \mu < +k\sigma\right) = C \tag{2.41}$$

where μ is the expected value of J_1 given by Eq. (2.39) and σ is standard deviation expressed by (2.40).

For confidence interval $C = 95\%$, according to standard normal tables k equals $k = 1.95$. Shooman (1968) recommended that for $N = 100\,000$ samples and p_f expected $p_f = 10^{-3}$ the error would be less than 20%. In general it can be assumed that, if p_f is the expected probability, then $100/p_f$ samples need to be generated. Hence, if p_f is of the order of $10^{-3} \div 10^{-5}$ as may be typical, $10^5 \div 10^7$ sample points should be taken into calculations. Mann et al. (1974) have suggested that the number of simulations may need to be of the order of 10000 ÷ 20000 for approximately 95% confidence limit.

The number N of simulations for a given confidence level C in the failure probability p_f can also be obtained from (see Melchers 1999)

$$N > \frac{-\ln(1-C)}{p_f} \tag{2.42}$$

Using Eq. (2.42) for a 95% confidence level and $p_f = 10^{-3}$ the required number of simulations is more than 3000.

It is not convenient to apply the above theoretical rules to the accuracy analysis in any particular Monte Carlo calculations. According to Melchers (1999) a useful tool for this purpose is to plot progressive results of the estimate of p_f and variance $\sigma^2_{J_1}$ (Eqs. (2.39) and (2.40) respectively). Such plots (see Fig. 2.8) will show that these measures decline when the number of samples rises and that a degree of stability is reached at a sufficiently high number of samples. This concept has been used, for example, by Araújo (2001).

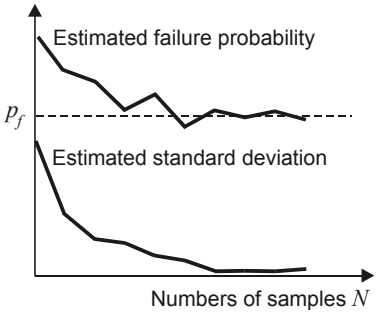

Fig. 2.8. Convergence of probability estimate with increasing sample size

The results may also be represented as a cumulative distribution function $F_G(g)$ (see Fig 2.9). The estimate of p_f in Eq. (2.39) may be improved by fitting an appropriate distribution function through the points for which $G(\cdot) \le 0$, i.e. the left-hand tail in Fig. 2.9 (Melchers, 1999). However, the choice of an appropriate distribution function may not stabilize until N is quite large (Moses and Kinser 1967). Grigoriu (1983) proposed fitting not a single distribution to the sample points but a sequence of distributions. The probability distributions function of a random variable $Z = R - S$ (see Fig 2.6) can also be approximated with polynomial functions (Er 1998). Li and Li (2002) combine the Monte Carlo simulation with approximation of the probability distribution functions, too.

The *Stratified Sampling* and *Latin Hypercube Sampling* techniques have been proposed to reduce the Monte Carlo calculation (Hurtado and Barbat 1998). They are briefly described in the next sections. A different reduction method can be found for example in Soh et al. (2004) where the integration of piecewise approach and the cell technique are applied. In Koutsourelakis et al. (2002) advantage is taken of lines instead of points to obtain greater accuracy using fewer samples.

An evident reduction of the samples can be achieved by using additional information about the problem to be solved, which creates the basis for *importance sampling* and similar techniques. For example, from see Fig 2.5 it is evident that only sampling in the region of overlap between $f_R(\cdot)$ and $f_S(\cdot)$ is important. An survey of the various strategies for sampling reduction called *Variance Reduction Techniques* is given by Rubinstein (1981) and by Warner and Kabaila (1968).

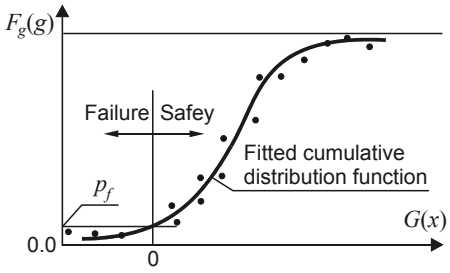

Fig. 2.9. Use of fitted cumulative distribution function to estimate p_f

Nevertheless the direct Monte Carlo method is still attractive. For example Schenk and Schuëller (2003) presented a complex analysis of the buckling of cylindrical shells with random geometric imperfections using this method. Reinforced concrete columns have been analysed (Araújo 2001, Frangopol et al. 1996) and prestressed, geometrical and material nonlinear structures by Biondini et al. (2004).

2.5.2. Stratified sampling

In the case of the *Stratified Sampling* method (Rubinstain 1981) the whole space of the variable is divided into subsets of equal probability. The acquired data are generated from each subset and an analysis is performed with corresponding sets of points (Fig. 2.10). A sample from inside the subset is taken either from the middle or randomly. In the case of reliability assessment the conventional strategy should be modified to increase its efficiency. For example, a careful selection of the number of samples from each subset must be made – those contributing to the reliability calculation should be sampled more intensively.

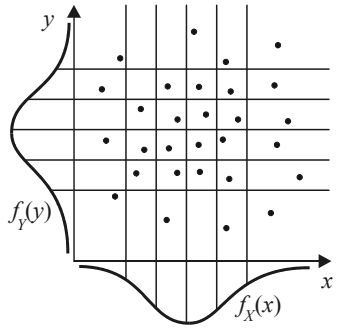

Fig. 2.10. Stratified Sampling

The failure probability is calculated in the following way (Hurtado and Bardat 1998)

$$\hat{p}_f = \sum_{i=1}^{l} P_i \sum_{j=1}^{n_i} I\left(G\left(\hat{\mathbf{x}}_i\right) \le 0\right) \tag{2.43}$$

where n_i is the number of samples of each of the l subregions into which the entire hypervolume has been divided, and P_i is the probability mass of each subregion.

It should be stressed that the Direct Monte Carlo and the Stratified Sampling Method can also be applied to those cases in which the limit state function $G(\mathbf{X})$ is not known. The efficiency of the methods to be dealt with in the next sections, e.g. Important Sampling or Directional Sampling depends greatly on establishing the state function.

2.5.3. Latin Hypercube Sampling

The *Latin Hypercube Sampling* method (Bazant and Liu 1985, Helton and Davis 2003) combines at random each subset number from each random variable with other subset numbers of the remaining variables only once (see Fig. 2.11). There are many variants of the method (see Florian 1992, Žiha 1995). Huntington and Lyrintzis (1998) used section-mean sampling to obtain a better accuracy in the simulated means and variance for each variable. Hora and Helton (2003) used a test for the presence of a monotonous relationship between the input and output variables to improve the standard Latin Hypercube Sampling. According to Olsson et al. (2003) the method is only slightly more efficient than the Direct Sampling for estimating small probabilities, and proposed a bridge between Latin and Importance Sampling. The so-called *descriptive sampling* which is based on values given for random variables can be related to the Latin hypercube sampling (see for example Žiha 1995).

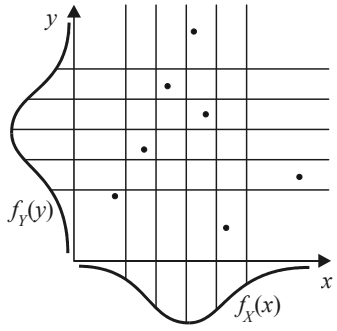

Fig. 2.11. Latin Hypercube Sampling

2.5.4. Importance sampling and search techniques

The integral (2.31) can be written using the indicator function $I[\cdot]$ as (see Melchers 1990, or Melchers 1999)

$$J = \int \ldots \int I\left[G(\mathbf{X}) \le 0\right] \frac{f_{\mathbf{X}}(\mathbf{x})}{h_{\mathbf{V}}(\mathbf{x})} h_{\mathbf{V}}(\mathbf{x}) d\mathbf{x} \tag{2.44}$$

where $h_{\mathbf{V}}(\mathbf{x})$ is termed the "importance-sampling" probability density function.

An unbiased estimate of J is given by (cf. (2.39))

$$p_f \approx J_2 = \frac{1}{N} \sum_{i=1}^{N} \left\{ I\left[G(\hat{\mathbf{v}}_i) \le 0\right] \frac{f_{\mathbf{X}}(\hat{\mathbf{v}}_i)}{h_{\mathbf{V}}(\hat{\mathbf{v}}_i)} \right\} \tag{2.45}$$

where $\hat{\mathbf{v}}_i$ is a vector of sample values taken from the importance sampling function $h_{\mathbf{V}}(\mathbf{v})$.

For a given level of confidence, far fewer sample points of $h_{\mathbf{V}}(\mathbf{v})$ are required than in the direct Monte Carlo method with $f_{\mathbf{X}}(\mathbf{x})$ as sampling distribution. The derivation of optimal $h_{\mathbf{V}}(\mathbf{v})$ functions is difficult and they are often selected on a priori grounds. Sometimes it is possible to estimate the point x^*, known as the point of "maximum likelihood" or the "design point", with $f_{\mathbf{X}}(\mathbf{x})$ having the largest influence on the limit state function (see Fig. 2.12). The point x^* may be found by a direct application of the numerical maximization techniques or the search algorithms. Once x^* is identified, the most common approach of choosing $h_{\mathbf{V}}(\mathbf{v})$ is to use the distribution $f_{\mathbf{X}}(\mathbf{x})$ shifted so that its mean is at x^*. Function $h_{\mathbf{V}}(\mathbf{v})$ suggested by Engelund and Rackwitz (1993) has proved to be very effective for a range of possible shapes of the limit state function.

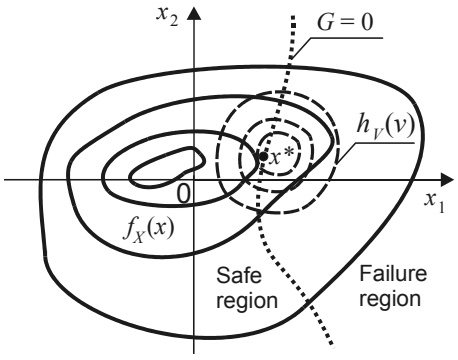

Fig. 2.12. Importance sampling function $I_{\mathbf{V}}[\,]$ in x space.

Adaptive sampling techniques apply modification of $h_{\mathbf{V}}(\mathbf{v})$, depending on the information being obtained from the search process (see Melchers 1999). First the initial location of $h_{\mathbf{V}}(\mathbf{v})$, described by a mean vector and a covariance matrix is assumed. A limited amount of sampling is then carried out. The samples which fall into the failure domain are used to relocate and change the form of $h_{\mathbf{V}}(\mathbf{v})$ (Bucher 1988). The convergence of this approach can be guaranteed to some extent (see Der Kiureghian and Dakessian 1998). In general, it requires good physical understanding of the problem being solved. The adaptive sampling technique has been used by Kleiber et al. (2002) to estimate reliability estimation of sheet metal forming operations, and by Mahadevan and Raghothamachar (2000) to large structures, frames and trusses.

In Ang et al. (1991), and Wang and Ang (1994) a method using the information of a previous simple random sampling is also proposed. The optimal importance sampling density is built up by averaging windowed kernel densities whose parameters are obtained from the previous analyses.

Ambartzumian et al. (1998) proposed an efficient sequential conditional importance sampling (SCIS) algorithm to compute the multinormal probability of rectangular domains by simulations. Royset and Polak (2004) used importance sampling to solve reliability-based optimal design problem. This technique can also be implemented to reliability estimation of dynamical systems (Au and Beck 2001, Bayer and Bucher 1999).

The importance sampling method makes allowance for the estimation of the sensitivity of failure probability to changes in random variables (Melchers 1999, Ambartzumian et al. 1998, Melchers and Ahammed 2004). Generally, if the effect of changing one or more variables on the failure probability is required to be evaluated, two Monte Carlo calculations, with or without a change should be performed. Such an analysis is unlikely to be very helpful. If the limit state function is analytical, then the differentials $\partial G / \partial X_i$ will give the sensitivity of $G(\mathbf{X})$ to a change in X_i.

In the case of the importance sampling the probability estimate for the modified problem with a changed random variable x_i is given by (Melchers, 1999)

$$p_f + \Delta p_i = \int_D f_{\mathbf{X}+\Delta X_i}(\mathbf{x})\, d\mathbf{x} \approx \frac{1}{N}\sum_{j=1}^{N} I\left[\hat{\mathbf{x}}_j\right] \frac{f_{\mathbf{X}+\Delta X_i}\left(\hat{\mathbf{x}}_j\right)}{h_{\mathbf{X}}\left(\hat{\mathbf{x}}_j\right)} \tag{2.46}$$

and the sensitivity can be estimated as follows

$$S_i = \left[\left(p_f + \Delta p_i\right) - p_i\right] \Big/ \Delta x_i \tag{2.47}$$

Bhattacharyya and Chakraborty (2002) have employed the Neumann expansion, the Monte Carlo simulation and the finite element method in computing the response sensitivity taking account of uncertainties in structural parameters.

2.5.5. Directional simulation and conditional expectation

In the directional simulation method use is made of a polar coordinate system (Ditlevsen et al. 1987). The n-dimensional Gaussian vector $\mathbf{Y} = R\mathbf{A}$ represents the directions in the standard normal space **y**. The random vector **A** represents the direction cosines. The radial distance R $(R \geq 0)$ is such that R^2 is χ_n^2-square distributed with n degrees of freedom. If R is independent of **A**, then, by conditioning on $\mathbf{A} = \mathbf{a}$ (see Fig. 2.13) the probability integral (2.31) can be written as (Bjerager 1988)

$$p_f = \int_{\mathbf{a}} P\left[g(R\mathbf{A}) \leq 0 \,\middle|\, \mathbf{A} = \mathbf{a}\right] \cdot f_{\mathbf{A}}(\mathbf{a})\, d\mathbf{a} \tag{2.48}$$

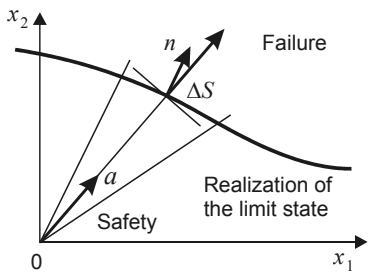

Fig. 2.13. A radial sample in direction $\mathbf{A} = \mathbf{a}$

where $f_{\mathbf{A}}(\mathbf{a})$ is the constant density of **A** on the unit sphere and $g(\mathbf{RA}) = 0$ is the limit state function in **y**-space.

The reliability can be estimated by generating randomly a standard normal unit vector $\hat{\mathbf{a}}_j$ and moving along the outward direction of this vector until the limit state function $g(r\hat{\mathbf{a}}_j) = 0$ is reached at $R = r$. From this expression it is possible to determine r. Trial and error calculations are usually implemented. The estimate of the failure probability is given by (Melchers 1999)

$$p_f = P\left[g\left(r\hat{\mathbf{a}}_j\right) \le 0 \right] = 1 - \chi_n^2\left(r\right) \tag{2.49}$$

The main advantage of the directional simulation method is that $\chi_n^2(\mathbf{r})$ can be evaluated analytically, effectively reducing the order of integration by one dimension. This approach is particularly useful for limit state surfaces which are nearly spherical in standard normal space **y**. Directional method has been used by Nie and Ellingwood (2000) and polar coordinates by Yonezawa and Okuda (1994).

In a situation where at least one of the random variables in (2.31) is an independent random variable, the Monte Carlo process can become more efficient by reducing the order of integration. This technique is known as *conditional expectation* (see Melchers 1999). For example, selecting one independent random variable X_1 with the largest uncertainty (variance), expression (2.31) can be rewritten as:

$$p_f = \int\limits_{G(\mathbf{X})\le 0} \int\limits_{n} f_{\mathbf{X}}\left(\mathbf{x}\right) dx = \int\limits_{G(\mathbf{X}')\le 0} \int\limits_{n-1} F_{\mathbf{X}_1}\left(\mathbf{u}\right) f_{\mathbf{X}}\left(\mathbf{u}\right) du \tag{2.50}$$

where $\mathbf{X}'$ represents the reduced vector of random variables.

The conditional expectation method gives better estimation than the equivalent direct formulation (Ayyab and Haldar 1984). Some additional variance reduction may be achieved through 'anti-thetic' variates in which the variates in sample sequences are given negative correlation (Rubinstein 1981).

Similar techniques are also developed, for example the *Axis-Orthogonal Simulation* (Fujita and Rackwitz 1987) and the *Generalized Conditional Expectation* (Ayyab and Haldar 1984) in which the simulation is governed by a subset of the random variables having low dispersion. An approach by Shao and Murotsu (1994) combines the traditional directional and adaptive importance sampling technique. Several new approaches for identifying directions towards evaluating the probability integral (Spherical *t*-design, Spiral Point, and Fekete Points) have been introduced by Nie and Ellingwood (2000 and 2004a). The same authors applied the neural methods in a directional reliability method (Nie and Ellingwood 2004b).

It should be mentioned that the described methods require a transformation of all random variables to the standard normal space. This can be very laborious in the case of a large number *n* of random variables. Moreover, there are in general *n*! ways to perform the transformation so that in principle all of them are assumed to detect the critical one (Dolinski 1983). This objective makes these methods useful only for improving the results calculated by analytical methods rather than for general analysis linked to an FE code.

2.5.6. Series and parallel systems

Many structural systems may be idealized into two simple categories: series and parallel. Combinations of these classes are also possible.

In a *series system* a failure of any element constitutes a failure of the structure. Thus, the failure probability in a structure composed of *m* members is (Freudenthal 1961, Freudenthal et al. 1966):

$$p_f = P\left(F_1 \cup F_2 \cup F_3 \cup ... \cup F_m\right) \tag{2.51}$$

where each failure mode F_i $(i = 1,...m)$ is represented by a limit state equation $G(\mathbf{X}) = 0$ in a basic variable space.

And so, the failure probability can be written as (Melchers 1999)

$$p_f = \int ... \int I\left[\bigcup_{i=1}^{m} G_i(\mathbf{x}) \le 0\right] f_{\mathbf{X}}(\mathbf{x})\, d\mathbf{x} \tag{2.52}$$

where the indicator function $I[\cdot]$ for a series system is generalized to

$$I\left[\bigcup_{i=1}^{m} G_i(\mathbf{x}) \le 0\right] = \begin{cases} 1 & \text{if} \quad I[\cdot] \text{ is true} \\ 0 & \text{if} \quad I[\cdot] \text{ is false} \end{cases} \tag{2.53}$$

and $G_i(\mathbf{x}) = 0$ represents the ith known limit state function, $i = 1, \ldots, m$.

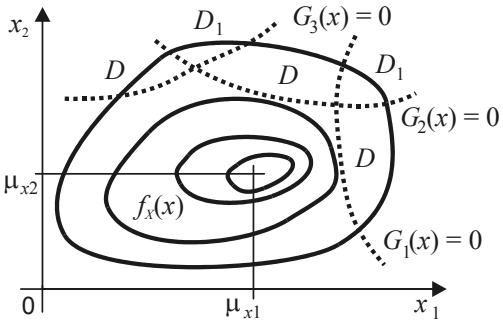

Fig. 2.14. Basic structural system reliability problem in two dimensions showing failure domain D (and D_1)

In a two-dimensional space, $I[\cdot]$ represents the integration domain D (and D_1) of Fig. 2.14. This formulation is applicable if the direct or importance sampling Monte Carlo approach is used.

In a *parallel system* to reach the limit state in one or more elements does not necessarily mean a failure of the whole system. The failure probability of an m-component parallel system is given by (Melchers 1999)

$$p_f = P\left(F_1 \cap F_2 \cap F_3 \cap ... \cap F_m\right) \tag{2.54}$$

where F_i is the event failure of the ith component.

In parallel systems the failure probability associated with the intersection of k limit states is given by (2.52) and $I[\cdot]$ is defined as

$$I\left[\bigcap_{i=1}^{k} G_i(\mathbf{x}) \le 0\right] \tag{2.55}$$

The most interesting regions are those which are bounded by appropriate limit state functions and are near their intersection (domains D_1 in Fig. 2.14).

The series and parallel system definition allow for a description of the *bounds of failure probability* when the failures are somewhere between completely independent and fully dependent modes (Cornell 1967)

$$\max_{i=1}^{m}\left[P(F_i)\right] \le P(F) \le 1 - \prod_{i=1}^{m}\left[1 - P(F_i)\right] \tag{2.56}$$

where $P(F)$ denotes the probability of failure, which can be expressed as $P(F) = 1 - P(S)$, and $P(S)$ is the probability of survival.

Unfortunately, in many practical structural systems the series bounds (2.56) are too wide to be meaningful (Grimmelt and Schuëller 1982, Ditlevsen 1979).

Second-order lower and upper bounds are determined by Ditlevsen (1979), and Vanmarcke (1973). The bounds obtained for a series of rigid-plastic frames were close to the direct Monte Carlo simulation results (Grimmelt and Schuëller 1982). Estimations of failure probabilities for intersections of non-linear states are given by Melchers and

Ahammed (2001). The concept of bounds has also been successfully applied to estimate seismic reliability of monumental buildings (Augusti et al. 2002).

It should be pointed out that a classification of the system as one with series, parallel or more complex subsystems is useful for other methods, particularly in conjunction with the FORM/SORM techiques.

2.5.7. Methods not dependent on limit function

Modern statistical theories based on expansion of the empirical density function of the response are mentioned by Hurtado and Barbat (1998) referring to: Cornish-Fisher expansion (Johnson et al. 1994), Saddlepoint expansion (Kolassa 1997), Edgeworth expansion (Hall 1992), and Normal expansion (Hong and Lind 1996). The probability of a response can be estimated on the basis of its own samples. Generally speaking, it can be asserted that there is little experience in the use of these methods in structural analysis. Some methods devised for sampling in very low probability regions of dynamic systems using the white noise processes must be mentioned (Pradlwarter et al. 1994). In a contribution by Pradlwarter and Schuëller (1997) the accuracy of the method is compared with that obtained with the less involved techniques known as *Russian Roulette* and *Splitting* (see for example Melnik-Melnikov and Dekhtyaruk 2000).

2.6. First- and Second-order Reliability Methods

The most important analytical tools for reliability calculation of failure probability are known as First- and Second-order Reliability Methods (FORM and SORM methods). Both of them require to take the following steps (Hurtado et al. 1998):

a) First the basic variables **X** are transformed into a set of standard normal variables **U**. The Rosenblatt transformation is usually used. The transformation is performed by the following algorithm:

$$\begin{aligned} U_1 &= \Phi^{-1} F\left(x_1\right) \\ U_2 &= \Phi^{-1} F\left(x_2 \middle| x_1\right) \\ &\cdots \\ U_n &= \Phi^{-1} F\left(x_n \middle| x_1,\, x_2, \ldots, x_n\right) \end{aligned} \tag{2.57}$$

b) In the second step the failure surface $G(\cdot)$ in the u-space in the neighbourhood of the most likely failure point is approximated. In the FORM method the approximation is performed by a tangent hyperplane using a first order Taylor expansion. In the SORM method a curved surface is obtained using the second order terms of the Taylor expansion or parabolas that make the multi-dimensional integration easy (Breitung 1984) (see Fig. 2.15).

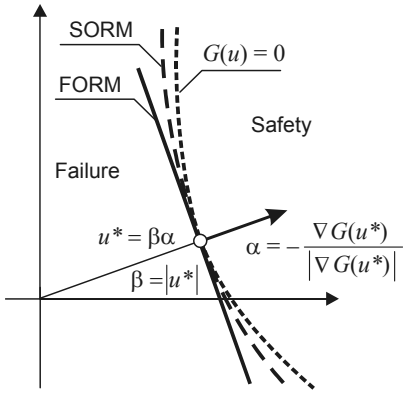

Fig. 2.15. FORM/SORM methods

c) The third step is to calculate the failure probability. In the FORM case it is approximated by

$$p_f = \Phi(-\beta) \tag{2.58}$$

where β is the distance from the origin to the approximating hypersurface in the *U*-space. It is called the first order reliability index, since it measures how far the most critical point is located from the mean value of the random variables, as can be seen in the figure.

Enormous problems are solved using the FORM and SORM techniques. For example, in (Gomes and Awruch, 2002) the FORM methods are employed to the reliability calculation of reinforced concrete structures. A multidimensional non-Gaussian stochastic field generation model is developed and used. Brząkała and Puła (1996) propose to implement the finite element method (FERM) based on FORM and SORM analysis to establish the reliability index β for a random layered subsoil. Lin (2000) compared the reliability of composite plates estimated by the use of three different methods: Monte Carlo, β method, and first order second moment method. All of them could produce reasonably good results. Val et al. (1997) combined FORM and a nonlinear finite element structural model to calculate the reliability of reinforced frames. Second-order third-moment reliability methods have also been proposed (Zhao et al. 2002).

2.7. Response surfaces

Response Surface Method is applied in a general field of experimental design, e.g. structural optimization, statistical description, etc. The main difference in the method compared with the Monte Carlo technique is that the experiments are not random but rather carefully planned (Hurtado and Barbat 1998). The objective is to obtain a description of the influence of all design variables and their possible combinations on the response of the system. Different strategies are developed. The most general technique is the *Factor Design* in which all the variables are combined with each other. Since the effect of some of them can be indistinguishable from other ones, the number of analyses can be reduced by applying a *Fractional Factorial Design*. A final step in the analysis is the calculation of a first or second order regression of the response variables with respect to the input ones. Usually conventional least square method is applied. It is also important to calculate error and variance statistics which can improve the experimental design and make it possible to take a decision about the system under analysis.

The method has been applied to reliability analysis in conditions where the limit state function $G(\mathbf{X})$ may not be known explicitly or is difficult to calculate (Melchers 1999, Faravelli 1989, Enevoldsen et al. 1994, Kim and Na 1997). For example, this might occur by the use of the finite element analysis, particularly when making iterative calculation of non-linear material or structural behaviour. The safe domain can be defined only through point-by-point finding for example by a repeated numerical analysis with different input values. If the values are specifically ordered the Response Surface method is implemented. An ordinary approach is to let $\bar{G}(\mathbf{X})$ be a second order polynomial whose coefficients are determined so as to minimize the error of approximation (Faravelli 1989, Bucher and Bourgund 1990, Rajashekhar and Ellingwood 1993, Maymon 1993):

$$\bar{G}(\mathbf{X}) = A + \mathbf{X}^T\mathbf{B} + \mathbf{X}^T\mathbf{C}\mathbf{X} \tag{2.59}$$

where the regression coefficients are defined by A, $\mathbf{B}^T = [B_1, B_2, \ldots B_n]$ and $\mathbf{C}$ is $n \times n$ symmetric matrix (Melchers 1999).

The coefficients may be obtained by conducting a series of structural analyses with input variables selected according to some "experimental design" (Melchers 1999). When the region of the failure domain or the design point is initially not known, the choice of the input variables may be difficult. A simple approach is to select the input variables as the mean value of the variables. An important step to be taken is to try to select the regression coefficients A, $\mathbf{B}$, $\mathbf{C}$ so that the total error is minimized.

Several methods of reducing the number of random variables involved have been proposed. One of them is simple replacement of random variables of low uncertainty with deterministic equivalents (Melchers 1999). Another approach is to reduce the set of random variables $\mathbf{X}$ to a smaller set describing their spatial averages, rather than allowing for their variation from point to point or from finite element to finite element.

Bucher and Bourgund (1990) suggested that the evaluation points might be chosen at a mean point $\mathbf{x}_m$ and at points given by $x_i = x_{mi} \pm h_i \sigma_i$ where h_i is an arbitrary factor and σ_i, is the standard deviation of X_i. Using these points, the approximating surface $\bar{G}(\bar{\mathbf{x}})$ can be determined. If $\mathbf{x}_m$ is not the design point, some other point $\mathbf{x}_D$ can be found on the surface $\bar{G}(\bar{\mathbf{x}})$. Then, a new mean point $\mathbf{x}_m^*$ can be obtained by linear interpolation between $\mathbf{x}_m$ and $\mathbf{x}_D$. The speed with which this technique approaches a sufficiently accurate fit depends on the selection of h_i (Rajashekhar and Ellingwood 1993). It is possible to modify the search algorithms to direct the search away from the design points already obtained (Der Kiureghian and Dakessian 1998).

A number of example applications of response surfaces have been given in the literature (Bucher and Bourgund 1990, Wu et al. 1990, Schuëller et al. 1991, Rajashekhar and Ellingwood 1993) and the software has been developed (Schuëller and Bucher 1991). These developments suggest that the concept of a response surface works well provided the point of maximum likelihood can be identified and that reasonable decisions can be made about the points to be used for fitting the response surface. Various suggestions relevant to this have been made (Kim and Na 1997). They include the use of iterative methods (Liu and Moses 1994), but it is difficult, particularly in large systems, because such points cannot always be identified without subjective interference. Falsone and Impollonia (2004) have presented a response surface method being insensitive to sampling point positions.

The Response Surface method has been applied to medieval tower reliability calculation by Griannini et al. (1996). Kmiecik and Soares (2002) applied this technique to determine the cumulative probability function of compressed plates strength. A comparison of the solution obtained with the help of neural network and the response surface method has been performed (Gomes and Awruch, 2004). Rajashekhar and Ellingwood (1995) applied the response surface method to the estimation of the reliability of reinforced-concrete cylindrical shells – a nuclear containment. Axisymmetric nonlinear finite-element analyses were performed to define the limit surface, and importance sampling was used for the calculation of limit state probability. Das and Zheng (2000) proposed a method for the cumulative formulation of the surface. In searching and improving process, a parameter h^s, which determines the distance from the central point to a sampling point, is reduced by iterations. They suggested that in case the SORM fails, the Monte Carlo simulation with variance reduction should be used. Melchers and Ahammed (2002 and 2004) have proposed estimation of gradients using a simplified (linear) response surface, i.e. the sensitivity of the outcomes to input information is estimated. Response surface method is also applied in dynamics analysis (Bucher and Brenner 1992).

Chapter 3

SIMULATION OF DISCRETE RANDOM FIELDS

Simulation of random fields plays an essential role in the solution of stochastic problems with the help of finite element methods. After theoretical foundations set out by Adler (1981) and Matheron (1975), and the pioneering works of Shinozuka and his co-workers (Shinozuka 1987a, Yamazaki and Shinozuka1990), several teams develop various methods of digital simulation of random fields defined on meshes (Grigoriu and Balopoulou 1993, Mignolet and Spanos 1992). These methods concern mainly the homogeneous fields encountered in the modelling of such phenomena as acoustics, turbulence, ocean engineering, tribology, earth sciences and others. Strategies for the simulation of nonhomogeneous fields are also proposed (Popescu et al. 1998). The conditional estimation is used by Nordgren and Conte (1999). The non-Gaussian field computation is presented by Gomes and Awruch (2002), who compared three methods, i.e. sub-domain decomposition, Cholesky or modal decomposition of the covariance matrix and spectral representation using cosine series, and who pointed out the last one as the most efficient one.

The presented here method is motivated by modelling the boundary value problems in civil engineering. In this domain the nonhomogeneous fields are typical. In the works by Bielewicz et al. (1985a, 1987, and 1994b), and Walukiewicz et al. (1995 and 1997) (see also Bielewicz et al. 1991, 1995b, and 1994a, and Górski and Walukiewicz 2000), a new approach to the simulation of such fields based on an effective version of the rejection theorem (Devroye 1986) and the conditional probability distribution formula has been developed. An important role in the calculations is played by the propagation base scheme covering sequentially the field points. In order to fulfil the geometric and the boundary conditions of the structure model, the realisations of random fields have to be bounded by an envelope. The use of the envelope is an original feature of this method.

The main goal of the simulation method is the generation of a set of field realizations in such a way that following the averaging procedure the prescribed mean value vector and the covariance matrix are reproduced accurately, in the statistical sense (Walukiewicz et al. 1995). The simulation results obtained for various second-order fields have proved that the adopted algorithm is correct (Walukiewicz et al. 1997).

The method has been successfully implemented in shell structure analyses (Bielewicz et al. 1994b), and in the examination of environmental (Jankowski and Walukiewicz 1997) and soil random problems (Przewłócki and Górski 2001).

The theoretical background is presented in section 3.1. The method is described in section 3.2. In section 3.3 the statistical experiments for the determination of the variance and the covariance estimators, as well as the estimators of the determinants of the covariance matrices are described.

3.1. Theoretical background

A continuous, second-order, real-valued, vector random field $\mathbf{X}(\mathbf{r},\omega)$ is specified by the expected (mean) value function

$$\bar{\mathbf{X}}(\mathbf{r}) = E\left(\mathbf{X}(\mathbf{r},\omega)\right) \tag{3.1}$$

and the correlation tensor function

$$\mathbf{K}_x(\mathbf{r}_1,\mathbf{r}_2) = E\left(\left(\mathbf{X}(\mathbf{r}_1,\omega) - \bar{\mathbf{X}}(\mathbf{r}_1)\right) \otimes \left(\mathbf{X}(\mathbf{r}_2,\omega) - \bar{\mathbf{X}}(\mathbf{r}_2)\right)\right) \tag{3.2}$$

where $E(\cdot)$ is the expectation operator, $\omega \in \Omega$ denotes an elementary event, the sign $\otimes$ denotes the tensor product, and $\mathbf{r}, \mathbf{r}_1, \mathbf{r}_2 \in \Re^3$. If $\bar{\mathbf{X}}(\mathbf{r}) = \text{const}$ and

$$\mathbf{K}_x(\mathbf{r}_1,\mathbf{r}_2) = \mathbf{K}_x(\mathbf{r}_1 - \mathbf{r}_2) \tag{3.3}$$

then the field is called homogeneous, i.e. stationary in space (Adler 1981).

Using discrete methods of simulation and analysis, it is necessary to consider the random fields in the form of multidimensional random variables **X** defined on regular or irregular meshes. Thus, the role of covariance function $\mathbf{K}_x(\mathbf{r}_1,\mathbf{r}_2)$ takes on the covariance matrix **K**, always symmetric and positively definite:

$$\mathbf{K} = E\left(\left(\mathbf{X}(\omega) - \bar{\mathbf{X}}\right)\left(\mathbf{X}(\omega) - \bar{\mathbf{X}}\right)^T\right) \tag{3.4}$$

where $\mathbf{X}(\omega)$ describes the discrete, second-order, real-valued random field and $\bar{\mathbf{X}}$ stands for the expected value vector

$$\bar{\mathbf{X}} = E\left(\mathbf{X}(\omega)\right) \tag{3.5}$$

It is also useful to define the degenerated field by the condition for the global covariance matrix **K**:

$$\det\mathbf{K} = 0 \tag{3.6}$$

The probabilistic foundation for the generation of arbitrary vector random variables has been formulated in the rejection theorem by Devroye (1986) and von Neumann (see Brandt 1998). The main theoretical assumption of the simulation method is that the probability density function f of an m-dimensional random vector **X** is defined on a compact domain in $\Re^m$ and obeys the condition $f(\mathbf{X}) < +\infty$. This assumption makes sense in structural mechanics. A random point Π uniformly distributed in $\Re^{m+1}$ can be generated in the following way:

$$\Pi(\omega) = (\mathbf{x},\ u) = \begin{cases} x_i = a_i + u_i(\omega)(b_i - a_i) \\ u\ = u_{i+1}(\omega)\, c f_{\max} \end{cases} \tag{3.7}$$

where $(a_i,\ b_i)$, $i = 1, 2, ..., m$ are the given intervals of the reals and $u_i(\omega),\ u_{i+1}(\omega) \in U[0,1]$ are the values of independent, uniform random variables. If $\Pi \in A$ (i.e. Π is not rejected), where $A = \{(\mathbf{x},u) : \mathbf{x} \in \Re^m,\ \ 0 \le u \le cf(\mathbf{X})\}$ and $c > 0$, then the generated random variable $X_i (i = 1, 2, ..., m)$ is

$$X_i = a_i + u_i(b_i - a_i) \tag{3.8}$$

The direct rejection method to generate vectors **X** introduces a new dimension: a uniform, independent random variable. In this extended $\Re^{m+1}$ space, the joint probability density defined on a suitable set, is uniform (Devroye 1986). Fig. 3.1 presents an interpretation of the proof in the case of $m = 1$.

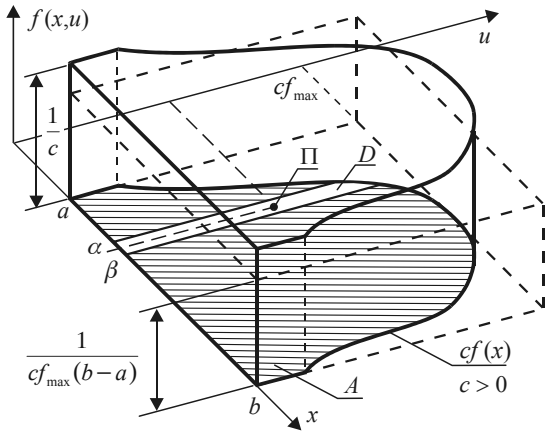

Fig. 3.1. An interpretation of Devroye theorem for $m = 1$

The random point Π is not rejected if it falls below the curve $cf(x)$ (Fig. 3.1). The probability of this event for the random variable uniformly distributed in the rectangle $cf_{\max}(b-a)$ becomes:

$$P(\Pi \in A) = \frac{\int_a^b cf(x)\,dx}{cf_{\max}(b-a)} = \frac{1}{f_{\max}(b-a)} \tag{3.9}$$

On the other hand, the probability for the point Π to fall below the curve $cf(x)$ (Fig. 3.1) in the interval $(\alpha,\ \beta)$ is equal

$$\frac{\int_\alpha^\beta f(x)\,dx}{f_{\max}(b-a)} \tag{3.10}$$

It follows that the ratio

$$\frac{P(\Pi \in D)}{P(\Pi \in A)} = \frac{\dfrac{\int_\alpha^\beta f(x)\,dx}{f_{\max}(b-a)}}{\dfrac{1}{f_{\max}(b-a)}} = \int_\alpha^\beta f(x)\,dx = P\left(x \in (\alpha,\ \beta)\right) \tag{3.11}$$

gives the required result.

However, the method is not effective (time inefficiency) for large values of m. For that reason a method of a sequential type, by applying a propagation scheme and conditional probability distributions has been proposed (Bielewicz et al. 1985a and 1994b, and Walukiewicz et al. 1997).

3.2. Simulation algorithm

As the proposed algorithm concerns discretized random problems, the random fields are described by the multidimensional random variables defined at the mesh nodes. The

covariance function is represented by the symmetric and positively defined covariance matrix $\mathbf{K}(m\times m)$. The random variable vector $\mathbf{X}(m\times 1)$ is divided into two blocks consisting of the unknown $\mathbf{X}_u(n\times 1)$ and the known $\mathbf{X}_k(p\times 1)$ elements $(n+p=m)$

$$\mathbf{X}=\begin{Bmatrix}\mathbf{X}_u\\ \mathbf{X}_k\end{Bmatrix}\begin{matrix}n\\ p\end{matrix} \tag{3.12}$$

described by a joint normal probability density $f(\mathbf{X})$

$$f(\mathbf{X})=(\det\mathbf{K})^{-\frac{1}{2}}(2\pi)^{-\frac{m}{2}}\exp\left(-\frac{1}{2}(\mathbf{X}-\bar{\mathbf{X}})^T\mathbf{K}^{-1}(\mathbf{X}-\bar{\mathbf{X}})\right). \tag{3.13}$$

where the covariance matrix $\mathbf{K}(m\times m)$ and the expected values vector $\bar{\mathbf{X}}(m\times 1)$ are also appropriately divided:

$$\mathbf{K}=\begin{bmatrix}\mathbf{K}_{11} & \mathbf{K}_{12}\\ \mathbf{K}_{21} & \mathbf{K}_{22}\\ n & p\end{bmatrix}\begin{matrix}n\\ p\end{matrix},\qquad \bar{\mathbf{X}}=\begin{Bmatrix}\bar{\mathbf{X}}_u\\ \bar{\mathbf{X}}_k\end{Bmatrix}\begin{matrix}n\\ p\end{matrix} \tag{3.14}$$

The unknown vector $\mathbf{X}_u$ can be estimated from the following conditional distribution

$$f(\mathbf{X}_u/\mathbf{X}_k)=\frac{f(\mathbf{X})}{f(\mathbf{X}_k)} \tag{3.15}$$

where $f(\mathbf{X}_k)$ is a normal probability density function of the known variables $\mathbf{X}_k$

$$f(\mathbf{X}_k)=(\det\mathbf{K}_{22})^{-\frac{1}{2}}(2\pi)^{-\frac{p}{2}}\exp\left(-\frac{1}{2}(\mathbf{X}_k-\bar{\mathbf{X}}_k)^T\mathbf{K}_{22}^{-1}(\mathbf{X}_k-\bar{\mathbf{X}}_k)\right) \tag{3.16}$$

Substituting (3.13) and (3.16) into formula (3.15) yields

$$\begin{aligned}f(\mathbf{X}_u/\mathbf{X}_k)=&\left(\frac{\det\mathbf{K}}{\det\mathbf{K}_{22}}\right)^{-\frac{1}{2}}(2\pi)^{-\frac{n}{2}}\\ &\cdot\exp\left(-\frac{1}{2}\left(\begin{Bmatrix}\mathbf{X}_u\\ \mathbf{X}_k\end{Bmatrix}-\begin{Bmatrix}\bar{\mathbf{X}}_u\\ \bar{\mathbf{X}}_k\end{Bmatrix}\right)^T\left(\begin{bmatrix}\mathbf{K}_{11} & \mathbf{K}_{12}\\ \mathbf{K}_{21} & \mathbf{K}_{22}\end{bmatrix}^{-1}-\begin{bmatrix}\mathbf{0} & \mathbf{0}\\ \mathbf{0} & \mathbf{K}_{22}\end{bmatrix}^{-1}\right)\left(\begin{Bmatrix}\mathbf{X}_u\\ \mathbf{X}_k\end{Bmatrix}-\begin{Bmatrix}\bar{\mathbf{X}}_u\\ \bar{\mathbf{X}}_k\end{Bmatrix}\right)\right)\end{aligned} \tag{3.17}$$

where **0** is a null matrix.

After simplification (see Jankowski and Walukiewicz 1997) formula (3.17) can be rewritten in the following way

$$f(\mathbf{X}_u/\mathbf{X}_k)=(\det\mathbf{K}_c)^{-\frac{1}{2}}(2\pi)^{-\frac{m}{2}}\times\exp\left(-\frac{1}{2}(\mathbf{X}_u-\bar{\mathbf{X}}_c)^{\mathrm{T}}\mathbf{K}_c^{-1}(\mathbf{X}_u-\bar{\mathbf{X}}_c)\right) \tag{3.18}$$

where $\mathbf{K}_c$ and $\bar{\mathbf{X}}_c$, described as conditional covariance matrix and conditional expected value vector, can be calculated as follows:

$$\mathbf{K}_c=\mathbf{K}_{11}-\mathbf{K}_{12}\mathbf{K}_{22}^{-1}\mathbf{K}_{21} \tag{3.19}$$

$$\bar{\mathbf{X}}_c=\bar{\mathbf{X}}_u+\mathbf{K}_{12}\mathbf{K}_{22}^{-1}(\mathbf{X}_k-\bar{\mathbf{X}}_k) \tag{3.20}$$

In the case of engineering applications the random variables are usually bounded by their upper and lower limits. For example, Young's modulus E can be estimated only by nonnegative values ($E \geq 0$), and no geometric discrepancies of any structures should cross a threshold set by relevant engineering codes. To fulfil this requirement a formula describing the Gaussian truncated distribution is introduced (Jankowski and Walukiewicz 1997)

$$f_t(x) = \frac{f(x)}{P} \tag{3.21}$$

where $f(x)$ is a Gaussian density function of one-dimensional random variable X, with standard deviation σ and mean value $\bar{x}$

$$f(x) = \frac{1}{\sigma\sqrt{2\pi}} \exp\left(-\frac{(x-\bar{x})}{2\sigma^2}\right) \tag{3.22}$$

and P is the area of the Gaussian density function described by the truncation parameter s

$$P = \frac{1}{\sigma\sqrt{2\pi}} \int_{\bar{x}-s\sigma}^{\bar{x}-s\sigma} \exp\left(-\frac{(x-\bar{x})}{2\sigma^2}\right) dx \tag{3.23}$$

Putting $z = (x-\bar{x})/\sigma$ into formula (3.23) it is easy to obtain

$$P = 2\mathrm{erf}(s), \tag{3.24}$$

where $\mathrm{erf}(s)$ is the error function

$$\mathrm{erf}(s) = \frac{1}{2\pi} \int_0^s \exp\left(-\frac{x^2}{2}\right) dx, \qquad \mathrm{s} \geq 0 \tag{3.25}$$

A variance of the random variable X of the Gaussian truncated distribution represents the following formula

$$\sigma_t^2 = \int_{\bar{x}-s\sigma}^{\bar{x}-s\sigma} (x-\bar{x})^2 f_t(x)\, dx \tag{3.26}$$

Substituting relations (3.21) and (3.24), and performing the required integration yields (see Jankowski and Walukiewicz 1997)

$$\sigma_t^2 = \sigma^2(1-t) \tag{3.27}$$

where

$$t = \frac{s \cdot \exp(-s^2/2)}{\sqrt{2\pi}\ erf(s)} \tag{3.28}$$

It is easy to notice that the assumption of the truncation parameter $s = 5$, usually used in the engineering applications, determines that $t \approx 0$.

Making use of the above formulas the truncated joint normal conditional distribution can be derived (Jankowski and Walukiewicz 1997)

$$f_t(\mathbf{X}_u/\mathbf{X}_k) = (1-t)^{-\frac{m}{2}} (\det \mathbf{K}_c)^{-\frac{1}{2}} (2\pi)^{-\frac{m}{2}} \exp\left(-\frac{1}{2(1-t)} (\mathbf{X}_u - \bar{\mathbf{X}}_c)^{\mathrm{T}} \mathbf{K}_c^{-1} (\mathbf{X}_u - \bar{\mathbf{X}}_c)\right) \tag{3.29}$$

The numerical analysis of the simulation method based on the conditional distributions (see, for example, Bielewicz et al. 1994b) has proved that the algorithm is efficient for meshes consisting of as many as 500 random values. To improve the numerical capability of the simulation algorithm some modifications are proposed. The changes make it possible to generate a field with a much larger number of random points.

To generate a discrete scalar random field use is made of a base scheme with random values. The scheme is placed at the nodal points of a mesh in such a way that it covers all the nodes i, $1 \le i \le MN$, $MN = M \times N$ (Fig. 3.2).

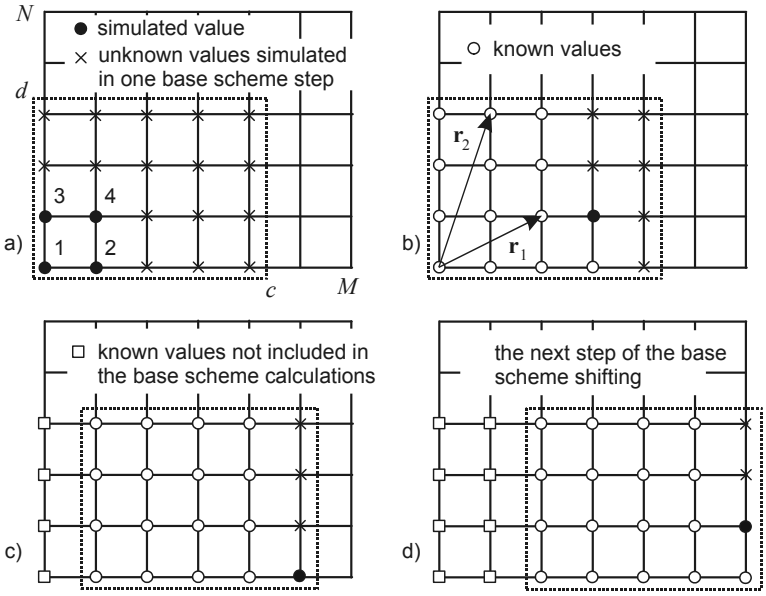

Fig. 3.2. Coverage of the field points with moving propagation scheme

The simulation process is divided into three stages. First, the four-corner random values are generated (see Fig. 3.2a). Next, a propagation scheme with a growing number of points covers a defined base scheme of the field mesh. In the example shown in Fig. 3.2b the dimension of the base scheme equals $c \times d = 5 \times 5 = 20$ random values (mesh points). In the third stage the base scheme is appropriately shifted, and the next group of unknown random values is simulated (see Fig. 3.2c and d). The base scheme is translated so as to cover all the field nodes.

Values of the random variables at the first four points of the mesh ($i = 1,..., 4$) are generated using the direct rejection method (see Eq. (3.7)). Substituting $p = 0$, and $m = n = 4$ into Eqs. (3.12) and (3.14), the following random vector of unknown variables, its expected values, and the appropriate covariance matrix are obtained:

$$\mathbf{X} = \mathbf{X}_u, \qquad \bar{\mathbf{X}} = \bar{\mathbf{X}}_u, \qquad \mathbf{K} = \mathbf{K}_{11} \tag{3.30}$$

The truncated density function of $\mathbf{X}$ is used in the generation

$$f_t(\mathbf{X}) = (1-t)^{-2} (\det \mathbf{K})^{-\frac{1}{2}} (2\pi)^{-2} \exp\left(-\frac{1}{2(1-t)} (\mathbf{X} - \bar{\mathbf{X}})^T \mathbf{K}^{-1} (\mathbf{X} - \bar{\mathbf{X}}) \right) \tag{3.31}$$

where t is the assumed truncated parameter whose value is assumed according to the generated field properties.

The generation process consists of the following steps (Bielewicz et al. 1987 and 1994b):

1. Generation of random vector $\mathbf{X}_u(4\times1)$ with the components:

$$X_i = a_i + (b_i - a_i)u_i, \quad i = 1,...,4, \tag{3.32}$$

where u_i are the random variables uniformly distributed in the interval [0,1], and $(a_i,\ b_i)$, $i = 1, 2, \ldots, m$ are intervals of the reals.

2. Generation of random variable u from the interval [0,1] and definition of the value

$$f_{\max} = u\Phi, \qquad \Phi = (1-t)^{-2}\left(\det \mathbf{K}\right)^{-1/2}(2\pi)^2 \tag{3.33}$$

where $\mathbf{K}(4\times4)$ is the local covariance matrix and $\mathbf{\Phi}$ bounds the conditional density function.

3. Calculation of the density function $f(\mathbf{X}_u)$

$$f(\mathbf{X}_u) = \Phi \exp\left(-\frac{1}{2(1-t)}J(\mathbf{X}_u)\right) \tag{3.34}$$

where

$$J(\mathbf{X}_u) = (\mathbf{X}_u - \bar{\mathbf{X}}_u)^T \mathbf{K}^{-1}(\mathbf{X}_u - \bar{\mathbf{X}}_u) \tag{3.35}$$

4. Checking the condition

$$f_{\max} \le f(\mathbf{X}_u) \tag{3.36}$$

If this condition holds, vector $\mathbf{X}_u(4\times1)$ is accepted and if not, the calculations are repeated.

For any point of the base mesh "i", $5 \le i \le (c\times d)$, where $(c\times d)$ denotes the dimension of the base scheme (see Fig. 3.2a) the only unknown random value is X_i, whereas other random variables $X_1 \div X_{i-1}$ are known.

In the calculations it is necessary to make the following substitutions in formulas (3.12) and (3.14): $m = i$, $n = 1$, $p = i - 1$. It is easy to notice that the problem is reduced to one-dimensional ($\mathbf{K}_c \equiv K_c$, $\bar{\mathbf{X}}_c \equiv \bar{X}_c$). It makes the generation easier and relatively fast. The calculations include the following operations:

1. Determination of the local covariance matrix $\mathbf{K}(i\times i)$, and determination of the known part of the random vector $\mathbf{X}_k((i-1)\times1)$, as well as the expected values vector $\bar{\mathbf{X}}(i\times1)$, according to formulas (3.12) and (3.14), respectively.
2. Calculation of the conditional variance K_c and the mean $\bar{X}_c$ on the basis of equations (3.19) and (3.20):

$$K_c = K_{11} - \mathbf{K}_{12}\mathbf{K}_{22}^{-1}\mathbf{K}_{21} \tag{3.37}$$

$$\bar{X}_c = \bar{X}_u + \mathbf{K}_{12}\mathbf{K}_{22}^{-1}(\mathbf{X}_k - \bar{\mathbf{X}}_k) \tag{3.38}$$

3. Generation of random variable X_i:

$$X_i = a_i + (b_i - a_i)u_i \tag{3.39}$$

4. Generation of the independent random variable u from interval [0,1] and definition of the value

$$f_{\max} = u\Phi, \qquad \Phi = (1-t)^{-(i-1)/2}\left(2\pi K_c\right)^{-1/2} \tag{3.40}$$

5. Calculation of the density function $f(X_i)$

$$f(X_i) = \Phi \exp\left(-\frac{1}{2(1-t)} J(X_i)\right) \tag{3.41}$$

where

$$J(X_i) = \frac{\left(X_i - \bar{X}_c\right)^2}{K_c} \tag{3.42}$$

6. Checking the condition

$$f_{\max} \le f(X_i) \tag{3.43}$$

If this condition holds, the random value X_i is accepted and if not, the calculation returns to point three.

Intervals (a_i, b_i) are fixed for every node. The assumed standard deviation σ_i at the node *i* is connected with the interval by equation

$$\left(\int_{a_i}^{b_i} (x_i - \bar{x}_i)^2 f(x_i)\, dx_i\right)^{1/2} = \sigma_i \tag{3.44}$$

The proposed method of covering the random field with the defined base schemes makes it possible to analyse the meshes with a large number of points. The maximum dimension of the covariance matrix **K** is defined by the base scheme size. The numerical analysis leads to the conclusion that 400 mesh points are an optimal base dimension. The symmetry of the matrix **K** (see Eq. (3.14)) significantly reduces the calculations.

It should be pointed out that according to the proposed algorithm the single random value is calculated on the assumption that the random values only in the close neighbourhood (the base mesh) are known. The specific way of covering the random field has a significant effect on the accuracy of the calculations. In strongly correlated fields the convergence of the simulation process can lead to considerable discrepancies.

This procedure can be used for simulation of arbitrary planes or three-dimensional random fields. The meshes can also be irregular. The implementation of the method is restricted only to the Gaussian fields.

3.3. Accuracy analysis of simulated random fields

Using the proposed generation procedure, various homogeneous and non-homogeneous Gaussian random fields can be simulated. To examine the correctness of the proposed method the following scalar, zero-mean value correlation functions have been considered in numerical examples:

— White noise field $N(\mathbf{r}, \omega)$

$$K_N(\mathbf{r}_1, \mathbf{r}_2) = \sigma^2 \delta(\mathbf{r}_1 - \mathbf{r}_2) \tag{3.45}$$

— the Wiener field (non-homogeneous) $W(\mathbf{r}, \omega)$

$$K_W(\mathbf{r}_1, \mathbf{r}_2) = \alpha^2 \min(r_{1x}, r_{2x}) \times \min(r_{1y}, r_{2y}) \times \min(r_{1z}, r_{2z}) \tag{3.46}$$

— the Brown field (locally non-deterministic)

$$K_B(\mathbf{r}_1,\mathbf{r}_2)=0.5\beta^2\left(\|\mathbf{r}_1\|+\|\mathbf{r}_2\|-\|\mathbf{r}_1-\mathbf{r}_2\|\right) \tag{3.47}$$

— Homogeneous (Shinozuka) field $S(\mathbf{r},\omega)$ (Shinozuka 1987a).

$$K_S(\mathbf{r}_1,\mathbf{r}_2)=\alpha_0^2\exp\left(-\alpha_1^2\left(r_{1x}-r_{2x}\right)^2-\alpha_2^2\left(r_{1y}-r_{2y}\right)^2-\alpha_3^2\left(r_{1z}-r_{2z}\right)^2\right) \tag{3.48}$$

where $\mathbf{r}\in\Re_+^2$ is the position vector (Fig. 3.2a) and α, β, α_0, α_1, α_2, α_3, ρ are arbitrary positive constants, $\|\cdot\|$ denotes the standard Euclidean norm (distance) and δ stands for the Dirac delta.

All presented functions are spatial but the calculations have been performed only for two-dimension cases. It should be mentioned that the developed computer program can be applied to generate any plane or spatial fields.

Statistical formulas give the estimators of the mean value $\hat{\mathbf{w}}$ and the global covariance matrix $\hat{\mathbf{K}}$ of the generated set of realizations:

$$\begin{aligned}\hat{\mathbf{w}}&=\frac{1}{NR}\sum_{i=1}^{NR}\mathbf{w}_i\\ \hat{\mathbf{K}}&=\frac{1}{NR-1}\sum_{i=1}^{NR}(\mathbf{w}_i-\hat{\mathbf{w}})(\mathbf{w}_i-\hat{\mathbf{w}})^{\mathrm{T}}\end{aligned} \tag{3.49}$$

where $\mathbf{w}_i$ is the random vector and *NR* is the number of realizations in the set.

The following definition of the global error G_{er} allows to compare the estimator of the covariance matrix $\hat{\mathbf{K}}$ with the theoretical one **K:**

$$G_{er}=\frac{\left(\|\mathbf{K}\|-\|\hat{\mathbf{K}}\|\right)}{\left(\|\mathbf{K}\|\right)}\times 100\% \tag{3.50}$$

where $\|\mathbf{K}\|=\sqrt{tr(\mathbf{K}^2)}$ is the Euclidean norm.

The error of variances V_{er} and the local error L_{er} of a single element of covariance matrix can also be used:

$$V_{er}=\sum_{i=1}^{MN}\frac{\left(k_{ii}-\hat{k}_{ii}\right)}{k_{ii}}\times 100\%,\qquad L_{er}=\frac{\max\left(k_{ij}-\hat{k}_{ij}\right)}{\sqrt{k_{ii}k_{jj}}}\times 100\% \tag{3.51}$$

where k_{ij} and $\hat{k}_{ij}$ denote the element of the theoretical covariance matrix and its estimator respectively.

The mesh dimensions of the simulated fields described by Equations (3.45) ÷ (3.48) are the same as the size of the engineering examples calculated in the next sections. In this way the correctness analysis is strictly related to the problems which are solved in the present work. Two different meshes for the generation of the random fields have been selected.

First, a plane square 11×11 mesh (121 nodes) is chosen. In all cases $r_x, r_y \in <1.0, 11.0>$ (Fig. 3.2). The values of the positive constant (see formula (3.45) ÷ (3.48)) are assumed to be: $\alpha=1.0$ (the Wiener field), $\beta=1.0$ (the Brown field), $\alpha_0^2=1.0$, $\alpha_1=\alpha_2=0.25$ (homogeneous field), and the parameter *s* (see the formula (3.28)) equals *s* = 5. For these 11 × 11 meshes the generation processes can be performed using a single base scheme (see Fig. 3.2 a and b).

To check if the errors of the fields generations decrease with the number of calculated realizations the following tests are performed. For each field (3.45) ÷ (3.48) one hundred independent trials ($NT = 100$) are carried out. Ten thousand realizations ($NR = 10\,000$) are generated in a single trial. The expected value of global errors of covariance matrix $E(G_{er})$ (Eq. (3.50)), error of variances $E(V_{er})$, and single element error $E(L_{er})$ (Eqs (3.51)) are calculated every 100th realizations using the following formulas:

$$\begin{aligned} E\left(G_{er}\right) &= \frac{1}{NT}\sum_{i=1}^{NT}\left(G_{er}\right)_i \\ E\left(V_{er}\right) &= \frac{1}{NT}\sum_{i=1}^{NT}\left(V_{er}\right)_i \\ E\left(L_{er}\right) &= \frac{1}{NT}\sum_{i=1}^{NT}\left(L_{er}\right)_i \end{aligned} \tag{3.52}$$

Also the variances of these errors are introduced:

$$\begin{aligned} D^2\left(G_{er}\right) &= \frac{1}{NT-1}\sum_{i=1}^{NT}\left(\left(G_{er}\right)_i - E\left(G_{er}\right)\right)^2 \\ D^2\left(V_{er}\right) &= \frac{1}{NT-1}\sum_{i=1}^{NT}\left(\left(V_{er}\right)_i - E\left(V_{er}\right)\right)^2 \\ D^2\left(L_{er}\right) &= \frac{1}{NT-1}\sum_{i=1}^{NT}\left(\left(L_{er}\right)_i - E\left(L_{er}\right)\right)^2 \end{aligned} \tag{3.53}$$

The results are presented in Fig. 3.3 ÷ Fig. 3.6. The plotted functions of the calculated mean errors and the standard deviations are different in each case of the random fields. The same characteristic features are common, for example:

— all the calculated error functions are visibly decreasing, in the most cases very fast,
— the maximal errors of a single element computation scatter much more in comparison with other estimators,
— the errors of the variance calculation are always smaller than other estimators.

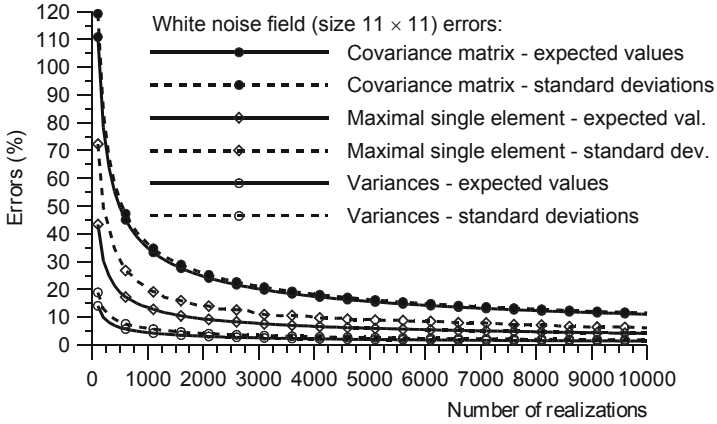

Fig. 3.3. Error analysis of white noise field generations (size 11 × 11)

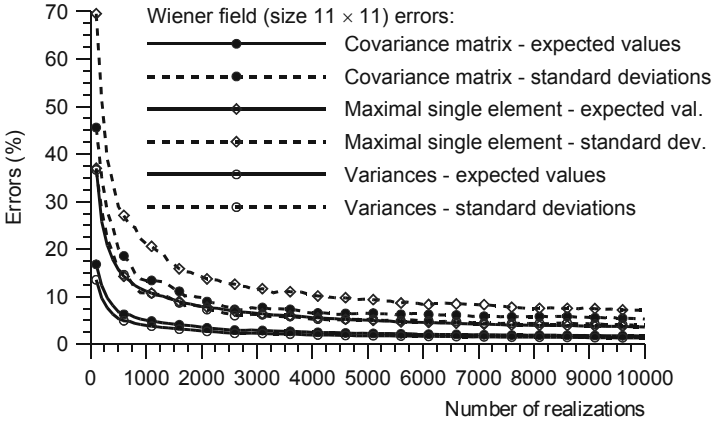

Fig. 3.4. Error analysis of the Wiener field generations (size 11 × 11)

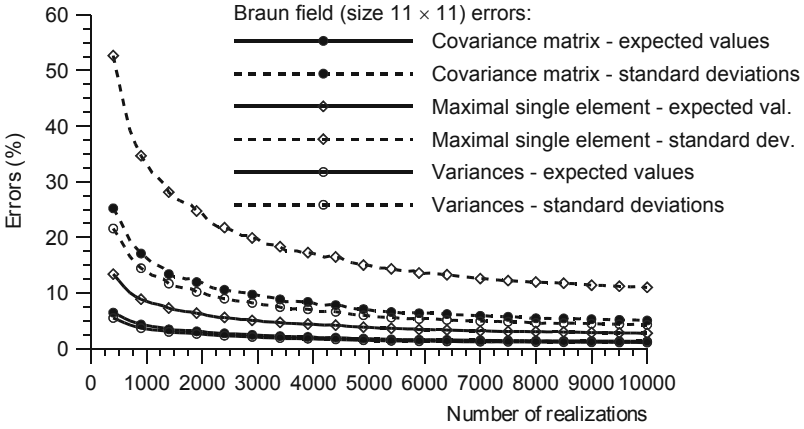

Fig. 3.5. Error analysis of the Braun field generations (size 11 × 11)

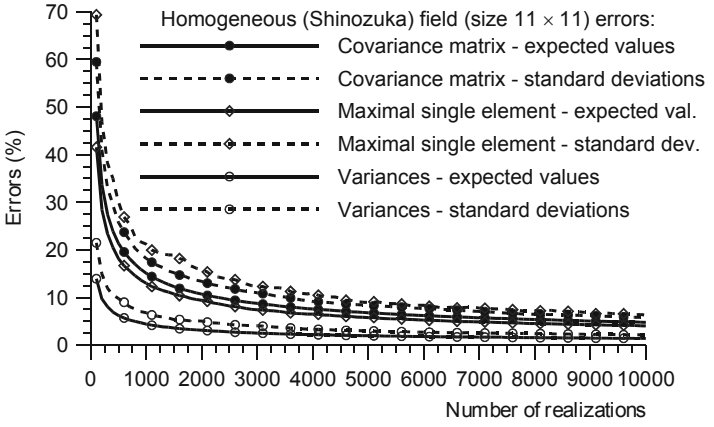

Fig. 3.6. Error analysis of homogeneous field generations (size 11 × 11)

In general it can be asserted that most crucial global errors of the covariance matrix $E(G_{er})$ start to be less than 10% from approximately $2000 \div 3000$ realizations (the white field is an exception). Also, from this number of realizations the errors stabilization is noticeable. For this reason it should be assumed that at least 2000 realizations is needed in order to reproduce the prescribed correlation functions properly. The exact number of simulation should be checked in each case individually.

Additionally, graphical comparisons between the theoretical covariance matrices $\mathbf{K}$ and the estimators $\hat{\mathbf{K}}$ (Eq. (3.49)) for the four random fields (3.45) ÷ (3.48) are created, and the results are presented in Fig. 3.7. In each case the lower triangle represents the generated field while the upper triangle the theoretical one. The figures allow for a visual check of the correctness of the simulated fields. Moreover, one can note that the selected correlation functions (3.45) ÷ (3.48) are very different, and because of that the verifying analysis has a comprehensive meaning.

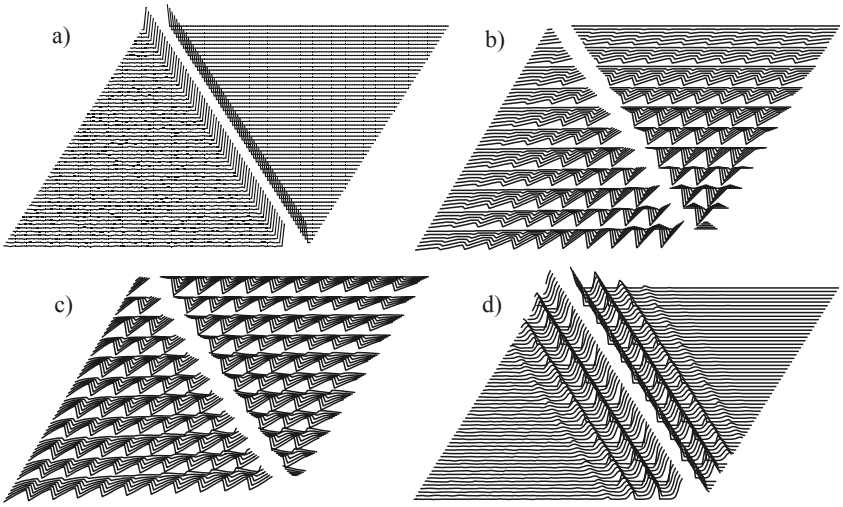

Fig. 3.7. Comparison of the target covariance matrices (upper triangles) with the simulated matrices (lower triangles): a) White noise field, b) the Wiener field, c) the Brown field, d) homogeneous field

Comparing the graphical presentations of the simulated fields (Fig. 3.7) and their errors function (Fig. 3.3 ÷ Fig. 3.6) an additional conclusion can be formulated. For example, the global covariance matrix errors is greater in the case of the white noise field (Fig. 3.3) and the homogeneous field (Fig. 3.6). Analysing the fields graphical presentation in Fig. 3.7a and d, it can be stated that a great part of the theoretical covariance matrix values equal zero. As the matrix element estimators have non-zero values (see Fig. 3.7) the calculated errors are remarkably high.

Some examples of the simulated single realizations are presented in Fig. 3.8. Also the graphical presentation of these realizations allows for specifying the type of the random field analysed. For example, observing the results presented in Fig. 3.7 and Fig. 3.8 one can find out if the field is a correlated one.

Next, a much bigger mesh is analysed. A plane discrete field, $16 \times 308 = 4928$ nodes has been chosen. The same dimension field (but described by different correlation function) is used in Chapter 7 to analyse a petrol tank with initial geometric imperfection. Only one

homogeneous (Shinozuka) correlation function (3.48) has been used in the generation process. This field seems to be an appropriate description of many two- and three-dimensional engineering problems, illustrating geometric imperfections of steel plates and shells or spatial variability of material parameters of soil, for example. The same values of the positive constant are assumed ($\alpha_0^2 = 1.0$, $\alpha_1 = \alpha_2 = 0.25$) as in the previous calculation. The size of the field determines the use of the shifted scheme method of generation (see Fig. 3.2). 16×16 points scheme has been chosen. It is easy to note that to cover all the random field points the scheme must be shifted 308 – 16 = 292 times. Only one series of calculations has been performed and the results are presented in Fig. 3.9.

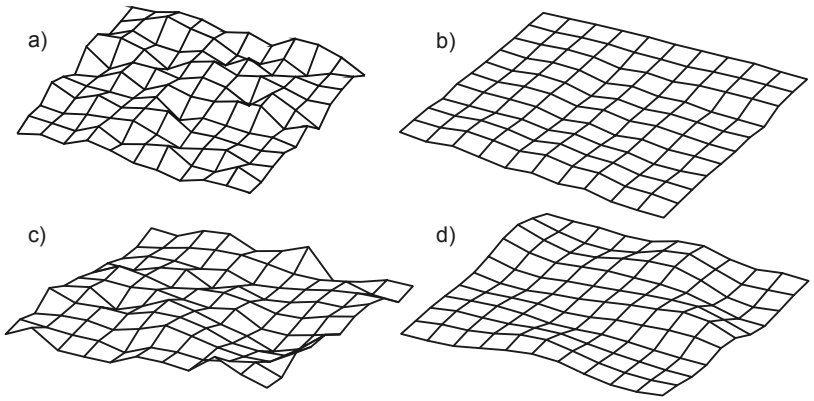

Fig. 3.8. Examples of realizations of the simulated fields: a) White noise, b) the Wiener field, c) the Brown field, d) homogeneous field

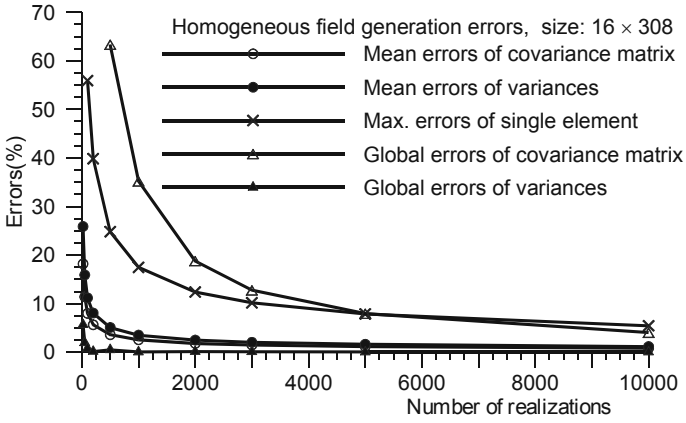

Fig. 3.9. Error analysis of Shinozuka (homogeneous) field generations (size 16×308)

Compared to the previous convergence analysis a standard mean error of covariance matrix and variances has also been calculated (see Fig. 3.9). The obtained global covariance error is bigger in comparison with the 11×11 field generation (Fig. 3.6). Nevertheless, the results proved that the generation of real engineering fields is possible and accurate.

To prove the correctness of the proposed generation method an additional test for the Brown and Wiener fields proposed by Walukiewicz has been performed (see Walukiewicz

et al. 1995). As in the first step of the analysis one hundred independent trials for 11 × 11 fields have been carried out. From the estimation theory (Krishnaiah, 1994) it is known that theoretical distributions of estimators for some characteristics of the multidimensional normal random variables can be derived on the basis of the Wishart (gamma) distribution. In the following the theoretical distributions of variances and covariances (local characteristic), as well as the distributions of the determinants of the covariance matrices (global characteristic) are calculated.

To start with, the probability distribution for the estimator of the covariance matrix $\hat{\mathbf{K}}$ was derived. Since $\hat{\mathbf{K}}$ is a symmetric matrix of dimension ($m \times m$), the following joint probability distribution is defined in space $\Re^{m(m+1)/2}$ (Walukiewicz et al. 1995)

$$f\left(\hat{\mathbf{K}}(NR),\mathbf{K}\right)=C(NR,m)\left(\mathbf{K}\right)^{-\frac{NR}{2}}\left(\hat{\mathbf{K}}\right)^{\frac{NR-m-1}{2}}\times\exp\left(-\frac{NR}{2}\mathrm{tr}\left(\mathbf{K}^{-1}\hat{\mathbf{K}}\right)\right) \tag{3.54}$$

where the constant $C(NR,m)$ is calculated from the normalization condition:

$$C(NR,m)=\left(NR^{-\frac{NR\times m}{2}}2^{\frac{NR\times m}{2}}\pi^{m(m-1)}\prod_{j=1}^{m}\Gamma\left(\frac{NR+1-j}{2}\right)\right)^{-1} \tag{3.55}$$

The condition $NR > m-1$ must be fulfilled for positively defined $\hat{\mathbf{K}}$ (almost surely). Function Γ is defined for positive real arguments or for some natural arguments as:

$$\Gamma(y)=\int_0^\infty x^{y-1}e^{-x}dx \tag{3.56}$$

or

$$\Gamma(NR)=(NR-1)! \tag{3.57}$$

If matrix $\hat{\mathbf{K}}$ is not positively defined then the probability distribution vanishes.

From formula (3.54) one obtains the probability distribution for a single variance estimator $\hat{\sigma}^2$ ($m=1$):

$$f\left(\hat{\sigma}^2\left(NR,\sigma^2\right)\right)=\frac{\left(\sigma^2\right)^{-\frac{NR}{2}}NR^{\frac{NR}{2}}\left(\hat{\sigma}^2\right)^{\frac{NR-2}{2}}}{2^{\frac{NR}{2}}\Gamma\left(\frac{NR}{2}\right)}\times\exp\left(-\frac{NR}{2}\frac{\hat{\sigma}^2}{\sigma^2}\right) \tag{3.58}$$

where σ^2 is the theoretical variance of the simulated field at a point.

The histograms of the variances of the Wiener and the Brown fields are presented in Fig. 3.10 and Fig. 3.11. These results show a very good agreement with the theoretical (Wishart) distribution.

Next, the first two moments of the estimated covariance matrix determinant ($\hat{\mathbf{K}}$) are calculated (Walukiewicz et al. 1995).

$$\begin{aligned}E\left(\ (\hat{\mathbf{K}})\right)&=\frac{1}{NR^m}\left[(NR-1)(NR-2)\ldots(NR-m)\right]\ (\mathbf{K})\\ E\left(\ (\hat{\mathbf{K}})^2\right)&=\left(\prod_{j=1}^{m}\left(1+\frac{1-j}{NR}\right)\left(1+\frac{3-j}{NR}\right)\right)\ (\mathbf{K})^2\end{aligned} \tag{3.59}$$

For the Wiener field and the Braun fields the sampled (100 samples) and the theoretical moments (formulas (3.59)) are calculated, as the functions of the number of realizations. These moments are presented in Fig. 3.12. One can observe a striking agreement of the estimated (generated) moments with the theoretical predictions.

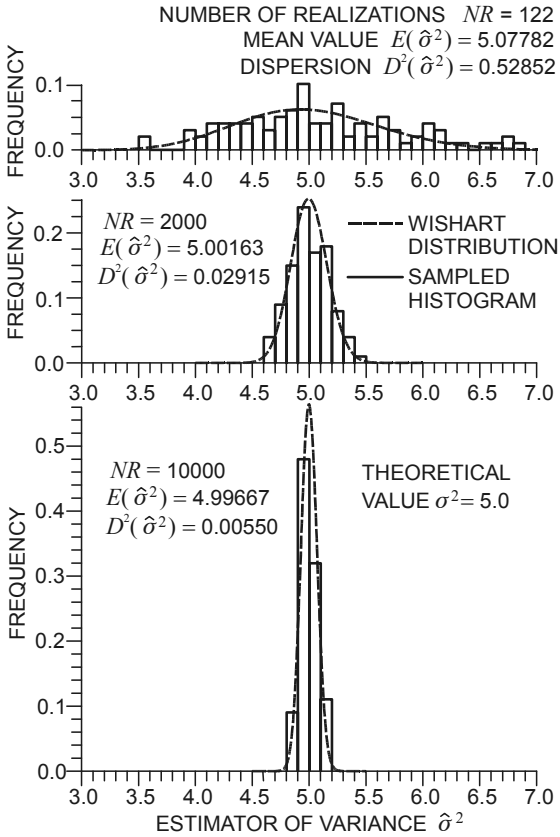

Fig. 3.10. Distribution of the Brown field sampled variances versus the Wishart distribution

Further investigation based on Shannon's measure of information (see, for example, Aczél and Daróczy 1975, Sobczyk 1973, or Sobczyk and Spencer 1996) has been performed by Walukiewicz (1997a and 1997b).

A statistical analysis of the simulated various homogeneous and nonhomogeneous, second-order random fields proved a high accuracy and some universality of the proposed method of simulation. The method will be especially useful in the simulation-based approach.

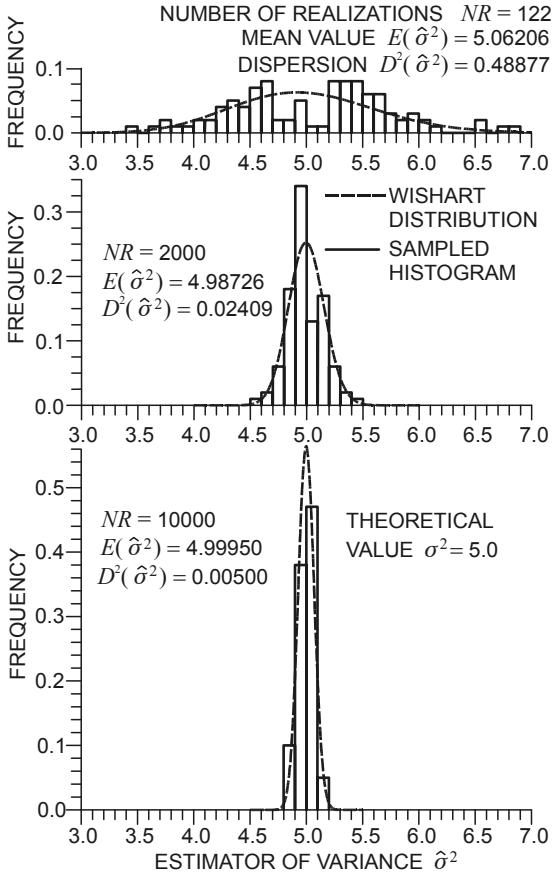

Fig. 3.11. Distribution of the Wiener field sampled variances versus the Wishart distribution

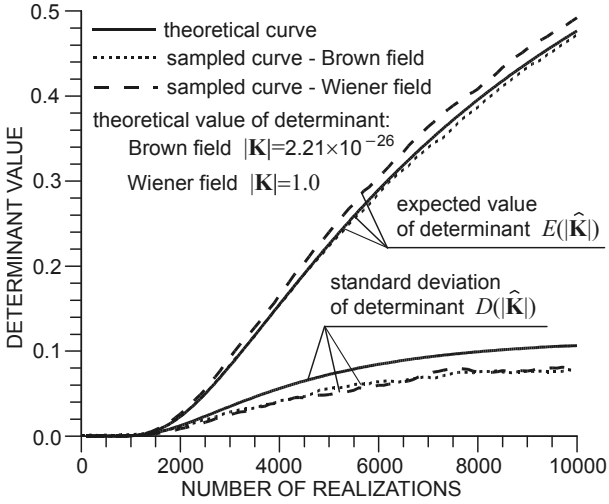

Fig. 3.12. Moments of sampled covariance matrix determinants versus theoretical moments

Chapter 4

SIMPLE RANDOM NONLINEAR MODELS

This Chapter considers the limit states of spatial nonlinear models with one and two degrees of freedom. The geometric and material imperfections of these models are taken in the form of random variables. The simulation of these random variables (the input data) and various versions of the Monte Carlo method are employed. The output results lead to the assessment of the reliability of the nonlinear models. Some of the results have been presented in Bielewicz and Górski (2002a).

Attention is concentrated on the following problems which are studied using these simple models:

— The direct Monte Carlo calculations are compared with stratified sampling methods. The influence of these calculation procedures on the structure reliability estimations is analysed. Additionally, a sensitivity analysis of the random variables is given.

Two approaches for the reliability assessment of the structure models are tested.

— The first is a standard one. Simulation of random imperfections and the Monte Carlo operation yield a histogram of the limit loads S. Assuming that the probability distribution of the applied load P is known, the structural reliability can be obtained according to the exact formula

$$R = \Pr(S > P) = \int_{-\infty}^{\infty} F_P(s) f_S(s) ds \tag{4.1}$$

where $F_P(s)$ is the cumulative distribution function of load P, and $f_S(s)$ stands for the probability density function of S.

— The second approach is more general. Its aim is a more precise description of the behaviour of a structure random model under random loading. The probability distribution of the limit state of the structure is introduced. Random imperfections of the structure and the applied loads are simultaneously generated at every Monte Carlo step. By making the imperfections constant it is possible to calculate the loading multiplier responsible for the structure failure. The set of all loading multipliers obtained in this way is used to define the histogram of the limit state of the structure. The histogram has a nondimensional form and is a numerical estimation of the probability distribution of the limit state. The area in the histogram above 1.0 determines the reliability, while the area below 1.0 determines the probability of failure. It should be pointed out that this approach can also be implemented also to problems for which the load distribution is not known and the samples are given as a set of values, for example, obtained from experiment.

— The calculation of the limit state of an imperfect nonlinear model of structures is, from the mathematical point of view, a transformation of random input data (imperfections) into random output results (load capacities). A statistical analysis of the output results leads to limit load or limit state histograms. In the transformation procedure the nonlinear operator of the model under consideration plays the most important role. The effects of stable and unstable operators are discussed.

The section is an introduction to a more complicated analysis of two-dimensional random problems.

4.1. Models with one degree of freedom

A model in the form of a rigid bar of length l is examined. The bar is hinged at the bottom and supported at the top by a linear, inclined spring of stiffness k [kN/m] (Fig. 4.1). This model is discussed in the monograph by Thompson and Hunt (1973) as an illustration of the asymmetric bifurcation point. The bar is loaded with a vertical eccentric (el) conservative force P. The angle of initial inclination (φ_0) of the vertical axis is also assumed as the input data. The position of the bar is defined by the angle of rotation φ.

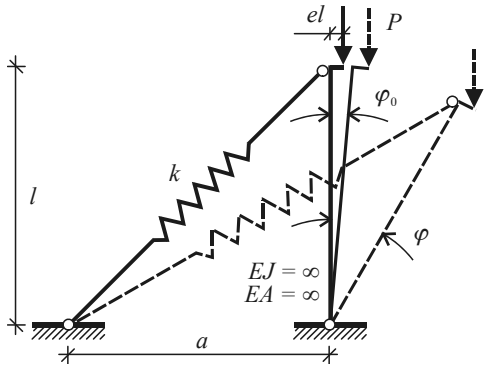

Fig. 4.1. Model of a rigid bar supported by a spring

The model allows for compression of the spring, and because of that it cannot be considered as an engineering example but only as an illustrative one. It should be mentioned that the results – probability distributions of the bar load capacity – are bi-modal functions. Therefore, they are close to the solution of the compressed shallow cylindrical shell (see Section 5). For example Náprstek (1999) tested simple Mises frames modelling strongly nonlinear behaviour of shallow shells with geometrical uncertainties. Consequently, the analysis of this simple model, even if it is only preliminary, enables to understand the stochastic mechanical response of much more complicated structures, for example, two-dimensional ones.

The elongation of the spring Δs (Fig. 4.1) equals

$$\Delta s = l\left\{\sqrt{1+\alpha^2+2\alpha\sin\varphi}-\sqrt{1+\alpha^2+2\alpha\sin\varphi_0}\right\} \tag{4.2}$$

The following equilibrium equation

$$\sum M_A = Pl\left(\sin\varphi + e\cos\varphi\right) - k\cdot\Delta s\cdot r = 0 \tag{4.3}$$

gives the load-angle relationship

$$P(\varphi) = ka\frac{\cos\varphi}{\sin\varphi+e\cos\varphi}\left\{1-\sqrt{\frac{1+\alpha^2+2\alpha\sin\varphi_0}{1+\alpha^2+2\alpha\sin\varphi}}\right\} \tag{4.4}$$

where $\alpha = a/l$.

Now, the energy of the model can be calculated

$$V = \frac{1}{2}k\left(\Delta s\right)^2 - Pl\left(\cos\varphi_0 - \cos\varphi + e\sin\varphi\right) \tag{4.5}$$

which allows for the definition of a curve $s(\varphi)$ separating the stable and unstable regions (the second variation is positively definite)

$$\frac{\partial V^2}{\partial \varphi^2} = 0 \quad \rightarrow \quad s\left(\varphi\right) = \frac{kl}{\cos\varphi - e\sin\varphi}\left\{\alpha^2\cos^2\varphi\frac{\sqrt{1+\alpha^2+2\alpha\sin\varphi_0}}{\left(\sqrt{1+\alpha^2+2\alpha\sin\varphi}\right)^3} + \right. \\ \left. + \alpha\sin\varphi\frac{\sqrt{1+\alpha^2+2\alpha\sin\varphi_0}}{\sqrt{1+\alpha^2+2\alpha\sin\varphi}} - \alpha\sin\varphi\right\} \tag{4.6}$$

Assuming that $\alpha = 1$ and $e = 0$, the admissible range of the force P value, versus the angle φ, and the sign of the initial inclination φ_0 are presented in Fig. 4.2. Analysis of stable and unstable points of bifurcations can be find for example in (Ikeda and Murota 1991).

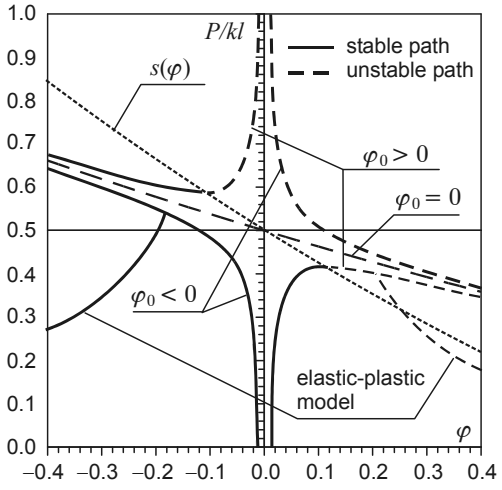

Fig. 4.2. The admissible range of the force P value versus the angle φ and the initial inclination φ_0

Next, the random inelastic model can be defined. It is assumed that the initial inclination φ_0 is a random variable and the spring is ideal elastic-plastic. The second assumption means that

$$-k\Delta s_{\text{ext}} \le k\Delta s \le k\Delta s_{\text{ext}} \tag{4.7}$$

where Δs is the elongation of the spring, and Δs_{ext} denotes the extreme elongation.

In this case the equilibrium paths show a sharp declining at the limit points (Fig. 4.2) as the result of the following equilibrium equation for $\varphi \ge \varphi_y$:

$$P\left(\varphi\right) = kl\left[\sqrt{1+\sin\varphi_y} - \sqrt{1+\sin\varphi_0}\right]\frac{\sqrt{1-\sin\varphi}}{\sin\varphi} \tag{4.8}$$

where φ_y is the angle corresponding to Δs_{ext}.

The spring elongation related to the plastic limit can be calculated from the following formula $\Delta s_{\text{ext}} = l\sqrt{2\varepsilon_y}$, where the yielding strain ε_y is an additional random normal variable (Brinkmann et al. 1990).

It is important to notice (see Fig. 4.2) that the variability of the imperfection parameter φ_0 generates three different types of the limit state of the structure – two types are the results of the bounds for the rotation φ (plastic limits) and one type is defined by the limit point on the post-buckling path for $\varphi_0 > 0$ (elastic range).

If the probability distribution of the initial inclinations φ_0 and/or the plastic limits ε_y are defined, it is possible to obtain the probability distribution of the critical load N_{cr}. And if the probability distribution of a real load *P* is given and *P* is stochastically independent of the critical load N_{cr}, then the reliability of the structure can be estimated.

The nonlinearity of the problem creates some difficulties when analytical formulas are used. A computer simulation based on the Monte Carlo methods brings, in this case, real advantages. A special computer code has been prepared to analyse the random problem comprehensively.

4.1.1. Direct Monte Carlo analysis

First, the direct Monte Carlo method is applied. To describe the bar model two independent random variables are taken into account: the initial inclination of the vertical axis φ_0, and the yield strain ε_y of the guy. They are described by the two independent normal random variables:

$$\begin{aligned} m_{\varphi_0} &= 0.00, \quad D_{\varphi_0} = 0.0116 \\ m_{\varepsilon_y} &= 0.09, \quad D_{\varepsilon_y} = 0.0059 \end{aligned} \tag{4.9}$$

where $m_{(\cdot)}$ describes the expected value, and $D_{(\cdot)}$ the standard deviation of the random variable $(\cdot)$.

One hundred of these random variables are generated. On the basis of $100 \times 100 = 10\,000$ pairs of the random values a histogram of the critical load N_{cr} is derived (Fig. 4.3). It can be noticed that it differs from the normal distribution. The histogram shape and its estimators characterize the mechanical behaviour of the bar model. For example, similar bi-modal distributions have been obtained in the case of compressed cylindrical shells (see Section 5) or concrete bending beams with medium level of reinforcement (see Henriques et al. 2002).

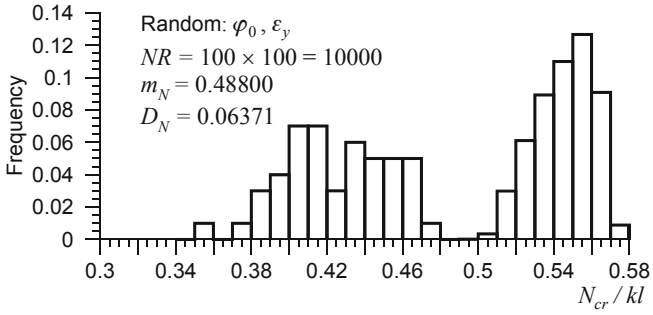

Fig. 4.3. Direct Monte Carlo – histogram of the critical load – $100 \times 100 = 10000$ samples

To estimate the model reliability one hundred random variables of the load P are additionally generated. The probability distribution of the load P is also assumed as normal distribution

$$m_P / kl = 0.36, \quad D_P / kl = 0.0289 \tag{4.10}$$

In this way, the reliability is calculated using $NR = 100 \times 100 \times 100 = 1\,000\,000$ samples. At first, the probability of failure is estimated (see Chapter 2.5)

$$p_f = \frac{n\left(P_i > N_{cr}^i\right)}{NR} = \frac{25400}{1000000} = 0.0254 \tag{4.11}$$

where $n(P_i > N_{cr}^i)$ is the number of forces P_i for which $P_i > N_{cr}^i$, N_{cr}^i is the critical load calculated according to the generated initial imperfection φ_0 and ε_y, and NR stands for the number of realizations (samples).

The reliability can be calculated according to the following formula

$$R = \Pr\left(N_{cr} > P\right) = 1.0 - p_f = 1 - 0.0254 = 0.9746 \tag{4.12}$$

It is also possible to create a histogram of the model limit state. To this end, at every Monte Carlo step i $(i = 1, 2, \ldots, NR)$ the following multiplier is calculated

$$\alpha_i = \frac{N_{cr}^i}{P_i} \tag{4.13}$$

A set of all multipliers obtained in this way defines the limit state histogram presented in Fig. 4.4. One of the characteristics of these histograms is reliability. It is easy to see that the area described by $\alpha_i < 1.0$ (the dashed domain in Fig. 4.4) estimates the probability of failure p_f (4.11). The obtained histogram describes the random mechanical response of the bar.

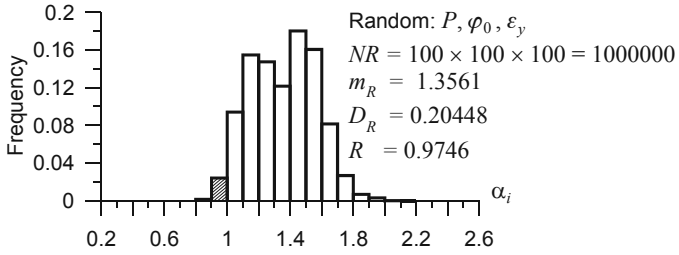

Fig. 4.4. Direct Monte Carlo – limit state histogram
$100 \times 100 \times 100 = 1\,000\,000$ samples

The direct Monte Carlo method, however very precise and easy in application to any linear or nonlinear problems, is inefficient and the calculations are time consuming. Alternative tools are usually used.

4.1.2. Stratified sampling method

According to the stratified sampling method (see Chapter 2.2) the analysis is performed taking advantages of selected random variables. The method is examined using the bar model (Fig. 4.1)

To begin with, 1000 random variables of the bar inclination φ_0, the yield strain of the guy ε_y and the load P are separately generated according to the formulas (4.9) and (4.10). Next, the obtained three random sets are divided into 100 equal subsets. In each subset the value close to its middle is chosen as a representative. Only the representative random variables are taken into consideration. In this way the problem reduces to $NR = N_{S\varphi} \times N_{S\varepsilon} \times N_{SP} = 100 \times 100 \times 100 = 1000000$ samples, where $N_{S\varphi}, N_{S\varepsilon}$, and N_{SP} are the numbers of subsets of φ_0, ε_y and P respectively. It should be noticed that in the numerical experimentation there is no need to randomize the order in which the experiments are done, because the results in this case is not affected by previous analysis. The numbers of samples in the direct and stratified methods are equal (1000000) but obtained in different ways. It should be pointed out that in the case of the stratified method some of the random subsets are empty, and in the example under consideration only 622288 values have to be analysed (the number was evaluated by the computer program).

In consequence, the probability of the single random variables is different in the direct and stratified methods. The samples of the first one have the prescribed equal probability $(p_i = 1/NR)$, while in the case of the stratified method it can be calculated in compliance with the following formula

$$p_i = \frac{N_{SP}^i \times N_{S\varepsilon}^i \times N_{S\varphi_0}^i}{NR} \tag{4.14}$$

where $N_{S\varphi_0}^i$, $N_{S\varepsilon}^i$, N_{SP}^i are the numbers of random variables of φ_0, ε_y and P belonging to the subset i.

In Fig. 4.5 the histogram of the critical load calculated with the help of the representatives of the generated φ_0, and ε_y values is presented. The estimators (the mean value m_N and the standard deviation D_N) are close to those obtained by the use of the direct Monte Carlo analysis (Fig. 4.5).

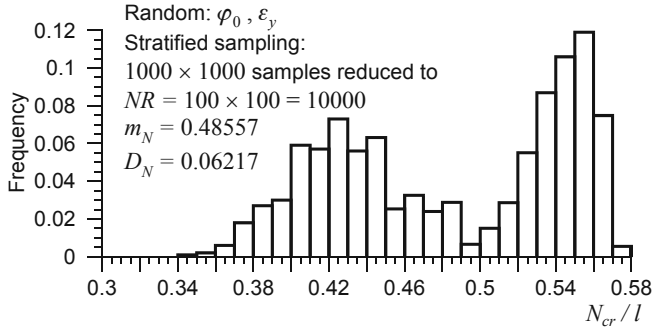

Fig. 4.5. Stratified Monte Carlo – histogram of the critical load – 1000 × 1000 samples reduced 100 × 100 = 10 000 samples

Then, the histogram of the model limit state is calculated using the definition of the α_i multipliers (see Eq. (4.13)). The histogram is presented in Fig. 4.6. The reliability obtained in this way

$$R = \Pr\left(N_{cr} > P\right) = 0.9747 \tag{4.15}$$

is identical to the value calculated by the application of the direct Monte Carlo method (4.12).

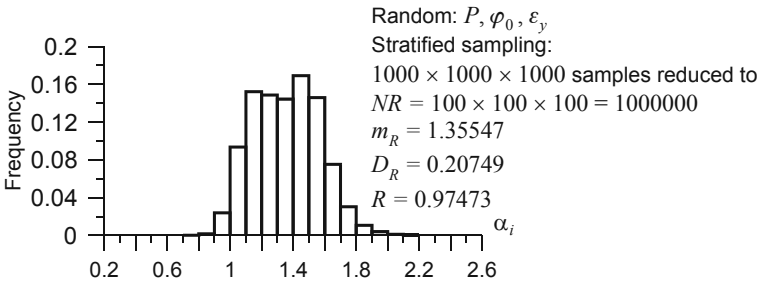

Fig. 4.6. Stratified Monte Carlo – limit state histogram
1000 × 1000 × 1000 samples reduced 100 × 100 × 100 = 1 000 000 samples

It is important to check how many reduced realizations should be considered without losing the accuracy of the reliability calculations. In Table 4.1 the results of the analysis for various numbers of subsets are presented. In each case the basic random set of 1000 variables was used to be next reduced to an appropriate magnitude. Additionally, a graphical presentation of the convergence calculations (Table 4.1) is given in Fig. 4.7.

Table 4.1

Stratified sampling method – accuracy analysis of the bar model reliability calculations

LS No. of subsets	NR number of realizations	Real number of realizations	m_N mean value of N_{cr}	D_N standard deviation of N_{cr}	m_R mean value of R	D_R standard deviation of R	R reliability
5	125	125	0.499838	0.068545	1.399988	0.224888	1.000000
6	216	216	0.472307	0.052851	1.320864	0.185134	0.972776
7	344	343	0.490629	0.066655	1.370597	0.219723	0.966254
8	512	512	0.475268	0.054465	1.328134	0.190319	0.971146
9	729	729	0.486959	0.064452	1.360627	0.214066	0.964001
10	1000	1000	0.476842	0.055169	1.331597	0.190811	0.974031
11	1331	1331	0.485703	0.062873	1.357137	0.209994	0.975572
12	1728	1728	0.496345	0.067657	1.385294	0.222137	0.978323
13	2197	2197	0.483720	0.061947	1.350190	0.206767	0.973149
14	2744	2744	0.493334	0.066477	1.377255	0.218929	0.974560
15	3375	3375	0.483020	0.060849	1.348333	0.204174	0.973800
17	4913	4624	0.482927	0.060980	1.348520	0.204761	0.973403
20	8000	7600	0.487248	0.063783	1.360456	0.211654	0.973754
30	27000	23490	0.483983	0.061080	1.351204	0.204921	0.973179
40	64000	53040	0.487604	0.063554	1.361301	0.211125	0.974097
50	125000	96922	0.485359	0.062217	1.355067	0.207577	0.974329
60	216000	159201	0.487623	0.063630	1.361208	0.211169	0.974510
70	343000	248235	0.486281	0.062694	1.357377	0.208725	0.974542
80	512000	340992	0.485294	0.061948	1.354776	0.206916	0.974511
90	729000	489048	0.485567	0.062171	1.355473	0.207487	0.974828
100	1000000	622288	0.485567	0.062171	1.355473	0.207487	0.974731

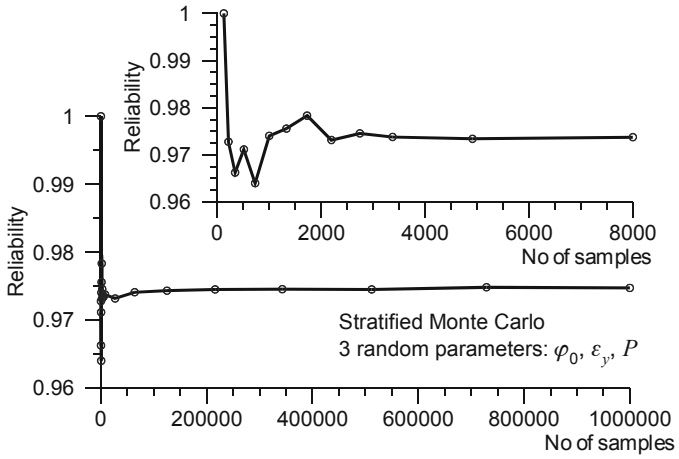

Fig. 4.7. Stratified Monte Carlo – analysis of reliability calculation convergence

Analysing the results one can conclude that at least 2000 samples should be applied to make the stratified Monte Carlo calculations. It means that the minimal number of reduced realizations when the reliability of the model is estimated is $NR = N_{S\varphi} \times N_{S\varepsilon} \times N_{SP} = 13 \times 13 \times 13 = 2197$.

The critical load and the reliability histograms obtained for this number of samples are presented in Fig. 4.8 and Fig. 4.9 respectively. There is an evident discrepancy between the critical load distribution obtained on the basis of 13×13 and 100×100 samples (compare Fig. 4.8 and Fig. 4.5). However, it is worthy of mention that the respective estimators of these histograms are close. The limit state distributions and their estimators in both cases are almost identical (compare Fig. 4.9 and Fig. 4.6).

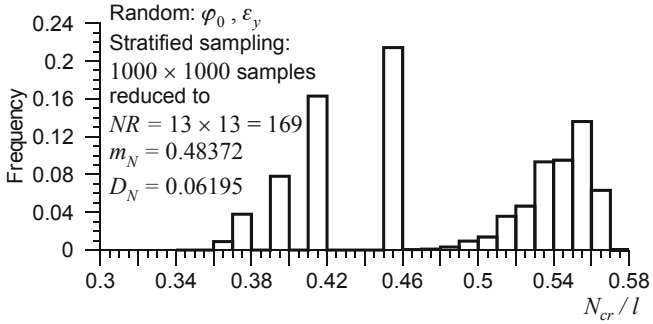

Fig. 4.8. Stratified Monte Carlo – histogram of the critical load – 1000 × 1000 samples reduced 13 × 13 = 169 samples

4.1.3. Level-3 reliability method

The stratified sampling method requires that all random variables have to be considered in the reliability calculations. In the case of the rigid bar model (Fig. 4.1) the realization number $NR = N_{S\varphi} \times N_{S\varepsilon} \times N_{SP}$. According to the level-3 reliability method only $NR = N_{S\varphi} \times N_{S\varepsilon}$ realizations should be taken into consideration. The critical load N_{cr}^i is

calculated for each random pair φ_0 and ε_y. This part of the calculation is similar to the stratified sampling method (see Chapter 4.1.2). An example of such a histogram calculated for $N_{S\varphi} \times N_{S\varepsilon} = 300$ is presented in Fig. 4.10a.

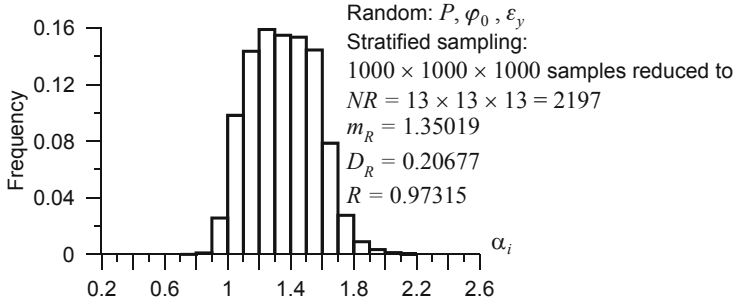

Fig. 4.9. Stratified Monte Carlo – limit state histogram
1000 × 1000 × 1000 samples reduced 13 × 13 × 13 = 2197 samples

The second part – the reliability calculation – differs from the direct or stratified Monte Carlo method. As in this case the formula (4.1) is applied, it is necessary to know not only the probability density function of the critical load but also the cumulative distribution function of the load F_P must be known. This is presented in Fig. 4.10a and b. The calculations according to the formula (4.1) are not performed on the basis of the presented distributions (Fig. 4.10) but by the computer program. The calculated reliability $R = 0.97508$ is close to the values obtained with the help of the direct and stratified methods.

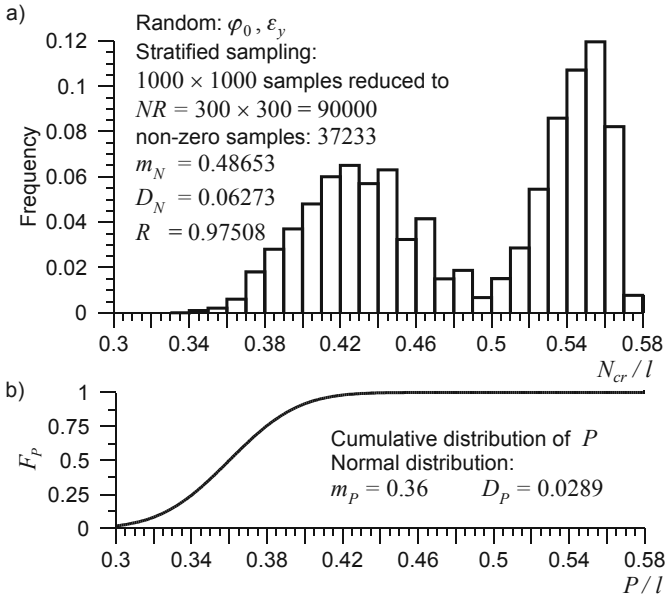

Fig. 4.10. Histogram of the critical load: 1000 × 1000 samples reduced 300 × 300 = 9000 samples (a), and the probability distribution of the compressive load (b)

To analyse the convergence of the applied reliability estimations a series of calculations has been performed (see Table 4.2). The same results are presented in Fig. 4.11.

Table 4.2

Level-3 method – accuracy analysis of the bar model reliability calculations

LS No. of subsets	NR No. of realizations	Real number of realizations	m_N mean value of N_{cr}	D_N standard deviation of N_{cr}	R reliability
5	25	25	0.499837	0.068545	0.980350
6	36	36	0.472308	0.052852	0.976341
8	64	64	0.475269	0.054465	0.973682
10	100	100	0.476842	0.055169	0.973103
12	144	144	0.496345	0.067658	0.975010
15	225	225	0.483021	0.060849	0.974926
20	400	380	0.487248	0.063783	0.974161
30	900	783	0.483983	0.061081	0.975039
40	1600	1326	0.487605	0.063554	0.974831
50	2500	1935	0.485360	0.062217	0.974999
60	3600	2646	0.487624	0.063631	0.974854
70	4900	3534	0.486282	0.062694	0.975192
100	10000	6460	0.485568	0.062172	0.975082
200	40000	19992	0.485663	0.062206	0.975115
300	90000	37233	0.486349	0.062728	0.975079

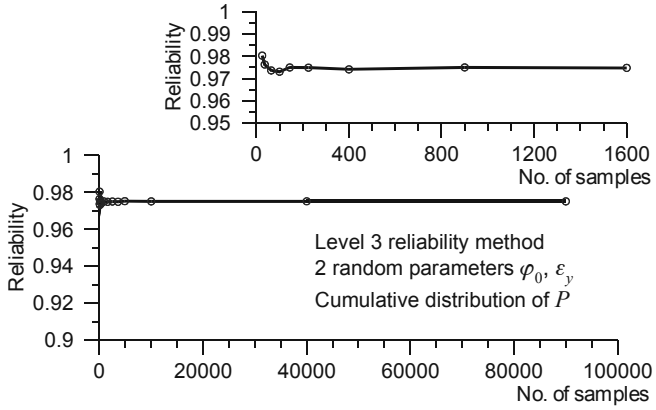

Fig. 4.11. Level-3 reliability method – analysis of the calculation convergence

The outcomes proved that the level-3 method indicates very fast convergence compared to the stratified Monte Carlo calculations (see Fig. 4.7 and Fig. 4.11). The minimal number of realizations can be estimated at 150, while in the case of stratified sampling at over 2000. It should be stressed that the results obtained by the level-3 method are only an approximation and the reliability values calculated according to these two methods vary only slightly (compare Table 4.1 and Table 4.2).

The level-3 method can also be combined with the direct Monte Carlo calculation technique. The convergence analysis is presented in Fig. 4.13. One can notice that the outcomes are also stable when at least 2000 are used in the calculations.

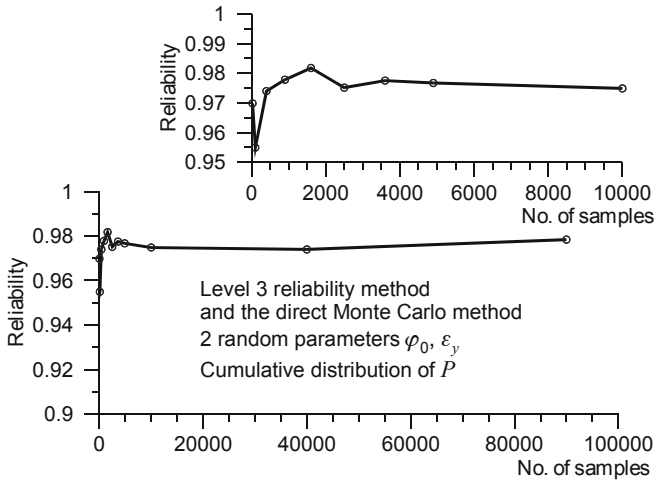

Fig. 4.12. Level-3 reliability method combined with the direct Monte Carlo – analysis of the calculation convergence

It is interesting to compare the results with the appropriate formula according to the level-2 method. This method takes into account only the first two moments of the probability distributions of P and N_{cr}. The structure reliability index β (Murzewski 1989, Thoft-Christensen and Murotsu 1986) is calculated on the assumption that the load and the resistance variables have the probability distribution close to normal

$$\beta = \frac{m_N - m_P}{\sqrt{D_N^2 + D_P^2}} = \frac{0.48653 - 0.36}{\sqrt{0.06273^2 + 0.0289^2}} = 1.8320 \tag{4.16}$$

where m_N, D_N, m_P, D_P are the expected values and the standard deviations of N_{cr} and P, respectively. Then

$$R^{(2)} = \operatorname{erf}(\beta) + 0.5 = 0.9329 + 0.5 = 0.9829 \tag{4.17}$$

where

$$\operatorname{erf}(\beta) = \frac{1}{\sqrt{2\pi}} \int_0^{\beta} e^{-\frac{t^2}{2}} dt \tag{4.18}$$

The results (4.17) are too optimistic against the reliabilities calculated according to the level-3 and the stratified Monte Carlo methods.

4.1.4. Random variable sensitivity analysis

In this Section sensitivity of all random variables affecting the reliability calculations of the bar model (Fig. 4.1) is considered. The proposed analysis is based on specific reliability calculations aided by the limit state histogram. Three random parameters are

analysed: the inclination φ_0, the strain ε_y, and the load P. Selecting one of this random value and making it constant a multiplier responsible for the structure failure is calculated. A set of all multipliers obtained in this way defines the limit state histogram of the structure. The histogram estimators and its shape make it possible to assess the sensitivity of the selected random variable.

First the sensitivity of the random load P obtained in the previous sections (see Fig. 4.6 or Fig. 4.9) is studied and calculated once more using an alternative method. The histogram of the critical load is estimated by the direct Monte Carlo method. 300 random variables of the initial inclination φ_0 and the yield strain ε_y are generated. Thus, the number of realizations $NR = 300 \times 300 = 90\,000$. The histogram is presented in Fig. 4.13. The results are close to those obtained according to the stratified method (see Fig. 4.5 and Fig. 4.10)

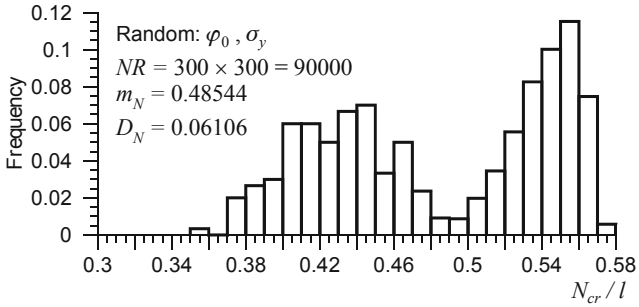

Fig. 4.13. Direct Monte Carlo – histogram of the reliability
300 × 300 = 90000 samples

In each realization, the calculation of the critical load N_{cr}^i is followed by the generation of a random variable of the load P_i. The results allow to determine the multiplier α_i, ($i = 1, 2, \ldots, 90000$) fulfilling the conditions of the formula (4.13). On this basis the limit state histogram (Fig. 4.14) and the structure reliability $R = 0.97701$ can be calculated. As in the case of critical load distribution, the results presented in Fig. 4.14 are close to those obtained with the help of the direct and stratified Monte Carlo methods.

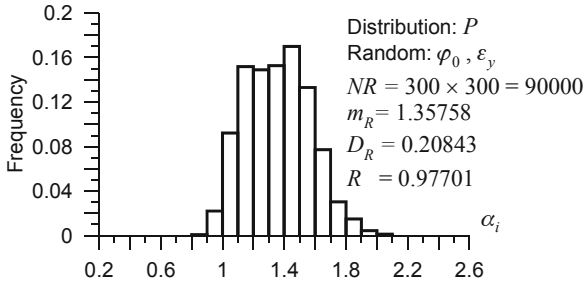

Fig. 4.14. Limit state histogram – sensitivity analysis of random load P

Further, the sensitivity of the initial angle of the bar inclination φ_0 is analysed. For this purpose 300 random variables of the yield strain ε_y and the load P are generated. Making use of the data the critical angle φ_{0cr}^i is calculated. The results enable to obtain the multiplier α_i, ($i = 1, 2, \ldots, 90000$) proceeding in accordance with to the following formula

$$\alpha_i = \frac{\varphi_{0cr}^i}{\varphi_0^i} \tag{4.19}$$

where φ_0^i is the random variable generated together with ε_y and P.

The results are presented in Fig. 4.15. As the dispersion of the limit state histogram is enormous three figures describing the different ranges of the α_i multipliers are outlined. The influence of the P load variability on the structure reliability is much more significant than the effect of the initial angle of the bar inclination φ_0. It is obvious that the calculated reliability is the same as in the previous case (R = 0.97703).

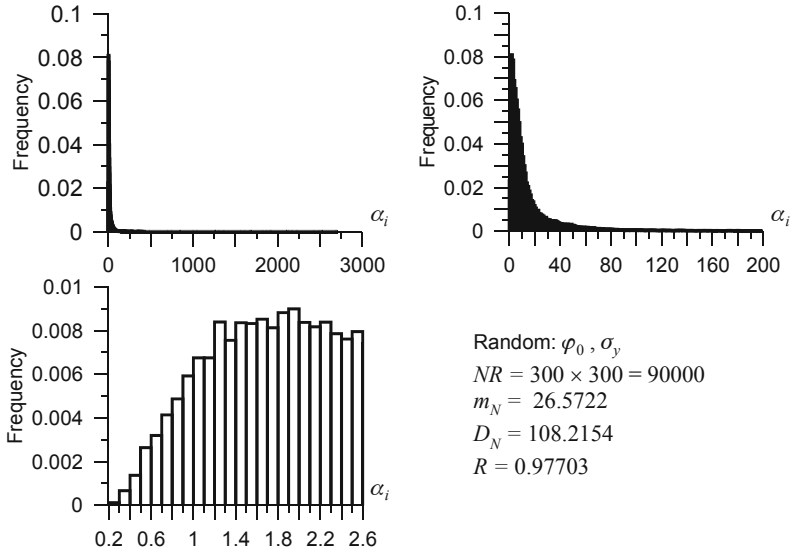

Fig. 4.15. Limit state histogram – sensitivity analysis of random parameter φ_0

The sensitivity analysis of the yield strain ε_y is carried out in a similar way. This time 300 random variables of the initial angle of the bar inclination φ_0 and the load P are generated. After calculating the critical strain ε_{cr}^i and generating the random variable ε_i the multiplier α_i, (i = 1, 2, …, 90 000) is obtained

$$\alpha_i = \frac{\varepsilon_{cr}^i}{\varepsilon^i} \tag{4.20}$$

The limit state histogram – three figures describing the different ranges of the α_i multipliers – is presented in Fig. 4.16. It should be pointed out that the histogram is not complete in the range $\alpha_i \le 0$. The reason is as follows: when the calculated $P_{\max}$ according to the generated φ_0^i is less that the generated value of P_i it is impossible to determine the appropriate value of the critical strain ε_{cr}^i and the multiplier α_i (4.20) does not exist. However, such a case (to not outlined in the limit state histogram) must be included in the reliability calculation as a failure. On this basis the structure reliability, identical to the earlier calculations is obtained (R = 0.97702).

According to the results one can notice that the variability of the yielding strains ε_y does not influence the structure reliability as much as the load P and its effect is similar to the initial inclination φ_0.

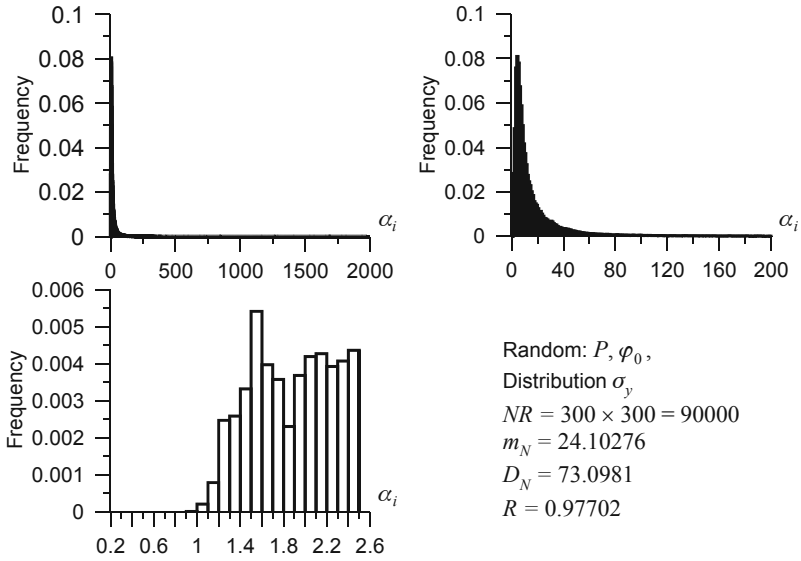

Fig. 4.16. Limit state histogram – sensitivity analysis of random parameter ε_y

The presented analysis shows versatile applications of the limit state histograms. On their basis not only the structure reliability (value) and the reliability feature (histogram) but also the sensitivity of the random parameters with respect to this reliability can be calculated.

4.1.5. Minimal and maximal random variable distributions

Using the simulation-based approach an interval of the structure reliability can be assessed. For this purpose the structure imperfections are described as the minimum and maximum values of a set of *n* random variables. The appropriate cumulative distribution functions for the two cases are as follows:

$$F_{\max}(x) = \left[F(x)\right]^n \tag{4.21}$$

$$F_{\min}(x) = 1 - \left[1 - F(x)\right]^n \tag{4.22}$$

where $F(x)$ describes the assumed cumulative distribution.

It is easy to apply the imperfection sets to the Monte Carlo analysis and to calculate the histograms of limit loads obtained in this manner. Then, using level-3 equation (4.1) two reliability values of the structure can be estimated. These values assess the interval of the structure reliability.

In this case, only the inclination of the bar is assumed as random. The angle φ_0 is described by the minimum and maximum values chosen from a set of three normal variables ($n = 3$) defined by $(4.9)_1$. The yield strain is constant $\varepsilon_y = 0.09$. In a numerical procedure three variables are automatically generated and the maximum and minimum values are selected. 3000 samples have been used to calculate the appropriate histograms of the critical loads (Fig. 4.17b and c). To compare the obtained results also the histogram of the critical load for 3000 samples of φ_0 has been derived (Fig. 4.17a)

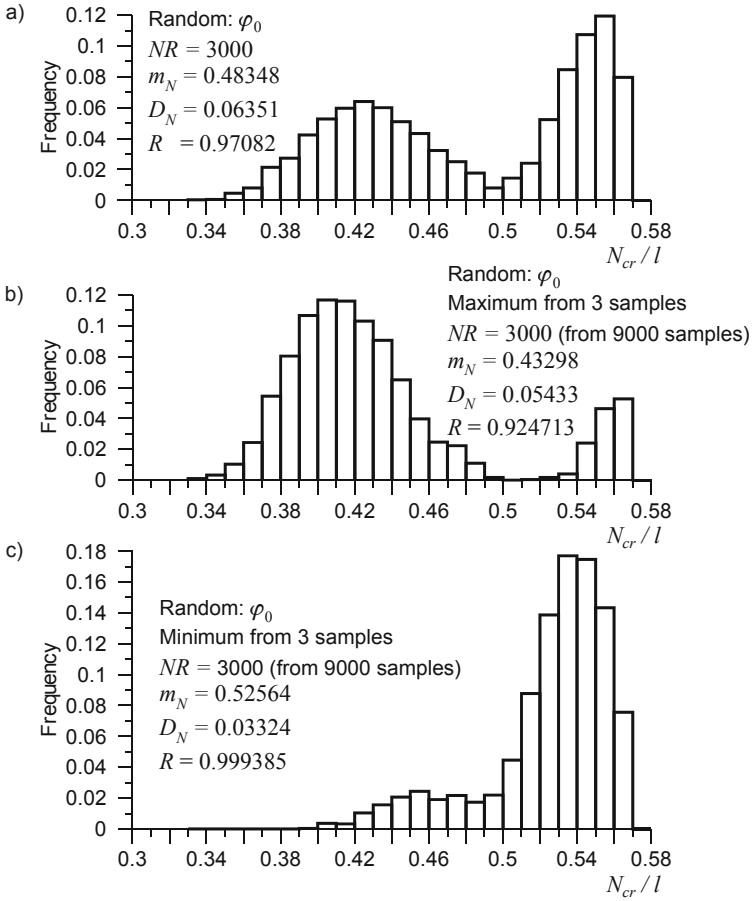

Fig. 4.17. Histogram of the critical load – 300 samples

Making use of these histograms the reliability of the bar model for minimum and maximum sets of random variables can be calculated according to the level-3 method:

$$\begin{aligned} R &= \Pr(N_{cr} > P) = 0.9708 \\ R_{\min} &= \Pr(N_{cr} > P) = 0.9247 \\ R_{\max} &= \Pr(N_{cr} > P) = 0.9994 \end{aligned} \tag{4.23}$$

These values form an estimated interval of the model reliability:

$$R_{\min} \le R \le R_{\max} \tag{4.24}$$

Similar calculations have been performed assuming $n = 2$ in formulas (4.21) and (4.22). The following interval has been obtained

$$0.94778 \le R \le 0.99557 \tag{4.25}$$

The interval is evidently too wide. In the case of real structure analysis, for which a great scattering of results can be observed, the estimation of the reliability interval can be an alternative and promising method.

It should be put forward that all the described techniques have limitations regarding the loading applied to the structure. Proportional loading situations are equivalent to the basic reliability problem (2.30) in which the applied extreme load is the maximum load for the lifetime of the structure. For complex system, usually load-path dependent are implemented. In such cases one possibility is to define the load combinations to be used in a reliability analysis in a manner analogous to that used in conventional structural design and for which only a limited number of combinations of loading is considered (see for example Ditlevsen and Madsen, 1996).

4.2. Models with two degrees of freedom

In this section a spatial nonlinear model of a rigid bar is analysed. Two cases are considered:

1) unstable case – an elastic solution,
2) stable case – an elastic-plastic solution.

To obtain these states appropriate springs supporting the bar are applied.

4.2.1. Case 1: elastic solutions

A model of a rigid bar of length l, hinged at the bottom and supported at the top by two linear springs of stiffness $k1$ and $k2$ (Fig. 4.18) is examined. The bar is loaded with a vertical conservative force P. The position of the bar is defined by the rotation angles φ and ψ, while φ_0 and ψ_0 are the angles of initial inclinations.

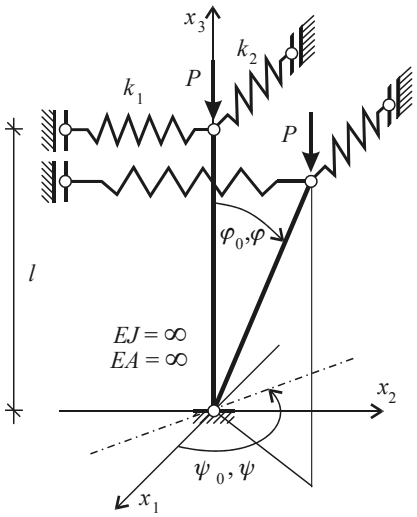

Fig. 4.18. Model of a rigid bar supported by elastic springs – Case 1

The potential energy of the model is

$$V(\varphi,\psi)=\frac{1}{2}k_1u_1^2+\frac{1}{2}k_2u_2^2-Pu_3 \tag{4.26}$$

where

$$u_1(\varphi,\psi) = l\left(\sin\varphi\sin\psi - \sin\varphi_0\sin\psi_0\right)$$
$$u_2(\varphi,\psi) = l\left(-\sin\varphi\cos\psi + \sin\varphi_0\cos\psi_0\right) \tag{4.27}$$
$$u_3(\varphi,\psi) = l\left(\cos\varphi_0 - \cos\varphi\right)$$

From the following elementary equations

$$\frac{\partial V}{\partial\varphi} = 0, \quad \frac{\partial V}{\partial\psi} = 0 \tag{4.28}$$

where

$$\frac{\partial V}{\partial\varphi} = k_1u_1\left(\cos\varphi\sin\psi\right) + k_2u_2\left(-\cos\varphi\cos\psi\right) - P\sin\varphi \tag{4.29}$$

$$\frac{\partial V}{\partial\psi} = k_1u_1\left(\cos\varphi\cos\psi\right) + k_2u_2\left(\sin\varphi\sin\psi\right) \tag{4.30}$$

the equilibrium parameters, angles φ and ψ, and load P related to them can be calculated.

It is easy to notice that the problem can be qualified as an unstable case (Case 1). Thus, the known energy considerations (the second variation of potential energy is positively defined) lead to the conclusion that the stable and unstable regions are separated by the following surface

$$\frac{\partial^2 V}{\partial\varphi^2}\frac{\partial^2 V}{\partial\psi^2} - \left(\frac{\partial^2 V}{\partial\varphi\partial\psi}\right)^2 = 0 \tag{4.31}$$

For example, for the fixed ψ_0 values ($\psi_0 = 5\pi/8$) and the spring stiffness relations $k2 = 0.1\times k1$ and $k2 = 0.9\times k1$, the value of force P versus angle φ is calculated. It should be pointed out that the equilibrium paths represent rather complicated spatial curves. The results presented in Fig. 4.19 are only their plane representations.

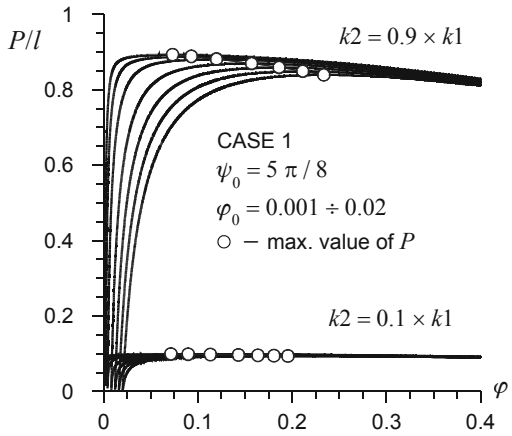

Fig. 4.19. Case 1 – equilibrium paths for the unstable model

The next step in the analysis concerns the random problem.

The inclination angles φ_0 and ψ_0 are assumed to be random variables. The uniform distributions in the following intervals are applied (see Fig. 4.18):

$$\varphi_0 \in \langle 0.0,\ 0.05 \rangle, \qquad \psi_0 = \langle \pi/2,\ \pi \rangle \tag{4.32}$$

When the random inclination variables have been defined it is possible to obtain the probability distribution of the critical load N_{cr}. The nonlinear problem is solved with the help of a computer program.

As many as 2000 initial inclinations of the bar have been simulated. For each random angle pair (φ_0 and ψ_0) the critical value of load N_{cr} is calculated. The critical load probability distribution for identical spring stiffness ($k2 = k1$) is presented in Fig. 4.20. Additionally, the expected values of the critical load m_n and its standard deviations D_n are calculated (Fig. 4.20).

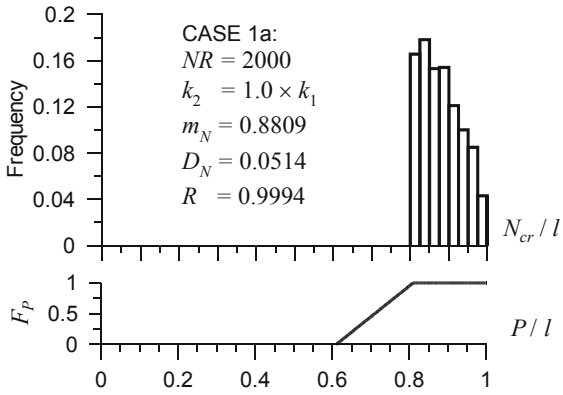

Fig. 4.20. Case 1a – histogram of the critical load N_{cr} and the probability distribution of load P

Assuming that the probability distribution of the applied load P is stochastically independent and uniformly distributed in the interval

$$P \in \langle 0.61, 0.81 \rangle \tag{4.33}$$

the structure reliability R can be calculated. The exact formula of level-3 method is applied (Eq. (4.1))

$$R = \Pr(N_{cr} > P) = 0.9994 \tag{4.34}$$

Next, similar calculations are performed for different values of the spring stiffness: $k2 = 0.95 \times k1$. Appropriate critical load probability distribution is presented in Fig. 4.21.

The reliability for this case is also calculated

$$R = \Pr(N_{cr} > P) = 0.9782 \tag{4.35}$$

In the following an alternative concept describing more precisely the behaviour of the model is proposed. 2000 random values of the independent, uniformly distributed load P are generated together with random imperfections φ_0 and ψ_0.

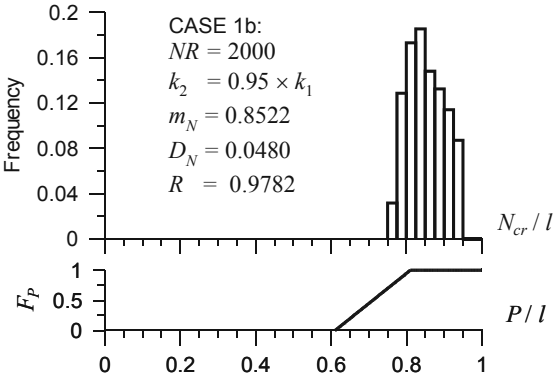

Fig. 4.21. Case 1b – histogram of the critical load N_{cr} and the probability distribution of load P

At every Monte Carlo step i ($i = 1, 2, \ldots, NR$) the multiplier satisfying Eq. (4.13) is calculated. A set of all multipliers obtained in this way defines the histogram of the limit state (see Fig. 4.22 and Fig. 4.23). In these simple cases the obtained reliability values are as follows:

$$\begin{aligned} &\text{Case 1:} \quad R = 0.9995 \\ &\text{Case 2:} \quad R = 0.9790 \end{aligned} \tag{4.36}$$

They are close to those obtained according to formula (4.1) – see Eqs. (4.34) and (4.35).

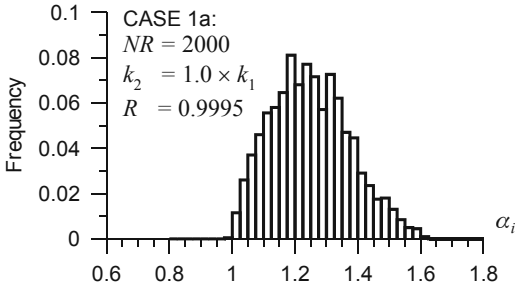

Fig. 4.22. Case 1a – histogram of the limit state

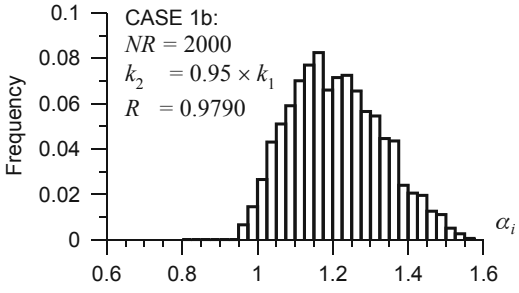

Fig. 4.23. Case 1b – histogram of the limit state

4.2.2. Case 2: elastic – plastic solutions

In this Section a model of a rigid bar supported by two springs of stiffness $k1$ and $k2$ (Fig. 4.24) is analysed. As in the first example the bar is loaded with a vertical conservative force P. The angles of initial inclinations φ_0 and ψ_0 of the vertical axis are assumed to be random, uniformly distributed values according to the formulas (4.32).

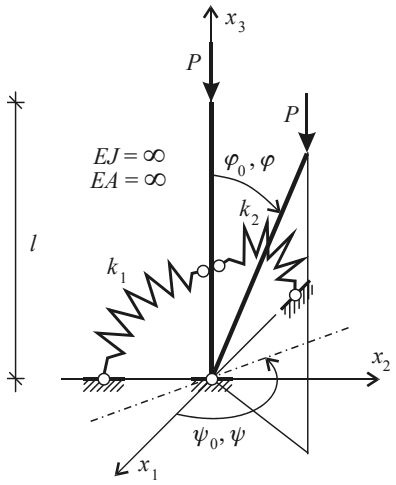

Fig. 4.24. Model of a rigid bar supported by elastic-plastic springs – Case 2

In this case the potential energy of the model is

$$V(\varphi,\psi)=\frac{1}{2}k_1\alpha_1^2+\frac{1}{2}k_2\alpha_2^2-Pu_3 \tag{4.37}$$

where

$$\begin{aligned}
&\sin\alpha_1(\varphi,\psi)=\sin\varphi\sin\psi-\sin\varphi_0\sin\psi_0\\
&\sin\alpha_2(\varphi,\psi)=-\sin\varphi\cos\psi+\sin\varphi_0\cos\psi_0\\
&u_3(\varphi,\psi)=l(\cos\varphi_0-\cos\varphi)
\end{aligned} \tag{4.38}$$

From the following equations:

$$\begin{aligned}
&\frac{\partial V}{\partial\varphi}=k_1\frac{\cos\varphi\sin\psi}{\sqrt{1-(\sin\varphi\sin\psi)^2}}\left[\sin^{-1}(\sin\varphi\sin\psi)-\sin^{-1}(\sin\varphi_0\sin\psi_0)\right]+\\
&+k_1\frac{\cos\varphi\cos\psi}{\sqrt{1-(\sin\varphi\sin\psi)^2}}\left[\sin^{-1}(\sin\varphi\cos\psi)-\sin^{-1}(\sin\varphi_0\cos\psi_0)\right]-Pl\sin\varphi=0
\end{aligned} \tag{4.39}$$

$$\begin{aligned}
&\frac{\partial V}{\partial\psi}=k_1\frac{\sin\varphi\cos\psi}{\sqrt{1-(\sin\varphi\sin\psi)^2}}\left[\sin^{-1}(\sin\varphi\sin\psi)-\sin^{-1}(\sin\varphi_0\sin\psi_0)\right]+\\
&+k_1\frac{-\sin\varphi\sin\psi}{\sqrt{1-(\sin\varphi\sin\psi)^2}}\left[\sin^{-1}(\cos\varphi\cos\psi)-\sin^{-1}(\sin\varphi_0\cos\psi_0)\right]=0
\end{aligned} \tag{4.40}$$

the equilibrium paths can be calculated. Some examples of these solutions are presented in Fig. 4.25.

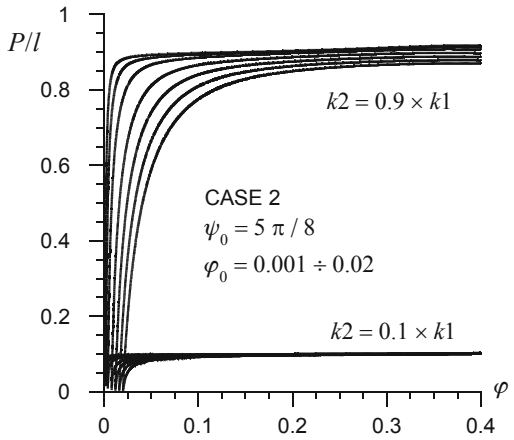

Fig. 4.25. Case 2 – equilibrium paths for the stable model

The second model presents a stable case (Case 2). It is easy to notice that the equilibrium paths do not exhibit any maximal points.

To obtain the histograms of critical load of ideal elastic-plastic springs are considered. The following plastic bound for rotations φ_y is assumed

$$\varphi_y = 0.20 \tag{4.41}$$

On the basis of 2000 simulations the histograms of the critical load N_{cr} are derived (Fig. 4.26 and Fig. 4.27).

The probability distribution of load P is accepted as in Case 1. In Fig. 4.26 and Fig. 4.27 the obtained reliability values are given.

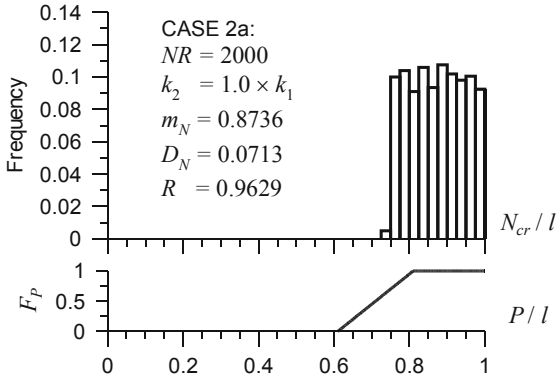

Fig. 4.26. Case 2a – histogram of the critical load N_{cr} and the probability distribution of load P

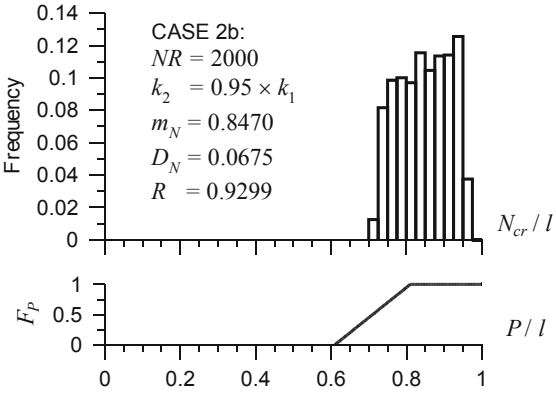

Fig. 4.27. Case 2b – histogram of the critical load N_{cr} and the probability distribution of load P

Alternative versions of the reliability values are also estimated. The multipliers α_i (Eq. 4.28) for $NR = 2000$ generated random values of load P_i are calculated. The results are presented in Fig. 4.28 and Fig. 4.29. In these cases the reliability values compared to those obtained by the level-3 formula show significant differences:

$$\begin{aligned} &\text{Case 1:} \quad R = 0.9645 \\ &\text{Case 2:} \quad R = 0.9340 \end{aligned} \tag{4.42}$$

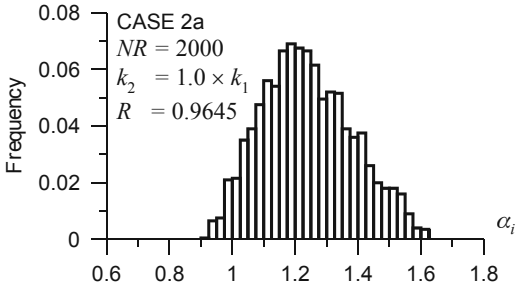

Fig. 4.28. Histogram of the limit state – Case 2a

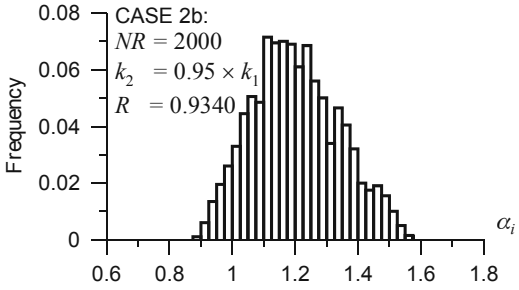

Fig. 4.29. Histogram of the limit state – Case 2b

In the elastic-plastic cases the method of the alternative calculating of the reliability with the help of multipliers describing the relations of simulated load values related to the critical loads can give valuable information on the structure mechanical behaviour.

The Chapter presents the power of the random sampling method when stochastic nonlinear models are taken into consideration. The method can easily be used for analysis of realistic models of masts with elastic-plastic guys randomly exposed for example, to wind action. The results can contribute to engineering design.

On the basis of the results two-dimensional models of structures can successfully be analysed.

Chapter 5

TWO-DIMENSIONAL RANDOM NONLINEAR MODELS

According to the simulation-based approach each realization of the nonlinear two-dimensional model of structure is solved using a finite element program and the incremental operations. These operations in the case of geometrically and/or materially nonlinear problems are time-consuming even for powerful computers. The accuracy of the calculations depends on the number of realizations. Therefore, it is important to know how many samples ought to be simulated in order to obtain satisfactory results.

In general, the problem of accuracy of the simulation-based approach can be solved by:
— an analysis of the input data (the description of the random structure parameters),
— an analysis of the output results (the structure response obtained in a numerical way).

5.1. Reduction methods of the random input data

The input data are usually presented as scalar, two-dimensional random fields of the second order. In numerical examples using the finite element method it is necessary to transform the continuous random fields into a discrete form. As a result, the random field takes the form of a multidimensional random variable and the covariance matrix plays the role of correlation function. The covariance matrix type and its parameters can be assumed according to some engineering knowledge, but their description should be mathematically sound. The establishment of International Data Bank, proposed by Arbocz and Hol (1995) would significantly help these investigations (see also Schenk and Schuëller 2003, and the reference cited there).

When the theoretical form of the imperfection fields has been assumed (for example: Wiener, Brown, homogeneous function or another) the simulation process is applied. Various methods and numerical programs can be used to generate a set of imperfection fields (see Chapter 2 and Chapter 3). The results can be compared with theoretical fields. The well known statistical formulas are the best and adequate for this comparison.

The simulation and the convergence analysis of the description for two-dimensional random fields (see Chapter 3) shows that the number of realizations depends on the quantity of nodes in the discretization mesh and the type of the generated field. Even for small meshes of $100 \div 200$ points a sufficient number of realizations must be of the order 2000. From the point of view of the efficiency of nonlinear numerical calculations such a numerous set of realizations is too big.

It is possible to reduce the number of the input realizations (see, for example, Hurtado and Barbat 1998).

In view of the above the following methods are presented in detail:
— reduction of the generated input realizations to a number of representative realizations with some prescribed probability (the stratified Monte Carlo analysis described in Chapter 2),
— selection of some specific, extreme input realizations from the generated set which are expected to give an extreme mechanical answer to the structure model.

In the second case the outcome of such parametric study of the generated set of input realizations is an evolution of the "worst" imperfection mode of the structure which leads to the lower bound of the critical load of the structure. This information is most significant as far as the structure safety is concerned, for example, shells (Deml and Wunderlich 1997).

The above methods are presented in the next sections. The structure uncertainties are described by degenerated (defined by one random variable. Eq. (3.6)), and two-dimensional random fields.

5.1.1. Direct and stratified Monte Carlo methods

As an illustration, a simply supported, shallow cylindrical shell, presented in Krätzig (1989), is considered (Fig. 5.1). The geometrical and material nonlinearities are taken into account. The shell is composed of an ideal elastic-plastic material. Only a compressive load is applied. The following data are assumed to be the deterministic values: $E = 2.06 \times 10^5$ MPa , $\nu = 0.3$, $\sigma_y = 245$ MPa , $a/R = 0.12$, $t/a = 0.01$ and $N_{\max} = a \times t \times \sigma_y$. Parameters E and ν describe the Young modulus and the Poisson coefficient respectively, and σ_y stands for the material yield stress value.

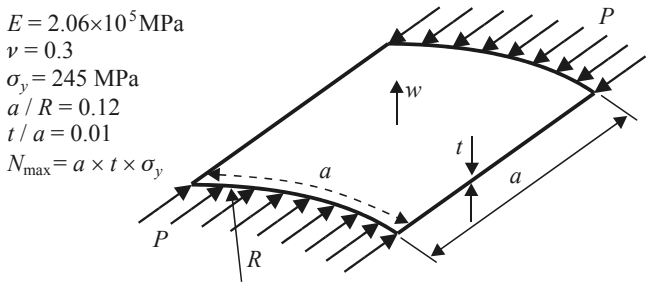

Fig. 5.1. Simply supported axially compressed shallow shell

To begin with, some introductory calculations are performed for ten arbitrarily chosen initial imperfection – displacements of the central point of the shell (see Fig. 5.2). In this way a double-symmetric problem is considered. For every assumed imperfection, the nonlinear calculation of the post-buckling behaviour of the shell is performed using the BOX program (Chróścielewski 1983, and 1996, and Chróścielewski et al. 1987). The results are presented in Fig. 5..

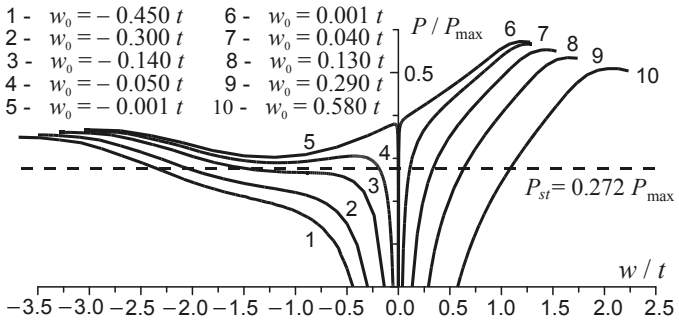

Fig. 5.2. Equilibrium paths of the shell central point – displacement w versus load P

Because of the symmetry of the model only one quarter of the shell is analysed ($12 \times 12 = 144$ finite elements with 24 degrees of freedom). The ideal elastic-plastic material is numerically described by $3 \times 3 = 9$ Gauss integration points in the middle plane of the element, with five points in the thickness direction. A single realization of the geometric imperfections is assumed in the form of transverse displacement in the middle surface of the perfect shell. The operation is performed using the BOX computer program as the forced displacement procedure at finite element nodes. The state of the shell is defined as stress free. Finally, the loading in an incremental steps is applied. A change of the geometry of the shell, and the stresses are controlled by the tangent stiffness matrix $\mathbf{K}_T(\lambda)$, where λ is the load parameter (see Fig. 5.1). The limit load S (Eq. (3.29)) is defined by $\det \mathbf{K}_T(\lambda) = 0$. Observing the equilibrium paths of the point on the middle surface of the shell (Fig. 5.2) the condition $\det \mathbf{K}_T = 0$ can correspond to the three different types of the shell response:

— the displacement w of the shell central point is directed upwards reaching the limit point in the plastic range,
— the displacement of the point is directed downwards reaching the limit point in the elastic range with the snap-through effect,
— the displacement of the point is directed downwards reaching the limit point in the plastic range.

It should be pointed out that a similar mechanical behaviour was noted in the simple rigid bar model analyzed in Chapter 4. For this reason, the conclusion formulated there can support the probabilistic solution of the shallow cylindrical shell problem.

5.1.1.1. Degenerated random fields described by single random variables

First, the geometrical imperfections are assumed in the form of a degenerated random field defined by one random variable at the central point of the shell (double-symmetric problem). The field is described by normal distribution with zero mean value and $0.1666t$ standard deviation. 300 variables with uniform probability (equal to 1/300) are generated. As the direct Monte Carlo method is applied the nonlinear calculations are performed for every simulated imperfection.

The load level $P_{st} = 0.272 P_{\max}$ close to the snap-through effect of the shell is assumed to be critical (Fig. 5.2). In this way the probability of the shell failure is formulated as the probability of the first passage of a given threshold (Bayer and Bucher 1999), i.e. the defined load level. For each imperfection, the displacement w at the central point of the shell corresponding to the load P_{st}, is numerically calculated. The following mean value and the standard deviations of the displacements are obtained:

$$\begin{aligned} \hat{w}/t &= -0.2997 \\ \hat{\sigma}_w/t &= 0.8436 \end{aligned} \tag{5.1}$$

The probability distributions of the geometrical imperfections w_0 and the resulting displacements w are presented in Fig. 5.3 and Fig. 5.4. The shape of these probability distributions indicates a nonlinear character of the considered problem – the normal distribution of the initial imperfections transforms into bi-modal distribution of the output results. It should be emphasized that the similar histogram shapes were obtained in the case of the rigid bar models (see Chapter 4). An advantage of these preliminary calculations is straightforward. Such a possibility of analysing complex structures throughout an alternative model is not new. For example, Náprstek (1999) tested simple Mises frames, modelling a strongly nonlinear behaviour of shallow shells with geometrical uncertainties.

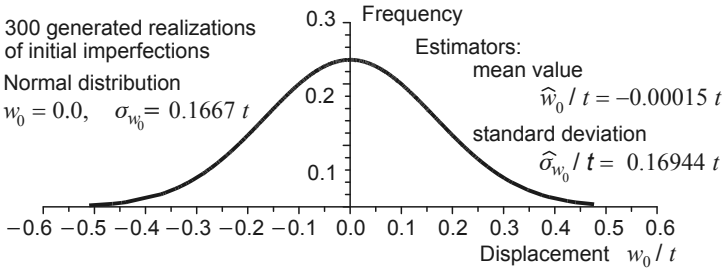

Fig. 5.3. Probability distribution of 300 initial geometrical imperfections w_0 at the central point of the shell

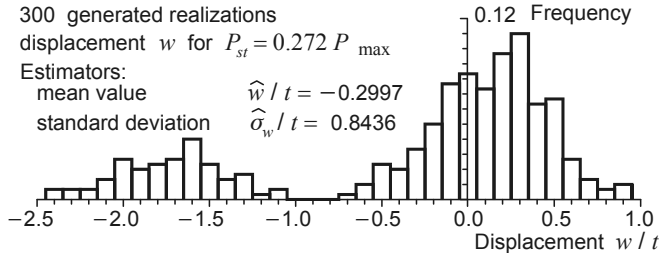

Fig. 5.4. 300 realizations of degenerated field – histogram of the shell central point displacement w for the load P_{st}

Next, the stratified Monte Carlo analysis is applied. In this simple, one dimensional case advantage is taken of the following reduction procedure. The initial imperfections are divided into intervals. One representative geometric imperfection is chosen from each interval. The probability of these representatives is described by the following formula

$$p_i = \frac{N_i}{NI} \tag{5.2}$$

where N_i is the number of the geometric imperfection belonging to the interval i, and NI is the number of all variables (in our case $NI = 300$).

The applied intervals $0.1t$, $0.05t$, $0.025t$, $0.02t$, $0.01t$, reduce the initial set to the number of the imperfections 11, 25, 37, 45, 75, respectively. For each reduced set of the realizations the following estimators are calculated:

— expected value $\hat{w} = \sum_{i=1}^{NRI} p_i w_i$

— standard deviation $\hat{\sigma}_w = \sqrt{\sum_{i=1}^{NRI} p_i (w_i - \hat{w})^2}$

— coefficient of variation $\gamma_1 = \frac{\hat{\sigma}_w}{\hat{w}}$ (5.3)

— central moment of the 3rd order $\mu_w^{(3)} = \sum_{i=1}^{NRI} p_i (w_i - \hat{w})^3$

— coefficient of asymmetry $\gamma_2 = \dfrac{\mu_w^{(3)}}{\hat{\sigma}_w^3}$

— central moment of the 4th order $\mu_w^{(4)} = \sum_{i=1}^{NRI} p_i (w_i - \hat{w})^4$

— coefficient of kurtosis $\gamma_3 = \dfrac{\mu_w^{(4)}}{\hat{\sigma}_w^4}$

where w_i is the representative imperfection from interval i and NRI is the reduced number of the imperfections in the set. The outcomes are presented in Table 5.1.

Table 5.1

Estimators of reduced sets of imperfections w_0

Estimators of initial geometrical imperfections w_0	300 generated realizations	Number of realizations in the reduced set:				
		11	25	37	45	75
Expected value $\hat{w}_0/t$	0.00015	0.00161	–0.00022	–0.00027	–0.00023	–0.00011
Standard deviation $\hat{\sigma}_{w_0}/t$	0.16916	0.17107	0.16900	0.16879	0.16927	0.16927
Coefficient of variation γ_1	1127.9	106.23	–761.61	–636.27	–748.33	–1537.4
Coefficient of asymmetry γ_2	–0.1719	–0.1595	–0.1814	–0.1729	–0.1699	–0.1680
Coefficient of kurtosis γ_3	3.0764	2.9560	3.0236	3.0774	3.0744	3.0687

For each reduced set of the realization the displacement w of the central point of the shell, corresponding to the load $P_{st} = 0.272 P_{\max}$ is calculated. It is assumed that the probability of this displacement is equal to the probability of the representative initial imperfection (5.2). The calculated estimators are presented in Table 5.2.

Table 5.2

Estimators of displacement w

Estimators of initial geometrical imperfections w	300 generated realizations	Number of realizations in the reduced set:				
		11	25	37	45	75
Expected value $\hat{w}/t$	–0.29968	–0.32643	–0.32305	–0.29930	–0.30197	–0.30166
Standard deviation $\hat{\sigma}_w/t$	0.84356	0.87050	0.85921	0.84266	0.84408	0.84405
Coefficient of variation γ_1	–2.8149	–2.6667	–2.6597	–2.8154	–2.7952	–2.7981
Coefficient of asymmetry γ_2	–1.0174	–0.8951	–0.9235	–1.0233	–1.0121	–1.0108
Coefficient of kurtosis γ_3	2.6627	2.3184	2.4087	2.6748	2.6533	2.6497

Considering the values of the estimators in Table 5.1 and Table 5.2, one can notice that the results of the reduced set of 37 realizations:

$$\begin{aligned} \hat{w}/t &= -0.2993 \\ \hat{\sigma}_w/t &= 0.8427 \end{aligned} \tag{5.4}$$

are close to those of the 300 generated realizations (5.1). Therefore, instead of analysing the 300 generated realizations it is possible to perform calculations only for the 37 realizations. Fig. 5.1 and Fig. 5.2 illustrate the input and output histograms.

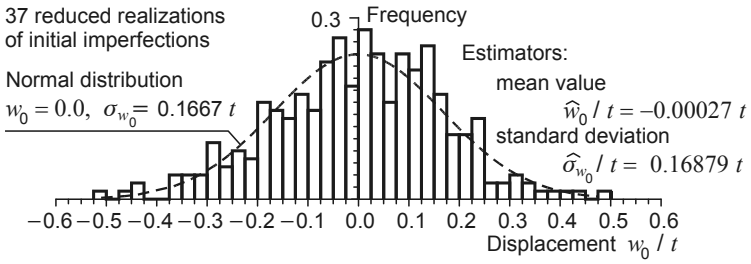

Fig. 5.1. Histogram of 37 reduced initial imperfections w_0 at the central point of the shell

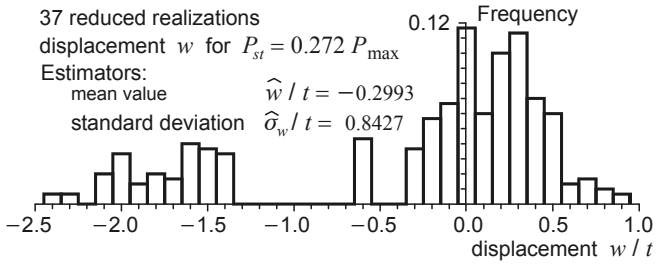

Fig. 5.2. 37 reduced realizations of degenerated field – histogram of the shell central point displacement w for the load P_{st}

For comparison the same analysis for 37 generated realizations (with equal probability 1/37) is made. The results presented in Table 5.3 indicate a significant discrepancy, especially in the case of the estimator values of the displacement w. The input and output histograms are presented in Fig. 5.7 and Fig. 5.8 respectively.

Table 5.3

Estimators for 37 generated realizations

Estimators	Initial imperfection w_0	Displacement w
Expected value $\hat{w}/t$	–0.0044	–2.6203
Standard deviation $\hat{\sigma}_w/t$	1.6622	0.78530
Coefficient of variation γ_1	–379.69	–2.9969
Coefficient of asymmetry γ_2	–0.03439	–1.1547
Coefficient of kurtosis γ_3	3.0417	3.2991

Comparing the results for the 37 generated and reduced realizations (see Fig. 5.6 and Fig. 5.8) one can see that the advantages of applying the reduction algorithm are obvious.

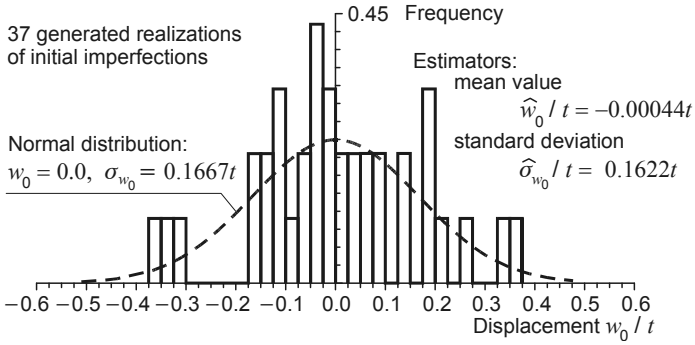

Fig. 5.3. Histogram of 37 generated initial imperfections w_0 at the central point of the shell

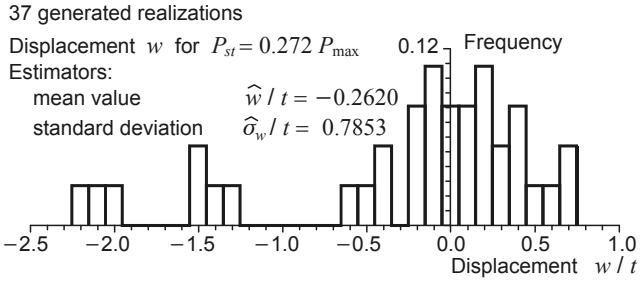

Fig. 5.8. 37generated realizations of degenerated field – histogram of the shell central point displacement w for the load P_{st}

It should be pointed out that in this example the solutions related to a few hundred realizations of the degenerated field give an appropriate probability distribution (Fig. 5.4). The reduction procedure for the degenerated field allows to minimize the calculations without losing the estimators accuracy (see Fig. 5.2). However to get the proper histograms of the probability distributions a much greater set of realizations should be analysed (compare Fig. , Fig. 5.2 and Fig.).

5.1.1.2. Two-dimensional random fields

In the second example the geometrical imperfections are described by the Wiener field $W(\mathbf{r}, \omega)$ (Eq. 3.29). This field is a prototype of the nonhomogeneous random fields.

The Wiener field defined on a regular mesh of 11×11 nodes is simulated according to the method presented in Chapter 3. The mesh is consistent with the finite element discretization of the shell structure, i.e. the random field is constant within the domain of the element. Thus, it is described by the random variable representing the value of the field at the element midpoint (see Chapter 2, and the work by Der Kiureghian and Ke 1988). The field envelope is assumed in the range $< -s\sigma(r_x, r_y),\ +s\sigma(r_x, r_y) >$, where $\sigma(r_x, r_y)$ is the standard deviation of the Wiener field calculated according to the formula (3.29) for $\mathbf{r}_1 = \mathbf{r}_2$ and $s = 5$ (see eq. 3.16). It is proved that for this range the density of the random variable with the normal conditional truncated distribution is approximately equal to the density of the random variable with the normal conditional distribution (see Jankowski and Walukiewicz 1997). The value of the α parameter, constant for all realizations, is so

assumed that the maximal simulated displacements do not exceed half of the shell thickness ($\alpha^2 = 0.096$). The analysis of the simulation procedure errors, calculated according to (3.33) and (3.34) formulas, is shown in Fig. 5.4. It is easy to note that the errors stabilize on a relatively low level, starting from a few hundred realizations.

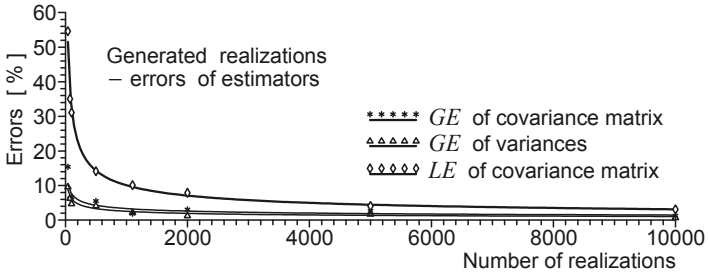

Fig. 5.4. Errors of estimators of the Wiener field with respect to the number of realizations

The Stratified Monte Carlo method is applied. In the case of two-dimensional random fields the reduction algorithm consists of several steps (Bielewicz et al. 1985a and 1993). First, the initial set of realizations *NR* is divided into classes of similar realizations. Three classification parameters are assumed:

— the number of sign changes *NCH*,
— the Euclidean norm of positive values *EP*,
— the Euclidean norm of negative values *EN*.

The values of these parameters calculated for all the realizations form some intervals.

Next, the obtained intervals are divided into a number of subintervals which create sets of classes (*NC* denotes the number of classes). Every class is described by one representative random vector **w**. All representatives of classes constitute a reduced set of realizations (*NRR* denotes the number of reduced realizations). The numerical tests show that *NRR* is much smaller than *NC*, as there is a considerable number of empty classes. In the reduced set of realizations the representatives of the classes have the following probability

$$p_i = \frac{N_i}{NR} \tag{5.5}$$

where N_i is the number of realizations belonging to the class *i* and *NR* is the number of all realizations in the set.

The following formulas present the estimators of the mean value $\hat{\mathbf{w}}_r$ and the covariance matrix $\hat{\mathbf{K}}_r$ (see Eqs (3.33) and (3.34)):

$$\begin{aligned} \hat{\mathbf{w}}_r &= \sum_{i=1}^{NC} p_i \mathbf{w}_i \\ \hat{\mathbf{K}}_r &= \sum_{i=1}^{NC} p_i (\mathbf{w}_i - \hat{\mathbf{w}}_r)(\mathbf{w}_i - \hat{\mathbf{w}}_r)^{\mathrm{T}} \end{aligned} \tag{5.6}$$

The reduction procedure adopted for 5000 realizations of the Wiener field is applied. The error analysis of the obtained results is presented in Fig. 5.5. The errors are approximately the same as in the case of the generated realizations without the reduction

procedure. While investigating the distributions of the generated and the reduced sets one can notice some stable characteristics in the reduced fields. Fig. 5.6 illustrates the marginal distributions of the norm of the negative values of the 54 generated and reduced realizations.

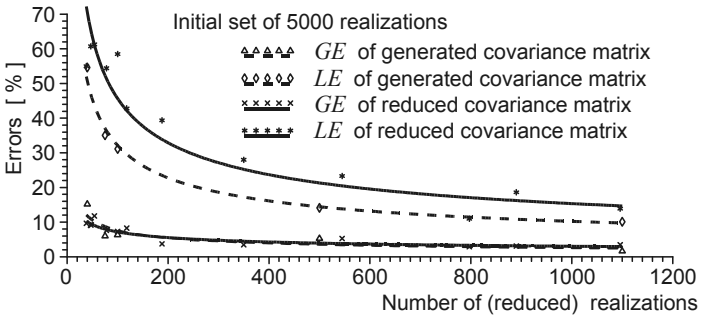

Fig. 5.5. Errors in initial and reduced sets of the Wiener field realizations

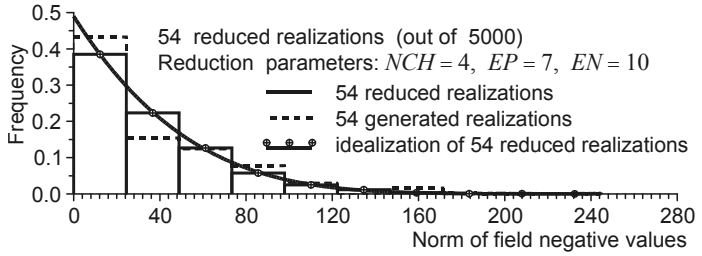

Fig. 5.6. Marginal distribution for 54 generated and reduced realizations of the Wiener field

To check the influence of the reduction magnitude on the results, two different analyses for arbitrarily chosen 54 and 296 reduced realizations are performed. A comparison of the obtained errors is presented in Table 5.4. It is easy to notice that only the error of the matrix single element increases significantly.

Table 5.4

Errors of generated and reduced sets of the Wiener field realizations

Errors [%]	5000 generated realizations	296 reduced realizations	54 reduced realizations
Global error (*GE*) of $\hat{\mathbf{K}}_r$	2.66	2.48	8.69
Error of variances of $\hat{\mathbf{K}}_r$	1.92	3.80	4.60
Local error (*LE*) of $\hat{\mathbf{K}}_r$	4.06	32.75	72.05

As in the previous section, in each sample of the 54 and 296 reduced realizations the displacement w at the central point of the shell, corresponding to the load level $P_{st} = 0.272 P_{\max}$ is numerically obtained. The estimators of these calculations are presented in Table 5.5, and their histograms in Fig. 5.7 and Fig. 5.8.

Table 5.5

Estimators of the structure responses to 296 and 54 reduced realizations of the Wiener field

Estimators	296 reduced realizations	54 reduced realizations
Expected value $\hat{w}$	–0.061993	–0.082622
Standard deviation $\hat{\sigma}_w$	0.35960	0.34994
Coefficient of variation γ_1	–5.8007	–4.2355
Coefficient of asymmetry γ_2	–2.5892	–2.2777
Coefficient of kurtosis γ_3	11.214	9.3370

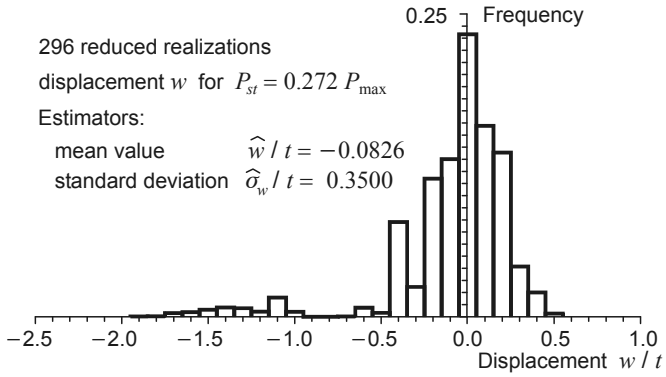

Fig. 5.7. 296 reduced realizations of the Wiener field – histogram of the shell central point displacement w for the load P_{st}

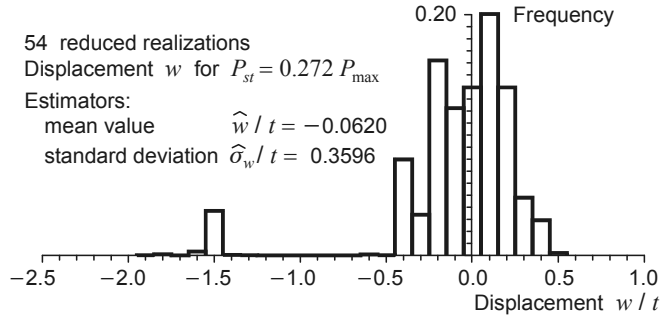

Fig. 5.8. 54 reduced realizations of the Wiener field – histogram of the shell central point displacement w for the load P_{st}

The results for the Wiener field indicate that its specific characteristics, especially number of realizations with dominant positive or negative amplitudes, play an essential role in the numerical analysis.

Comparison of the obtained histograms for the Wiener and the degenerated fields (see Fig. and Fig. 5.7) shows that the influence of the type of the initial imperfections is significant.

5.1.1.3. Estimation of the structure reliability

In the previous Sections attention was focused on reduction methods of various two-dimensional random fields. The calculation was performed for the specified value of the load P_{st}. In this Section a reliability analysis of the same shell is made. For this purpose, using the simulated-based approach, a histogram of the critical load have to be obtained.

To this end the direct Monte Carlo method is applied. Three hundred initial geometrical imperfections are under consideration. The two-dimensional degenerated random fields are taken to study the input geometric imperfection (Bielewicz et al. 1994b). In the numerical solution a double sinusoidal-like surface with a random amplitude has been chosen. The transverse displacement of the middle point has been assumed as the normal random variable: $m_w = 0.$ $D_w = 0.1667t.$ As a consequence of this assumption a histogram of the critical load is obtained (Fig. 5.9).

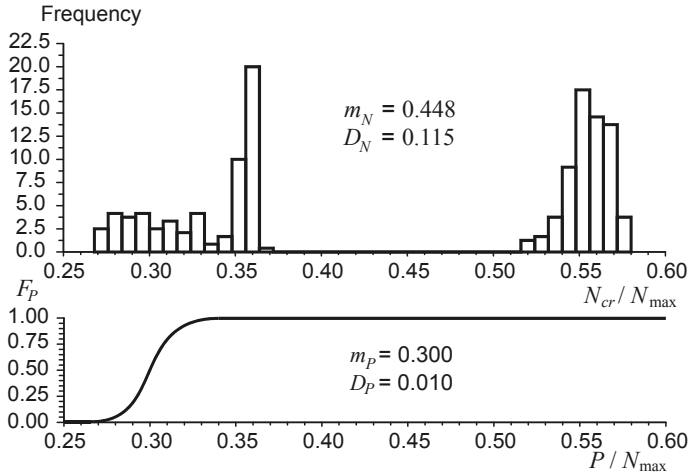

Fig. 5.9. Histogram of the critical load and the probability distribution of the compressive load

Next, the exact reliability of the model was calculated from the formula (4.1) using the histogram. Allowance was made for the normal probability distribution of the compressive loads, described by the mean value $m_P = 0.3,$ and the standard deviation $D_P = 0.03.$ According to the level-3 method, the reliability equals

$$R^{(3)} = \Pr\left(N_{cr} > P\right) = 0.8887 \tag{5.7}$$

It is also worth comparing the results with the formula of level-2 method Eq. (4.1). In this case the reliability index $\beta = 1.282$ and

$$R^{(2)} = \Pr\left(N_{cr} > P\right) = 0.9001 \tag{5.8}$$

Since $R^{(3)} < R^{(2)},$ the example proves that the reliability of such structures should be computed by use of the exact formula (level-3 method).

5.1.2. Selection of the extreme input realizations

In Section 5.1.1 it has been shown that in the nonlinear structural model analysis, the application of the direct Monte Carlo method is very difficult (the nonlinear calculations require an enormous amount of time). By applying the stratified method a considerable reduction of the calculation time is possible. In this Section, an alternative approach, which gives a more radical reduction of the calculation time, is presented. To obtain the lower bound of the critical load of the structure some characteristic random variable vectors are selected from the generated set of realizations. These vectors can be characterized by:
— maximal or minimal random values in the set,
— maximal or minimal number of positive or negative random values,
— maximal or minimal mean value of the random vector,
— components which are close to an eigen-form of the relevant linearized operator,
— any other interesting features distinguishing the random vector from the set.

The selected vectors, as the initial data, describe the extreme, in some sense, structure material variability. Using a finite element program a set of outcomes could be obtained. On this basis one could estimate the structure response.

To illustrate this, a concrete, simply supported, uniformly compressed, shallow cylindrical shell presented in Fig. 5.10 is analysed (see Chróścielewski et al. 1994).

$E_0 = 34000.0$ MPa
$\nu = 0.2$
$\sigma_{y0} = 20$ MPa
$R = 83.3$ m
$a = 10$ m
$t = 0.1$ m
$P_{\max} = t \times \sigma_{y0}$
λ – load factor

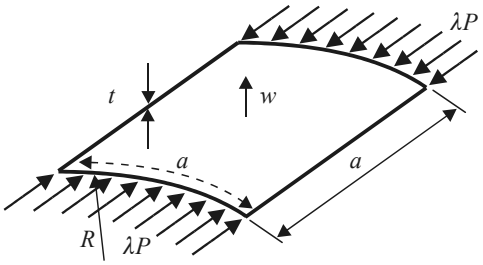

Fig. 5.10. Simply supported axially compressed shallow shell

The material and geometrical nonlinearities are taken into consideration. For the reason that only testing calculations are performed, the concrete is described by the elastic-plastic material (the concrete cracking and the reinforcement are neglected). The number of finite elements (*NEL*) is assumed according to the number of the random field variable values $NEL = 11 \times 11 = 121$, and in this way the midpoint discretization method is applied.

The shell response due to the material uncertainties is analysed. To describe the material imperfections, the zero-mean fields characterized by the white noise $N(\mathbf{r}, \omega)$ (Eq. (3.28)) and the homogeneous Shinozuka field $S(\mathbf{r}, \omega)$ (Eq. (3.31)) the correlation functions are generated. For example, Carmeliet and Hens (1994) applied an alternative, a three-parameters Weibull distribution function to describe the concrete initial damage threshold. They also introduced two different length parameters: the characteristic length of the nonlocal damage model and the correlation distance of the random field.

In this case, use is made of the method of generation of two-dimensional random fields presented in Chapter 3. It should be pointed out that the white noise field does not impose any correlations between the material parameters at different points of the structure. On the other hand, the homogeneous (Shinozuka) field introduces not only such correlations, but also relates them to the distance between the structure points. In concrete structures this

feature seems to be of considerable importance. For every finite element i Young's modulus E_i and the yield stress σ_{yi} are calculated according to the formulas:

$$\begin{aligned} E_i &= E_0\left(1+f_1X_i\right) \\ \sigma_{yi} &= \sigma_{y0}\left(1+f_2X_i\right) \end{aligned} \tag{5.9}$$

where E_0 and σ_{y0} are the expected values of Young's modulus and the yield stress, variables X_i are components of the generated random vectors, f_1 and f_2 are scaling factors:

$$f_1 = \frac{5000.0}{\left|X^{\max}\right|}, \qquad f_2 = \frac{6.0}{\left|X^{\max}\right|} \tag{5.10}$$

where $X^{\max}$ is the extreme random value in the set. In this way the modulus E_i and the yield stresses σ_{yi} for any finite element i are assumed to be:

$$\begin{aligned} 29000.0 \le E_i &\le 39000.0 \qquad [\text{MPa}] \\ 14.0 \le \sigma_{yi} &\le 26.0 \qquad [\text{MPa}] \end{aligned} \tag{5.11}$$

Due to the fact that Young's modulus E_i and the yield stress σ_{yi} are described by the same random field, a full correlation between these parameters is introduced.

Six various characteristic – extreme in some sense – random vectors (three from each field) are chosen from the generated sets of the white noise and the homogeneous Shinozuka fields realizations. The selection has been made according to the minimal random values in the set, the maximal number of negative random values, and the minimal mean value of the random vector.

Using the BOX program (Chróścielewski 1983), the nonlinear post-buckling calculations are performed. Force P_t of 1/5000th intensity of the reference load (imperfection load) is applied to the centre of the shell in order to obtain the post-buckling responses of the model. Two calculations are made for each realization: the transverse force P_t is directed upwards and downwards. The results are presented in Fig. 5.11 and Fig. 5.12.

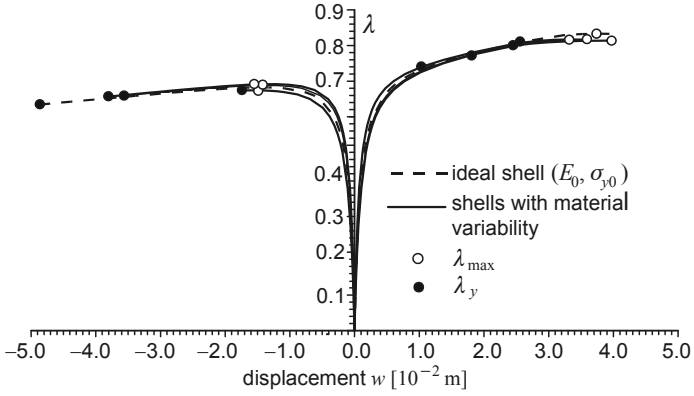

Fig. 5.11. White noise field – displacement w at the centre of the shell versus load parameter λ

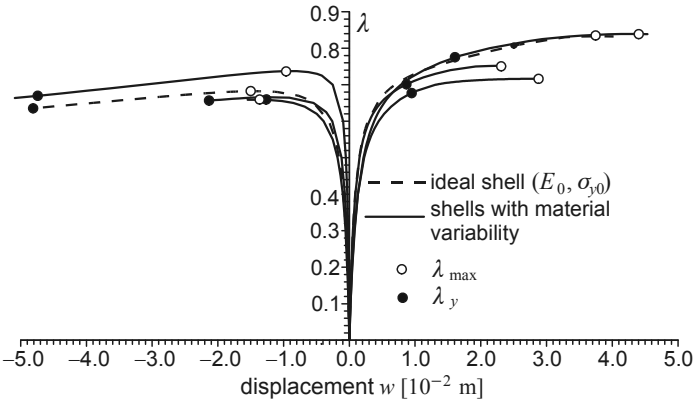

Fig. 5.12. The homogeneous (Shinozuka) field – displacement w at the centre of the shell versus load parameter λ

Two characteristic points of the equilibrium paths are selected:
— the maximal value of P (i.e. $\lambda_{\max}$) and the corresponding displacement w,
— the point where the shell responses change from elastic to plastic (λ_y, w_y).
The results are presented in Table 5.6.

Some qualitative conclusions can be formulated as follows:
— the equilibrium paths are sensitive to the type of random fields (the white noise and the homogeneous fields),
— the critical displacements w_y are highly sensitive to the type of material variability,
— the effect of randomness is smaller in the case of $P_{\max}(\lambda_{\max})$ calculations.

Table 5.6

Characteristic points on the equilibrium paths of the shell

Material variability	Downward displacement				Upward displacement			
	λ_y	w_y 10^{-2} m	$\lambda_{\max}$	w 10^{-2} m	λ_y	w_y 10^{-2} m	$\lambda_{\max}$	w 10^{-2} m
ideal shell	0.634	–4.89	0.682	–1.49	0.830	2.58	0.833	3.77
white noise 1	0.674	–1.69	0.674	–1.58	0.740	1.03	0.817	3.34
white noise 2	0.660	–3.53	0.689	–1.39	0.800	2.41	0.817	3.61
white noise 3	0.656	–3.62	0.692	–1.22	0.775	1.83	0.814	3.98
Shinozuka 1	0.657	–2.13	0.666	–1.26	0.680	0.97	0.716	2.88
Shinozuka 2	0.670	–4.73	0.737	–0.98	0.780	1.69	0.839	4.34
Shinozuka 3	0.658	–1.20	0.659	–1.37	0.700	0.86	0.752	2.35

On the basis of these outcomes, the shell model reliability could be estimated for engineering purposes. In the case under consideration the normal cumulative distribution function of the load $F_P(x)$ with $m_P = 0.300$, $D_P = 0.1$ is assumed. Taking the value $\min(\lambda_{\max}) = 0.659$ from Table 5.6 and using formula (2.1) the equation takes the form

$$\min R^{(3)} = \int_{-\infty}^{\infty} F_P(x)\,\delta(x-0.659)\,dx = F_P(0.659) = \\ = \frac{1}{2} + \operatorname{erf}\left(\frac{0.659-0.300}{0.100}\right) = 0.99983 \tag{5.12}$$

The proposition of a selection of a characteristic (extreme) sample and the application of formula (5.12) seems to be useful in reliability assessments.

5.2. Convergence analysis of the output results

This Chapter is connected with an alternative version of random input data reduction in the simulation-based approach.

The input data are transformed by a nonlinear operator (according to Eq. 1.1) into description of the limit state of the structure. The method of the analysis of these random output results differs significantly from the statistical analysis of the random input data presented in Chapter 5.1. The analytical solutions of the stochastic nonlinear problems are unknown. A comparative analysis of the output results obtained from different numbers of realizations seems to be the only way for the convergence assessment. Such calculations are frequently applied. For example, Araújo (2001) used this method for probabilistic description of reinforced concrete columns. The analysis has proved that only 200 Monte Carlo samples are sufficient to obtain satisfactory results. In similar calculations made by Mirza (1998) related to some eccentrically loaded concrete columns, 500 samples were taken into account. Also in Bhattacharyya and Chakraborty (2002) and Chakraborty and Dey (1999) analogous analyses are applied to compute the response sensitivity concerning uncertainties in the structural parameters. In the case of plane stress and plate bending problems about 200 ÷ 300 samples have proved to be sufficient to achieve the satisfactory results. Carmeliet and Hens (1994) used 200 Monte Carlo samples of initial damage thresholds to obtain the tensile strength distribution for concrete beams in three-point bending tests. In their study no use was made of convergence analysis of the results. However Jeong and Shenoi (2000) applied as many as 1000 samples to estimate the reliability of fibre reinforced plastic laminated plates. There, the sensitivity of the basic design variables have also been included in their calculation.

In the above mentioned works no systematic convergence analyses have been performed. It is obvious that the choice of convergence to describe the numerical results influences the results. Thus, the following statistical formulas are proposed:

$$\hat{m}_N = \frac{1}{NR}\sum_{i=1}^{NR} N_{cr}^i, \qquad 2 < NR < NR_{\max}$$

$$\hat{D}_N^2 = \frac{1}{NR}\sum_{i=1}^{NR}\left(N_{cr}^i - \hat{m}_N\right)^2$$

$$\left\|\hat{\mathbf{K}}\right\| = \sqrt{tr\left(\hat{\mathbf{K}}_w\right)^2} \tag{5.13}$$

$$\hat{\mathbf{K}}_w = \frac{1}{NR-1}\sum_{i=1}^{NR}\left(\mathbf{w}_i - \hat{\mathbf{w}}\right)\left(\mathbf{w}_i - \hat{\mathbf{w}}\right)^T, \qquad \hat{\mathbf{w}} = \frac{1}{NR}\sum_{i=1}^{NR}\mathbf{w}_i$$

where: NR – number of realizations, $\mathbf{w}_i$ – displacement vector related to the critical force N_{cr}^i, $\hat{\mathbf{w}}$ – the mean vector of displacements $\mathbf{w}_i$, $\hat{m}_N$ – expected values and $\hat{D}_N$ – standard deviation of the critical load force N_{cr}, $\hat{\mathbf{K}}_w$ – covariance matrix estimators of the displacement vector $\mathbf{w}$ related to forces N_{cr}, $\|\hat{\mathbf{K}}\|$ – the norm of covariance matrix $\hat{\mathbf{K}}_w$.

Using the above equations the convergence of the numerical calculations can be checked. When the fluctuation of the estimated values of $\hat{m}_N$, $\hat{D}_N$ and $\|\hat{\mathbf{K}}\|$ are meaningless it is possible to assume that the analysed set of sampling is sufficient. Thus, the maximal number of realization $NR_{\max}$ depends on the progress of the nonlinear calculation of the structure under consideration. This form of the accuracy assessment of the sampling can be additionally verified by comparing the histograms of the limit loads for the chosen number of realizations.

It seems rational to assume that in engineering applications the convergence analysis can be limited only to the output results.

5.2.1. Random fields described by one random variable

In the following the proposed convergence analysis of structure reliability calculations is examined in detail. For this purpose, once more, a simply supported, uniformly compressed, shallow cylindrical shell (Fig. 5.13) is considered.

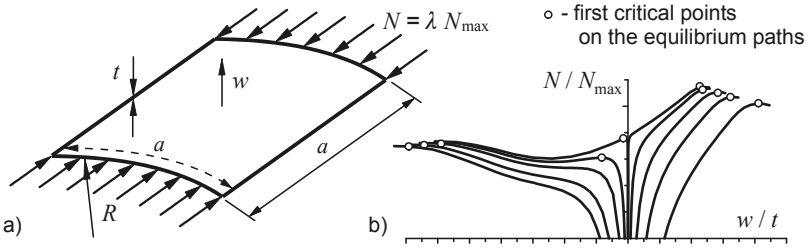

Fig. 5.13. Model of a simply supported shallow cylindrical shell (a) and equilibrium paths at the middle point of the shell (b)

An extensive analysis of a similar problem, i.e. critical load estimation of compressed cylindrical shells with random imperfections, has been provided by Arbocz and his co-workers (see for example Arbocz 2000, Arbocz and Hol 1991, and 1995, Arbocz and Starnes 2002, Cederbaum and Arbocz 1996a, 1996b and 1997, and many others).

In the present analysis the shell is composed of an ideal elastic-plastic material. The following data are assumed to be the deterministic values: $E = 2.1\times10^5$ MPa, $\nu = 0.3$, $\sigma_y = 250$ MPa, $a/R = 0.12$, $t/R = 0.00036$ and $N_{\max} = a\times t\times\sigma_y$. Parameters E and ν describe Young modulus and Poisson coefficient respectively and σ_y stands for the material yield stress value.

The shell geometric imperfection fields $w(x, y)$ are described by double sinusoidal-like surfaces with random amplitudes w_0 (see Fig. 5.13a) defined as:

— a random variable with the uniform probability density function (section 6.1.1),
— a minimum, and a maximum value selected from a set of three uniform random variables (section 6.1.2).

5.2.1.1. Direct Monte Carlo method

First, the initial transverse displacement w_0 at the middle point of the shell is assumed as the uniform random variable from the following range: $-2t < w_0 < 2t$. The mean value and the standard deviations are: $m_w = 0$ and $D_w = 1.16t$.

In this case the accuracy analysis is restricted to the output level. Using the direct Monte Carlo method, it is necessary to assume the minimum number of realizations describing properly the mechanical behaviour of the shell model. To achieve this, the expected values $\hat{m}_N$, the standard deviations of the limit compressive force $\hat{D}_N$, and the norm of covariance matrix estimators $\|\hat{\mathbf{K}}\|$ (Eq. (5.13)) of the displacement vector **w** related to the forces N_{cr} are checked in every realization (Fig. 5.14).

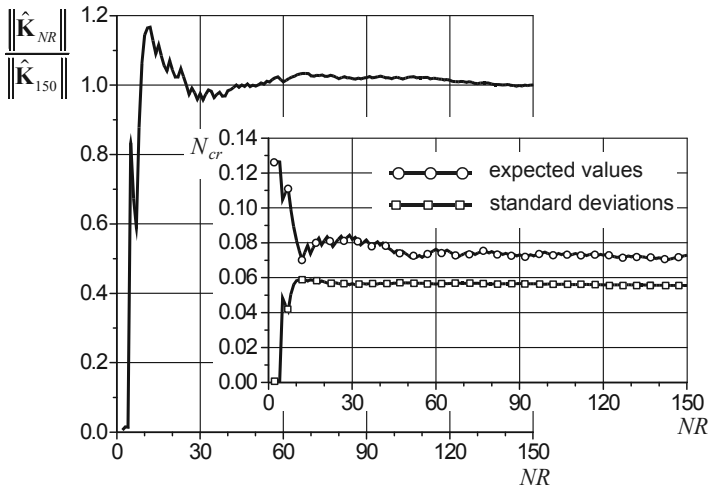

Fig. 5.14. Uniform random variable – estimators of critical load characteristics vs. the number of realizations

It is easy to notice that the expected values of the critical load, the standard deviations, and the norm of covariance matrices stabilize approximately above 50 realizations. The histograms of the critical compressive loads for 50 and 150 realizations of initial imperfections are presented in Fig. 5.15. The results for $NR_{\max} = 150$ can therefore be assumed as an adequate solution. The analysis has proved that an engineering sound solution can be obtained on the basis of the first 50 realizations.

On the basis of the obtained histograms the reliability of the shell model can be calculated. The uniform probability distribution of the compressive load P (Fig. 5.15) is taken into account. According to the level-3 formula (2.1) and on achieving an exact integration, the following values of reliability for a different number of realizations are calculated:

$$NR = 50: \qquad R_{uni}^{50} = \Pr\left(N_{cr} > P\right) = 0.8467 \tag{5.14}$$

$$NR = 150: \qquad R_{uni}^{150} = \Pr\left(N_{cr} > P\right) = 0.8778 \tag{5.15}$$

A change of these values is rather small and the shapes of both histograms are similar.

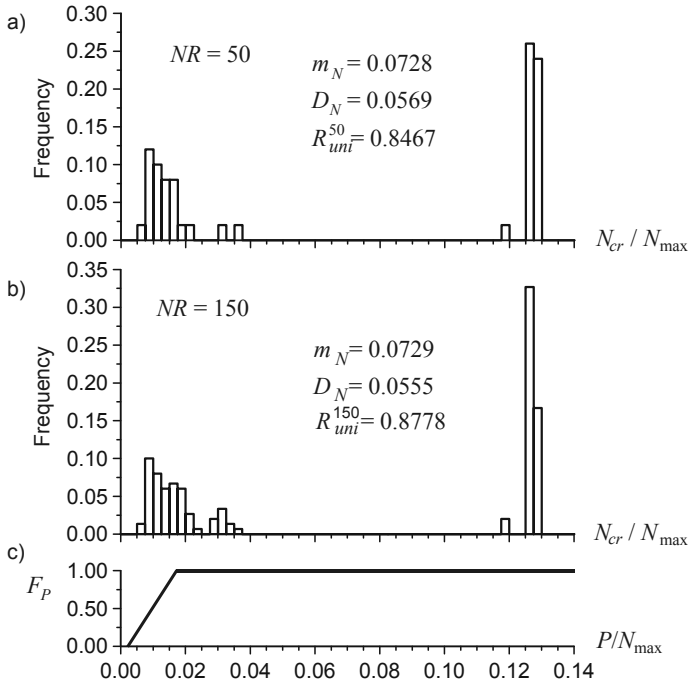

Fig. 5.15. Histograms of the critical load for $NR = 50$ and $NR = 150$ realizations of the initial imperfections and the probability distribution of the compressive load P

5.2.1.2. Interval of structure reliability

In the second part of the analysis the geometric imperfections are described by minimal and maximal values chosen from a set of three uniform variables (see Chapter 4). The sets of random variables are obtained with the help of the cumulative distribution functions (4.21) and (4.22) where function $F(x)$ is characterized by the uniform distribution and the exponent is taken as $n = 3$. The exact analytical cumulative distributions of the random variables defined for the interval (0, 1) are presented in Fig. 5.16 (solid lines).

For a uniform random variable the mean value m is equal to 0.5 and the standard deviations $D = 0.288$. With respect to the minimum value selection and $n = 3$, $m_{\min} = 0.25$ and $D_{\min} = 0.194$. For the maximum value selection $m_{\max} = 0.75$ and $D_{\max} = 0.194$. Taking $n > 3$ the above probability distributions will tend to the deterministic values of 0 and 1, respectively. Comparing the minimum and the maximum distribution estimators for $n = 3$, a medium value of the random effect is expected.

In the numerical procedure three variables are automatically generated and the maximum and minimum values are selected. The distributions obtained for 50, 150 and 1000 random values are presented in Fig. 5.16 (dashed lines). It is easy to notice that a satisfactory description of the minimum and maximum random variables can be obtained when the number of realizations is greater than 150. The initial transverse displacements w_0 at the middle point of the shell calculated in this way are characterized by the mean value $m_w = 0$ and the standard deviations $D_w = 1.16t$.

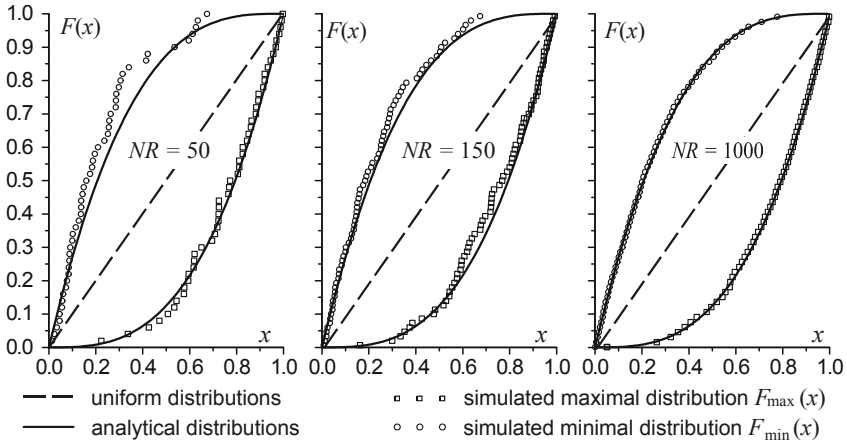

Fig. 5.16. Cumulative distribution functions of the maximum and minimum values

The calculation convergence analysis is restricted to the output level. Using the simulation-based approach, it is necessary to assume the minimum number of realizations describing properly the mechanical behaviour of the shell model. To achieve this, the expected values $\hat{m}_N$, the standard deviations of the limit compressive force $\hat{D}_N$, and the norm of covariance matrix estimators $\|\hat{\mathbf{K}}\|$ of the displacement vector **w** related to forces N_{cr} are checked in every realization (see Eq. (5.13)).

The results of these calculations in the case of the minimum value selection input of three random variables are presented in Fig. 5.17. The convergence of the critical force estimators is noticeable. Differences between the estimators calculated for 120 up to 200 realizations are meaningless. It can be questionable if the engineering sound solution is obtained on the basis of the first 200 realizations.

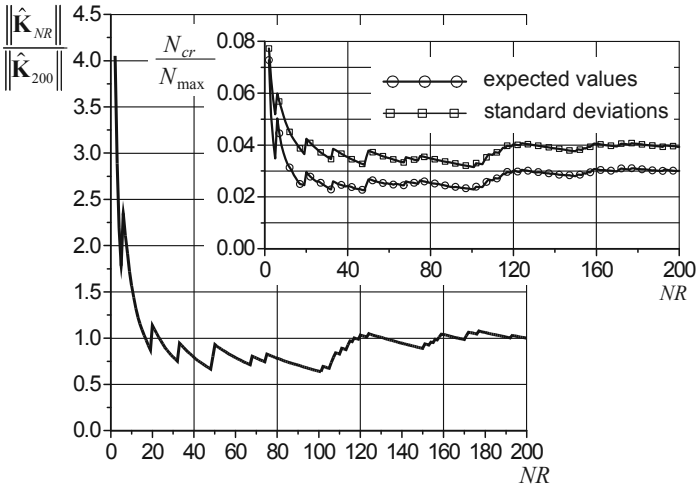

Fig. 5.17. Minimum of 3 random variables – estimators of critical load characteristics vs. numbers of realizations

Formulas (5.13) concern the accuracy of the displacement vector in relation to the number of realizations treated as a basic step in the study. The result of this analysis can additionally be verified by the probability distribution calculation of the limit load used in the reliability estimation of the shell model. To illustrate this appropriate histograms for 150 and 200 realizations of minimum selection of three random variables are compared in Fig. 5.18. The results are almost identical.

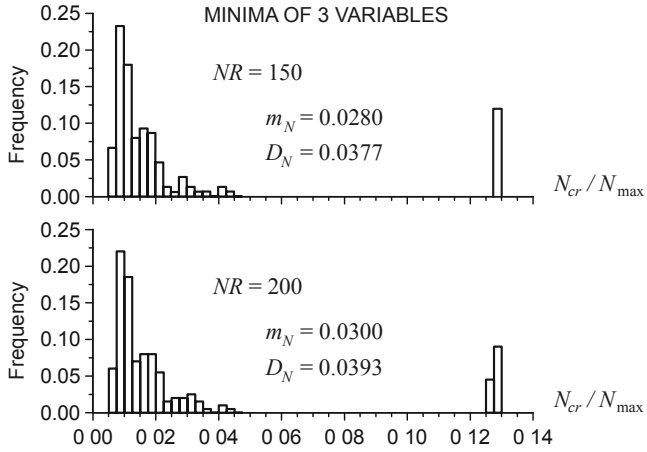

Fig. 5.18. Histograms of the critical loads for 150 and 200 realizations

With regard to the maximum value selection of three random variables, the critical force estimators become much more stabilized and only 150 realizations are needed to obtain a satisfactory stabilized solution (Fig. 5.19).

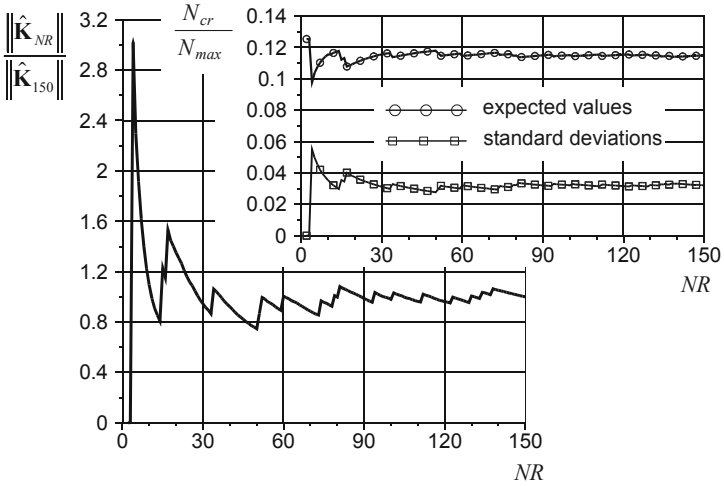

Fig. 5.19. Maxima of 3 random variables – estimators of critical load characteristics vs. the number of realizations

The histograms of the critical loads for the minimum and maximum value selection of three random variables of the initial imperfections are presented in Fig. 5.20. Making use of these results the reliability of the shell model can be calculated. A uniform probability distribution of compressive load P is assumed (Fig. 5.20).

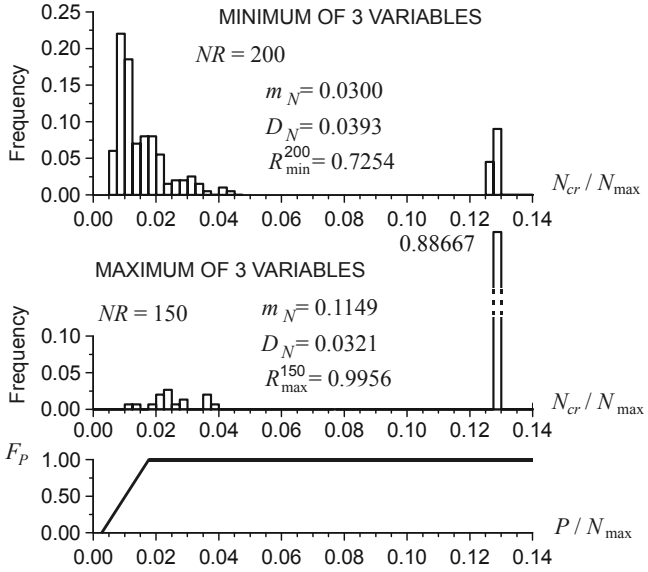

Fig. 5.20. Histograms of the critical loads for the minimum and maximum of three sets of random variables and probability distributions of the compressive load

The reliability for minimum and maximum sets of random variables has been calculated

$$R_{\min}^{200} = \Pr(N_{cr} > P) = 0.857 \tag{5.16}$$

$$R_{\max}^{150} = \Pr(N_{cr} > P) = 0.999 \tag{5.17}$$

These values form an estimated interval of the shell reliability:

$$0.857 < R < 0.999 \tag{5.18}$$

5.2.2. Two-dimensional random field

The above results a worthy of comparison with a more realistic field of continuous imperfections. To this end the following two-dimensional random field describing the geometric imperfections is assumed:

$$w(x,y) = \overline{w}\left[1 + \alpha\beta(x,y)\right] \tag{5.19}$$

where $\overline{w}$ is the expected value of the geometric imperfection, α is the coefficient of variation, and $\beta(x,y)$ stands for the normalized homogeneous random field. The homogeneous field is described by the following correlation function:

$$K_w(x,y) = e^{-\lambda_x \Delta x}\left(1+\lambda_x \Delta x\right) \quad e^{-\lambda_y \Delta y}\left(1+\lambda_y \Delta y\right) \tag{5.20}$$

The field point distances for the mesh discretization (20×20 elements) are $\Delta x = \Delta y = a/20$, where a is the shell length (see Fig. 5.13). The decay coefficients are $\lambda_x = \lambda_y = 5$, which means that the correlation between the field points is significant in the range of one quarter of the shell.

The method of generating the two-dimensional random fields presented in Chapter 3 is applied.

The finite element method imposes the field discretization that can significantly influence the results. To reduce the effect of the element mesh dimensions the procedure of local averages of the random fields proposed by Vanmarcke (1983) is adopted. The appropriate functions of variances D_w and covariances K_w of the homogeneous field (5.20) are (Knabe et al. 1998):

$$D_w(\Delta x,\Delta y) = \frac{2}{\lambda_x \Delta x}\left[2+e^{-\lambda_x \Delta x}-\frac{3}{\lambda_x \Delta x}\left(1-e^{-\lambda_x \Delta x}\right)\right]\frac{2}{\lambda_y \Delta y}\left[2+e^{-\lambda_y \Delta y}-\frac{3}{\lambda_y \Delta y}\left(1-e^{-\lambda_y \Delta y}\right)\right] \tag{5.21}$$

$$K_w(\Delta x,\Delta y) = \frac{e^{\lambda_x \Delta x}}{\left(\lambda_x \Delta x\right)^2}\left\{\left[\cos\left(\lambda_x \Delta x\right)-\sin\left(\lambda_x \Delta x\right)\right]+2\lambda_x \Delta x-1\right\} \frac{e^{\lambda_y \Delta y}}{\left(\lambda_y \Delta y\right)^2}\left\{\left[\cos\left(\lambda_y \Delta y\right)-\sin\left(\lambda_y \Delta y\right)\right]+2\lambda_y \Delta y-1\right\} \tag{5.22}$$

The critical forces are calculated for 50 simulated realizations of the imperfection field. The resultant estimators and the critical force histogram are presented in Fig. 5.21 and Fig. 5.22 respectively. With this in view the reliability becomes

$$R_{2-D}^{50} = \Pr\left(N_{cr} > P\right) = 0.950 \tag{5.23}$$

It belongs to the calculated reliability range (5.18).

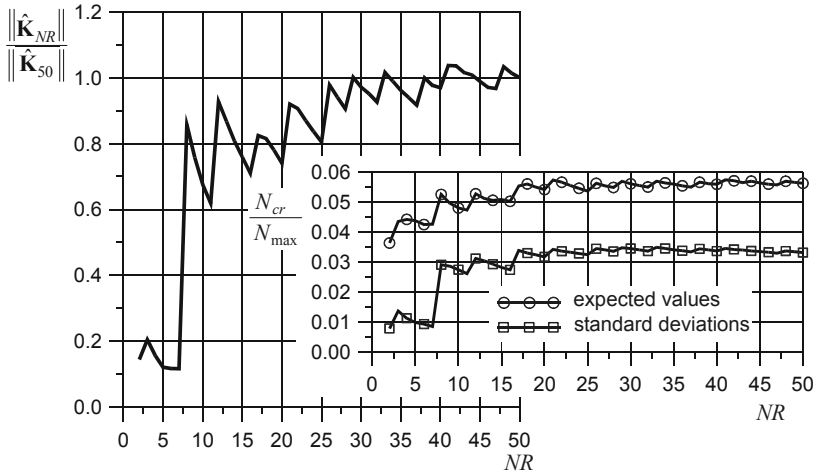

Fig. 5.21. Estimators of critical load characteristics vs. the number of realizations – the homogeneous field of imperfections

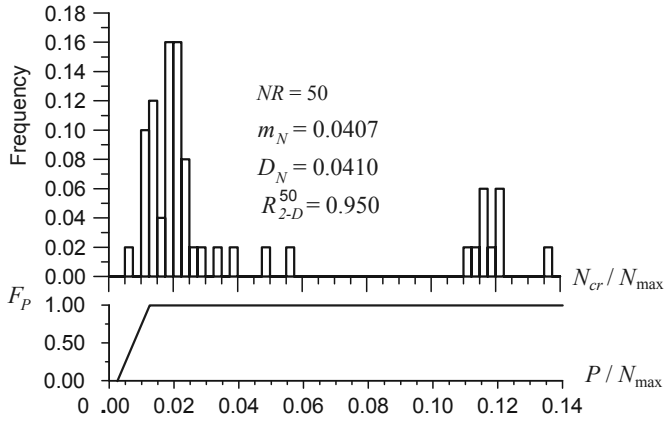

Fig. 5.22. Histogram of the critical load for random field of imperfection and distribution of the compressive load

The analysis of estimators shows that 50 realizations of the homogeneous field of imperfections are a sufficient number of samples for the shell model under consideration. One can notice that the shape of the critical force histogram (Fig. 5.22) corresponds to the histogram obtained for a minimum selection of three random variable distributions (Fig. 5.20).

It should be pointed out that the numerical calculations of the shell with imperfections described by a two-dimensional field are extremely laborious compared with the description by a single random variable. In the last case the finite element calculations are performed only for one quarter of the shell and the nonlinear incremental solution is much more stabilized.

Moreover a stiffening behaviour of the shell with a two-dimensional random field is observed. It is worth mentioning that this stiffening behaviour was also confirmed by Papadopoulos and Papadrakakis (2004) and by Deml and Wunderlich (1997) in shells with small slenderness and large imperfection amplitudes. The stiffening behaviour makes the calculation extremely difficult.

For this reason the reliability calculations using the simulation-based approach and the interval estimation seem to be a better solution to assess the reliability of the nonlinear models of shells and similar complex structures.

Chapter 6

IDENTIFICATION OF GEOMETRIC IMPERFECTIONS

It is well known that the effect of structural geometric imperfections can dramatically decrease the nominal load carrying capacity of engineering structures (Arbocz and Starnes 2002**,** Khamlichi et al. 2004, Papadopoulos and Papadrakakis 2004). An analysis of these imperfections can improve the design process (Arbocz 1998) but it is difficult and expensive to measure them in situ or by laboratory models, specially in the case of two-dimensional structures, like plates and shells. Moreover, the degree of the imperfection sensitivity depends not only on the magnitude but also on the shape of the initial imperfections (Arbocz and Starnes 2002). For example, it is not sufficient to check the shell surface for the maximum imperfection amplitude by carrying out selected circumference or axial measurement scans. A complete surface map of the measured structure should be provided. Papadimitriou et al. (2001) showed that the structural reliability computed before and after using additional dynamics data could differ significantly. Therefore, the measured response of a structure, whenever available, should be used to update its reliability.

Comprehensive numerical analyses of this problem can be found, for example, in Schenk and Schuëller (2003) where buckling behaviour of cylindrical shells with random geometric imperfections is examined. A concept of the numerical prediction of a large scatter in the limit load observed in experiments using the direct Monte Carlo method, the simulation technique, and the nonlinear finite element method is introduced. The geometric imperfections are modelled as a two dimensional, Gaussian stochastic process with prescribed second moment characteristics based on data bank of the measured imperfections. The tests are aided by the Karhunen-Loéve expansion method. Owing to this it is possible to give the second moment characteristics of the limit load.

Stefanou and Papadrakakis (2004) presented a stochastic triangular shell element in the case of combined uncertain material (Young's modulus and the Poisson ratio) and geometric (thickness) properties. The properties are described by uncorrelated two dimensional homogeneous stochastic fields. The spectral description of the random fields in conjunction with the Monte Carlo simulation is used for the computation variability. Two examples are analysed, the Scordelis-Lo roof and a hyperboloid shell. In Papadopoulos and Papadrakakis (2004) using the same methodology a parametric study is performed to evaluate of the sensitivity of the buckling load of a cylindrical panel to the amplitude and the shape of the initial imperfections. One- and two-dimensional stochastic imperfections of shapes, the modulus of elasticity and the shell thickness are introduced individually or in combination. The influence of the shape and magnitude of the imperfections on the form and magnitude of the distributions of the panel buckling loads is investigated. In the case of one-dimensional combined imperfections a drastic reduction of about 50% of the mean value of the buckling load is observed, whereas in two-dimensional combined imperfections such a reduction has not been proved and the buckling load remains the same and is almost equal to the buckling load of a perfect shell.

With regards to compressed cylindrical shells a reliability based knockdown factor is derived to describe the allowable load applied (Arbocz and Starnes 2002). It can replace the empirical knockdown factor so chosen that when multiplied by the calculated perfect shell buckling load, a "lower bound" relating to all existing experimental data is obtained.

In this Chapter two real engineering structures are considered (Górski 2001a, b, and c, Górski and Jasina 2001a and b, and Górski and Mikulski 2005). The first one concerns the analysis of the measured discrepancies obtained for cylindrical vertical tanks. The second deals with the geometric imperfections of longitudinally stiffened ship's hull panels. The simulation technique presented in Section 3 is used to generate the initial geometric imperfections. In both cases the estimators of the obtained realizations of the imperfections are compared with the test data.

The following problems are discussed:

— identification of random fields of structure imperfections on the basis of experimental data,
— simulation of large random fields describing the tank imperfections as an illustration of circular data (see Fisher 1993 or Watson 1983),
— simulation of random fields of imperfections bounded by envelope which model the – specific structure shape and the boundary conditions of plates with ribs,
— the influence of the initial geometric imperfections on the numerical results.

6.1. Random imperfections of cylindrical vertical tanks

In Orlik (1976) a detail description of cylindrical vertical tank discrepancies can be found. Nine sets of measured in situ imperfections of tanks of $V = 5000 \div 50000$ m^3 capacity were analysed (see Table 6.1, Fig. 6.1 and Fig. 6.2). The tank basic statistic parameters, i.e. mean values, standard deviations, and maximal values of the initial geometric imperfections are presented in Table 6.2. It is easy to notice that the discrepancies between the parameters are significant. Only the first two tank imperfections are similar (compare also Fig. 6.1a and b). Even in the case of tanks nos. 3 and 4, the dimensions of which are the same as in the first two, the initial discrepancies differ evidently. The differences result from the tank dimension, the construction method used and the precision of the tank assembly. The last reason seems to be the most important.

Table 6.1

Cylindrical vertical tank data (Orlik 1976)

Tank no.	V [m^3]	Diameter d [m]	Height h [m]	Tank assembly method	Mesh dimension [mm]	Nos. of measure-ing point	Nos. of points along perimeter	Nos. of points along height
1	5000	23.75	11.98	rolled strike	396×750	3232	202	17
2	5000	23.75	11.98	rolled strike	396×750	3232	202	17
3	5000	23.75	11.98	rolled strike	396×750	3030	202	15
4	5000	24.50	11.80	sheets, hand welding	4810×1500	128	16	9
5	13000	36.58	13.45	sheets, hand welding	442×750	168	12	14
6	30000	49.50	16.44	sheets, hand welding	370×1500	3780	420	9
7	30000	49.50	16.44	sheets, hand welding	5981×750	572	26	22
8	32000	54.10	14.40	sheets, hand welding	6060×800	448	28	16
9	50000	65.00	18.01	sheets, automatic welding	400×1500	5100	510	10

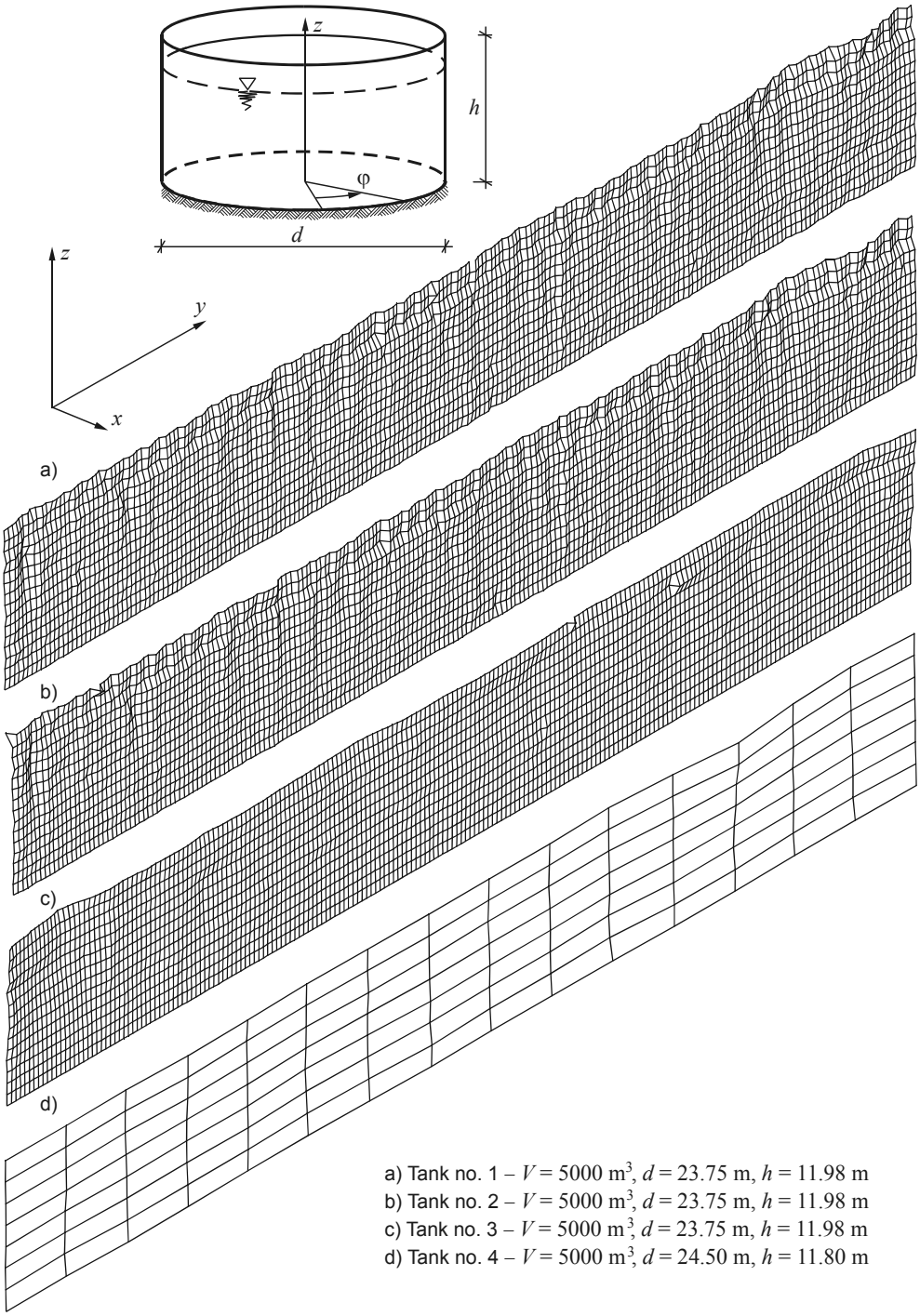

Fig. 6.1. Petrol tank (cylindrical shell) measured geometric imperfections ($V = 5000$ m^3 capacity)

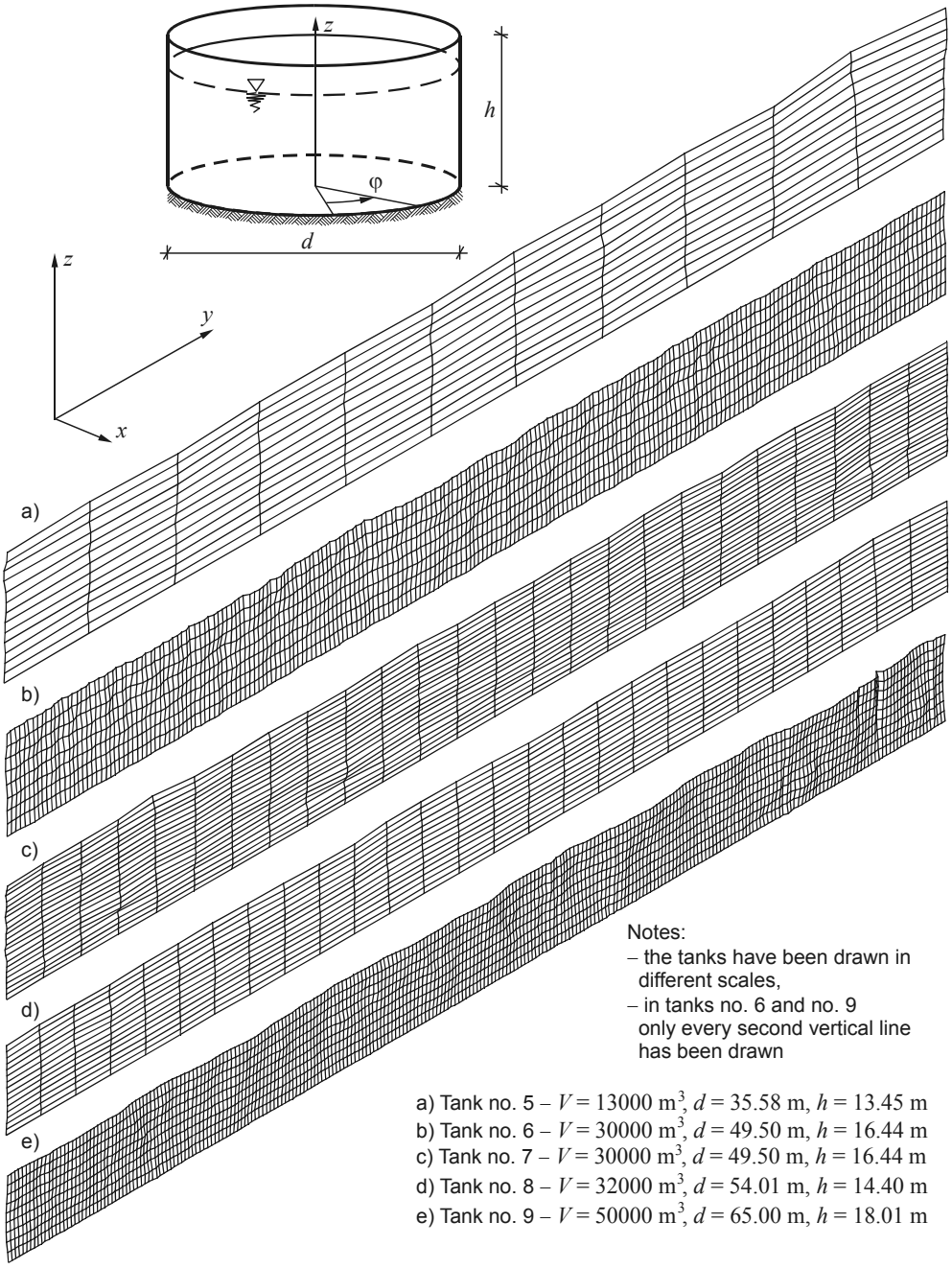

Fig. 6.2. Petrol tank measured geometric imperfections (V = 13000÷50000 m^3 capacity)

Some other detailed statistical descriptions of the tank imperfection fields as well as methods of their measurement in situ can be found in Orlik (1976). In this section, use is

made of these data including identification and simulation of the geometric imperfection maps. The effect of the tank side discrepancies on the numerical results is also analysed.

Table 6.2

Measured initial geometric imperfections of tanks – statistical parameters

Tank no.	d [m]	Mean value $\bar{x}$ [m]	St. dev. σ_x [m]	$\lvert x_i^{\max} \rvert$ [m]	$\bar{x}/d$	σ_x/d	$\lvert x_i^{\max} \rvert / d$
1	11.875	-0.763×10^{-2}	0.233×10^{-1}	0.159	-0.643×10^{-3}	0.197×10^{-2}	0.134×10^{-1}
2	11.875	-0.988×10^{-2}	0.240×10^{-1}	0.163	-0.832×10^{-3}	0.202×10^{-2}	0.137×10^{-1}
3	11.875	-0.485×10^{-2}	0.153×10^{-1}	0.110	-0.408×10^{-3}	0.129×10^{-2}	0.926×10^{-2}
4	12.250	-0.216×10^{-1}	0.213×10^{-1}	0.075	-0.176×10^{-2}	0.173×10^{-2}	0.612×10^{-2}
5	17.790	-0.994×10^{-3}	0.329×10^{-1}	0.139	-0.559×10^{-4}	0.185×10^{-2}	0.781×10^{-2}
6	24.750	-0.361×10^{-2}	0.302×10^{-1}	0.167	-0.146×10^{-3}	0.122×10^{-2}	0.675×10^{-2}
7	24.750	0.118×10^{-1}	0.252×10^{-1}	0.097	0.476×10^{-3}	0.101×10^{-2}	0.392×10^{-2}
8	27.005	0.297×10^{-2}	0.278×10^{-1}	0.108	0.110×10^{-3}	0.103×10^{-2}	0.400×10^{-2}
9	32.500	0.109×10^{-2}	0.491×10^{-1}	0.226	0.334×10^{-3}	0.151×10^{-2}	0.696×10^{-2}

6.1.1. Identification of the measured geometric imperfections

Examining the shapes of the initial geometric imperfection fields (see Fig. 6.1, Fig. 6.2, and Table 6.2) it is easy to describe them as accidental or even chaotic. Thus, only probabilistic methods can define these fields properly.

The tank side surface discrepancies can be considered in terms of a two-dimensional scalar random field described by a probability density function. The choice of this function can significantly influence the results. According to the analysis presented by Wilde (1981) and Orlik (1976) the following hypothesis can be put forward:

— the stochastic process is stationary and ergodic,

— the random variables can be described by a Gaussian probability density function.

Using the above assumption, and taking into consideration the essential features of the imperfection fields, the following nonhomogeneous correlation function is formulated:

$$K(y_1, y_2, z_1, z_2) = \alpha z_1 z_2 h^{-2} \cos\left(\omega(y_2 - y_1)\right) \exp\left(-\beta|y_2 - y_1| - \gamma|z_2 - z_1|\right) \qquad (6.1)$$

where: y_1, y_2, z_1, z_2 are the point coordinates (see Fig. 6.1), constants α, ω, β, and γ are the correlation coefficients, and h denotes the tank height.

The first term $\alpha z_1 z_2 h^{-2}$ determines a linear change of the standard deviations $\sigma_x = \sqrt{\alpha}\, z/h$ along the vertical line with zero value at the tank bottom and maximum at the top. The element $\cos\omega(y_2 - y_1)$ assumes that the random variables permute along the perimeter according to the cosine function. The last term, $\exp(-\beta\,|y_2 - y_1| - \gamma\,|z_2 - z_1|)$ describes how fast the correlation between the neighbouring points vanishes, in horizontal and vertical directions.

The correlation function parameters α, ω, β, and γ are estimated on the basis of the measured data. Only the imperfection fields of tanks nos. $1 \div 3$ ($V = 5000\ \mathrm{m}^3$), no. 6 ($V = 30000\ \mathrm{m}^3$), and no. 9 ($V = 50000\ \mathrm{m}^3$) were measured using fine meshes (see Fig. 6.1 and Fig. 6.2 or Table 6.1). Thus, the five data sets were used to determine the constants of Eq. (6.1). The assumption that the random field of imperfections is ergodic, makes it

possible to analyse not single (the measured) but hundreds of realizations. For example, in the first case (tank no. 1), as the imperfection values are given in 202 vertical lines, the same number of field realizations can be considered. For the reason that 16 points were measured along the vertical line the dimension of the random vector $\mathbf{x}_i$ equals $16 \times 202 = 3232$. The global experimental covariance matrix $\mathbf{K}_e$ (size 3232×3232) of the measured imperfection field was obtained according to the following statistical formulas:

$$\mathbf{K}_e = \frac{1}{NR-1}\sum_{i=1}^{NR}\left(\mathbf{x}_i - \overline{\mathbf{x}}\right)\left(\mathbf{x}_i - \overline{\mathbf{x}}\right)^T, \qquad \overline{\mathbf{x}} = \frac{1}{NR}\sum_{i=1}^{NR}\mathbf{x}_i \tag{6.2}$$

where $\mathbf{x}_i$ is the measured imperfection vector, NR is the number of realizations, and $\overline{\mathbf{x}}$ represents the mean value of the imperfection vector $\mathbf{x}_i$ ($i = 1, \ldots NR$). Making use of the calculated matrix $\mathbf{K}_e$ (6.2) the parameters of the correlation function (6.1) are determined by the standard regression analysis (Schaefer and Anderson 1989).

First, the minimal dimension of the covariance matrix needed to calculate the correlation parameters (6.1) is determined. For this purpose only the data of tank no. 1 are analysed. Three different sizes of random imperfection vectors $\mathbf{x}_i$ being equal to 16×16, 16×32, and 16×50 are taken into consideration. It should be pointed out that the number of the measured horizontal lines is 16, and because of that the vectors differ only in the number of the vertical lines which were included in the calculations. The results are presented in Table 6.3. It has been assumed that the random vector $\mathbf{x}_i$ of dimension 16×16 is sufficient for the calculations. This simplification has significantly reduced the time of the regression analysis.

Table 6.3

Tank no. 1 – determination of the correlation parameters and the size of the covariance matrix

$\mathbf{x}_i$ size	$\mathbf{K}_e$ size	Correlation parameters				Errors	
		α	ω	β	γ	G_{er}	V_{er}
16×16	256×256	0.000716	0.317389	0.175900	0.058001	4.54	26.88
16×32	512×512	0.000666	0.342336	0.112336	0.045077	5.93	31.99
16×50	800×800	0.000655	0.350614	0.113872	0.037591	7.28	32.82

In Table 6.3 the following definitions of the global G_{er} and variances V_{er} errors enable to compare the experimental covariance matrix $\mathbf{K}_e$ with its estimator $\hat{\mathbf{K}}_e$

$$G_{er}\left(\mathbf{K}_e, \hat{\mathbf{K}}_e\right) = \frac{\left|\left\|\mathbf{K}_e\right\| - \left\|\hat{\mathbf{K}}_e\right\|\right|}{\left\|\mathbf{K}_e\right\|} \times 100\% \tag{6.3}$$

where $\left\|\mathbf{K}\right\| = \sqrt{tr\left(\mathbf{K}\right)^2}$ is the Euclidean norm. The error of variances V_{er} of the covariance matrix is also used:

$$V_{er}\left(k_{ii}^e, \hat{k}_{ii}^e\right) = \frac{1}{MN}\sum_{i=1}^{MN}\frac{\left(k_{ii}^e - \hat{k}_{ii}^e\right)}{\left(k_{ii}^e\right)} \times 100\% \tag{6.4}$$

where k_{ii} denotes the diagonal element of the covariance matrix.

Inserting the parameters presented in Table 6.3 to the correlation function (6.1), the covariance matrix estimator $\mathbf{K}_e$ and its errors (6.3) and (6.4) can be obtained. Comparing the errors one can observe that they are bigger in the case of finer meshes calculations. It should be pointed out that taking into consideration more elements of the covariance matrix (i.e. more vertical line of the measured discrepancies) the experimental correlations (6.2) are also more complicated and the function (6.1) seems to be too elementary. Nevertheless, the obtained results could be considered as acceptable.

A graphical representation of the experimental covariance matrix values and their estimator are given in Fig. 6.3. Only the correlations between the points along the selected horizontal line ($z = 6$ m) are provided. The plots show that the scattered pattern of imperfections has been modelled accurately.

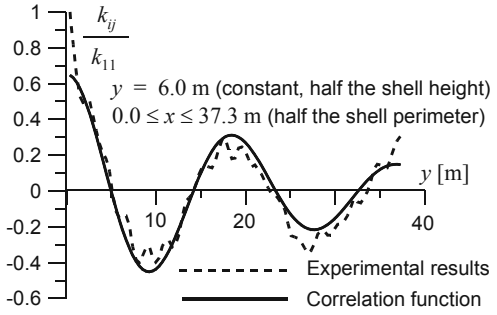

Fig. 6.3. Graphical representation of identified correlation matrix of imperfection field

Using the same approach identical calculations of the correlation parameters for the tanks nos. 2, 3, 6 and 9 are performed. The results are presented in Table 6.4. Only the first two sets of parameters describing the discrepancies for the tank no. 1 and no. 2 are similar. The results confirm the conclusions formulated after analysing the measured data (see Table 6.2). It is obvious that the characteristics of geometric imperfections vary depending on different dimension tanks. Also the difference between the tanks of the same capacity (tanks nos. $1 \div 2$ and no. 3) can be easily predicted. Comparing Fig. 6.1a, b, and c one can notice that tank no. 3 was built much more precisely.

Table 6.4

Correlation parameters of the covariance function

Tank no.	Random vector $\mathbf{x}_i$ dimension	Correlation parameters of Eq. (6.1)				Errors	
		α	ω	β	γ	G_{er}	V_{er}
1	16 × 16	0.000716	0.317389	0.175900	0.058001	4.49	26.84
2	16 × 16	0.000707	0.329261	0.163659	0.050385	3.04	29.00
3	16 × 16	0.000533	0.421175	0.113103	0.098789	8.25	15.75
6	28 × 9	0.001397	0.154658	0.061831	-0.00861	1.84	22.21
9	26 × 10	0.005234	0.134896	0.040879	0.001564	0.78	6.40

The same correlation coefficient estimation can be made in the case of the limited measured data, i.e. for tanks nos. 4, 5, 7, and 8. For example, using the data of tank no. 4 (see Fig. 6.1d) the following parameter values have been obtained:

$$\alpha = 0.013612, \quad \omega = 0.299437, \quad \beta = 0.062983, \quad \gamma = -0.009868 \tag{6.5}$$

The associated global and local errors are:

$$G_{er} = 16.51\%, \quad V_{er} = 4.48\% \tag{6.6}$$

In this case the calculations were performed with the help of the all available data (mesh 9×15, 128 measured points). Despite the fact that tank no. 4 (capacity $V = 5000$ m^3) is almost identical to tanks $1 \div 3$ the results differ significantly (compare parameters (6.5) and Table 6.4). The differences result mainly from the limited data used in the calculations, i.e. 15 vertical lines in tank no. 4, and 202 in the case of tank no. 1. The differences in the initial imperfection shapes and magnitudes (see Fig. 6.1a, d, and Table 6.2) seem to have minor influence.

To indicate the effect of the number of the measured imperfections on the correlation parameter values an additional simple analysis has been performed. The measured data of tank no. 1 have been reduced in such a way that their size is close to the data of tank no. 4, i.e. $8 \times 17 = 136$ points. On this basis the following correlation parameters have been estimated:

$$\alpha = 0.009893, \quad \omega = 0.335382, \quad \beta = 0.024198, \quad \gamma = -0.013186 \tag{6.7}$$

As expected the results differ significantly from those obtained for the 16×202 measured points of tank no. 1 (see Table 6.3). Thus the imperfection data for tanks 4, 7, 8, and 9 seem to be insufficient to describe the random fields properly. The method of identification of the imperfection fields on the basis of limited data is an open problem.

The analysis makes it possible to formulate the following conclusions:

— the number of the imperfection measuring points depends on the quality of the tank assembly,

— the data necessary for the adequate definition of the random field of imperfections depend more on precisely measurement of a limited part of the tank (for example one quarter) than the entire tank side using a rough mesh.

It is important to decide if it is possible to establish a general rule describing the relation between the tank dimensions and the correlation parameters. To this end the parameter values (Table 6.4) are presented versus the tank perimeters (see Fig. 6.4a).

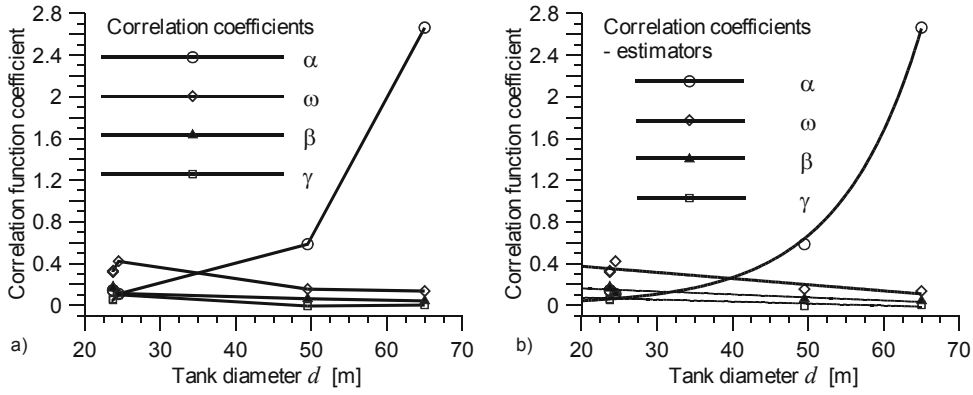

Fig. 6.4. Correlation coefficients (Eq. (6.1)) vs. tank diameter (see Table 6.4)
a) discrete values, b) described by functions (regression analysis)

Analysing the graph (Fig. 6.4a) and taking into consideration the statistic data presented in Table 6.2 one can notice that the available data are too scattered to build a reliable general expression describing the random field of the tank imperfections. Only a draft formula can be estimated. For this purpose the standard regression analysis is applied. The first coefficient α (Eq. (6.1)) is described with the help of an exponential function, and coefficients ω, β and γ are defined be straight lines (see Fig. 6.4b):

$$\begin{aligned} \alpha &= 0.006733 \cdot \exp\left(0.091963 \cdot d\right) \\ \omega &= -0.005894 \cdot d + 0.491321 \\ \beta &= -0.002876 \cdot d + 0.218356 \\ \gamma &= -0.001931 \cdot d + 0.112063 \end{aligned} \tag{6.8}$$

where d is the tank diameter.

It should be stressed that the formulas (6.8) cannot be recommended as general ones. The correlation should be built as a function not only of the tank diameters but also of such parameters as the standard deviations of imperfections, their extreme values, coefficients which describe the tank assemble method, and other available data. Thus, the formulas (6.8) are only the first approximations. They can be improved when new data are included in the calculations (for example, Kowalski 2004).

But in spite of the conclusion the presented identification analysis can be utilized for generation of random imperfection fields to be used in the numerical calculation of petrol vertical tanks.

6.1.2. Envelopes of the tank geometric imperfections

It is possible is to assume the correlation function as an envelope of the extreme imperfections. For this purpose the standard deviations of the tank discrepancies for each horizontal level are calculated and plotted (see Table 6.5 and Fig. 6.5). Examining these data it is easy to notice that the tank side discrepancies start from the bottom and their values indicate the same order as the imperfections measured at higher levels. Therefore, the simplest solution is to approximate the standard deviation to a parabolic function

$$\sigma = \sqrt{\alpha}\sqrt{\frac{z}{h}} \tag{6.9}$$

Then, the correlation function of the imperfection field takes the form

$$K\left(y_1, y_2, z_1, z_2\right) = \alpha\sqrt{\frac{z_1}{h}}\sqrt{\frac{z_2}{h}}\cos\omega\left(y_2 - y_1\right) \times \exp\left(-\beta\left|y_2 - y_1\right| - \gamma\left|z_2 - z_1\right|\right) \tag{6.10}$$

The correlation coefficient α is assumed in such a way that the standard deviation value at the top of the tank is increased by 10%. Thus, in the case of tank no. 1 $\sqrt{\alpha} = 0.0364$ and its graph is presented in Fig. 6.5a. Fig. 6.5b presents the normalized envelope for all available tank data. The results have proved that the adopted envelope in the parabolic shape describes precisely all the possible maximal discrepancies of imperfections. The values of the other correlation parameters ω, β, and γ (see Eq. (6.10)) have not been changed (Table 6.4).

Table 6.5

Tank no. 1 – statistical description of the geometric imperfections along the horizontal lines

Horizontal lines no.	z [m]	Mean value $\bar{x}$ [m]	Maximal value x_{max} [m]	Minimal value x_{min} [m]	Extreme value x_{extr} [m]	Standard deviation σ_x [m]	x_{extr} / σ_x
1	0.7488	-0.12426×10^{-2}	0.021	–0.033	0.03176	0.006978	4.5511
2	1.4975	0.44752×10^{-2}	0.032	–0.021	0.02753	0.008445	3.2591
3	2.2462	0.24752×10^{-4}	0.033	–0.026	0.03298	0.009406	3.5052
4	2.9950	0.48515×10^{-2}	0.030	–0.025	0.02515	0.010194	2.4670
5	3.7438	-0.15990×10^{-2}	0.021	–0.033	0.03140	0.006960	4.5117
6	4.4925	-0.14406×10^{-2}	0.029	–0.034	0.03256	0.011226	2.9003
7	5.2412	0.32228×10^{-2}	0.035	–0.034	0.03178	0.013185	2.4101
8	5.9900	-0.27079×10^{-2}	0.026	–0.045	0.04230	0.015669	2.6991
9	6.7388	0.14109×10^{-2}	0.043	–0.052	0.05059	0.017939	2.8201
10	7.4875	-0.63960×10^{-2}	0.030	–0.065	0.05860	0.019059	3.0749
11	8.2363	-0.30248×10^{-2}	0.040	–0.074	0.07098	0.022272	3.1867
12	8.9850	-0.94257×10^{-2}	0.035	–0.092	0.08257	0.023256	3.5507
13	9.7338	-0.61238×10^{-2}	0.038	–0.080	0.07388	0.024531	3.0115
14	10.482	-0.35752×10^{-1}	0.013	–0.123	0.08725	0.025896	3.3692
15	11.231	-0.30460×10^{-1}	0.034	–0.136	0.10554	0.028299	3.7295
16	11.980	-0.37941×10^{-1}	0.041	–0.159	0.12106	0.033137	3.6533

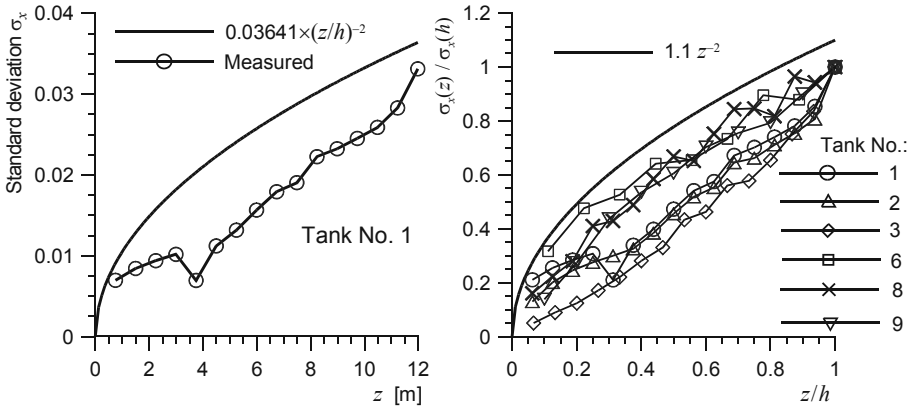

Fig. 6.5. Standard deviations of vertical tanks calculated separately for each level

The proposed correlation functions (6.1) and (6.10), and the estimated values of the parameters α, ω, β, and γ make it possible to generate the vertical tank geometric imperfections.

6.1.3. Generation of the measured tank imperfections

The generation process is presented using the data of tank no. 1. Two cases are analysed, i.e. generation of the measured imperfections as precisely as possible, and generation of maximal imperfection values but still possible in the engineering sense.

Having the correlation function (6.1) and the estimated constants (see Table 6.4) the imperfection field can be numerically simulated. According to the method of generation presented in Chapter 3 the values of the random field – the lower (a_i) and the upper boundary (b_i) – have to be defined for each mesh point *i*. The parameters determine the theoretical maximum value of the imperfections and they should be related to their standard deviations. Since the imperfection field is assumed as ergodic the same boundary values are assigned to each horizontal line. To estimate them the imperfection mean values and standard deviations presented in Table 6.5 are analysed, once more.

The discrepancies between the magnitude of the extreme imperfection related to the standard deviation σ_x / x_{extr} reach from 2.4101 (the 7th line) to 4.5511 (bottom line) and their average equals 3.294 (see Table 6.5).

The same calculations have been performed for all data (9 tanks). The extreme imperfections concerning their standard deviations are presented in Table 6.6. They appeared on the different tank levels (*z/h* in Table 6.6). Only in two cases the extreme values occurred on the tank edges (tank nos. 6 and 7). The maximal value $\sigma_x / x_{extr} = 4.7730$ appeared in tank no. 9 ($V = 50000$ m^3).

Table 6.6

Statistical description of the geometric imperfection along the horizontal lines

Tank no	Extreme values		Tank edge
	z/h	x_{extr} / σ_x	x_{extr} / σ_x
1	0.0625	4.5511	3.6533
2	0.1250	4.5764	3.5357
3	0.7333	3.8638	3.3294
4	0.3750	2.3853	1.6780
5	0.8571	2.5232	2.3843
6	1.0000	3.6732	3.6732
7	1.0000	2.6984	2.6984
8	0.0625	3.3931	2.4055
9	0.1000	4.7730	2.8431
	The means:	3.6042	2.9112

Analysing the data presented in Table 6.5 and 6.6, it is appropriate to assume the following values for the random field boundary:

$$a_i, b_i = \pm s\sigma_i = \pm 5\sigma_i \tag{6.11}$$

where σ_i is the standard deviation at point *i* (see Eq.(6.1)) and s is the truncation parameter (see Eq. (3.28))

$$\sigma_i = K\left(y_i, y_i, z_i, z_i\right) = \alpha z_i^2 h^{-2} \tag{6.12}$$

The boundary formula (6.11) allows for using the Gauss field for which the number of the cut off variates, defining by the parameter $s = 5$ are meaningless. The choice of the boundary values (6.11) determines that the random field is also mathematically (statistically) sound.

The next generation parameters, i.e. the simulation base scheme (see Chapter 3) is defined as a rectangle of dimension 16×16 points. This base scheme is moved horizontally step by step to cover all mesh points. The procedure allows for generating

the tank imperfections, i.e. along the cylindrical surface. As many as 2000 realizations have been generated. Using formulas (6.3) and (6.4) the following errors in the field simulation occurred:

$$\begin{aligned} G_{er} &= 3.30\% \\ V_{er} &= 3.48\% \end{aligned} \tag{6.13}$$

The values (6.13) indicate excellent convergence of the field estimators. Additionally few samples of the generated field of imperfections, presented in Fig. 6.6, prove that the essential features of the measured imperfection map have been numerically reproduced.

6.1.4. Generation of the extreme tank imperfections

The same calculation can be performed in order to obtain the extreme geometric imperfection field. For this purpose the Eq. (6.10) with the following correlation coefficient are implemented:

$$\begin{aligned} \sqrt{\alpha} &= 0.0364 \\ \omega &= 0.317389 \\ \beta &= 0.175900 \\ \gamma &= 0.058001 \end{aligned} \tag{6.14}$$

The same boundary values (6.11) are used. After generating 2000 realizations the following errors occurred

$$\begin{aligned} G_{er} &= 0.15\% \\ V_{er} &= 0.41\% \end{aligned} \tag{6.15}$$

A sample of the generated initial imperfection vector is presented in Fig. 6.7. The vector characterizes the extreme mean value chosen from all 2000 samples in the set. Thus the sample is an extreme one.

Some general conclusions can be formulated.

The method of generating initial imperfections can be directly used to estimate the theoretical capacity of an imperfect tank. For this purpose, when an appropriate field of random vectors is assumed and generated some extreme samples can be selected and on their basis it is possible to calculate the stress field of the construction (Chapter 5.1.2). The selection criteria for the characteristic imperfection samples are, for example: extreme single imperfection, norms of vector values, number of sign changes (number of waves) along the horizontal lines. The choice of the parameters plays an important role in the analysis. Also the definition of the theoretical capacity of the vertical petrol tank should be established.

The method can help in the design process. According to the existing measured imperfection data, their appropriate standard deviation and the correlation function can be assumed. Then, the generation procedure and numerical analysis of the tank with geometric imperfections is applied. In this way a “capacity lower bound” relating to all generated but realistic data can be obtained.

It is also possible to establish the reliability of the tanks by using the Monte Carlo method presented for example in Schenk and Schuëller 2003, Bielewicz and Górski 2002b or Melchers 1999. However in this case more samples should be considered.

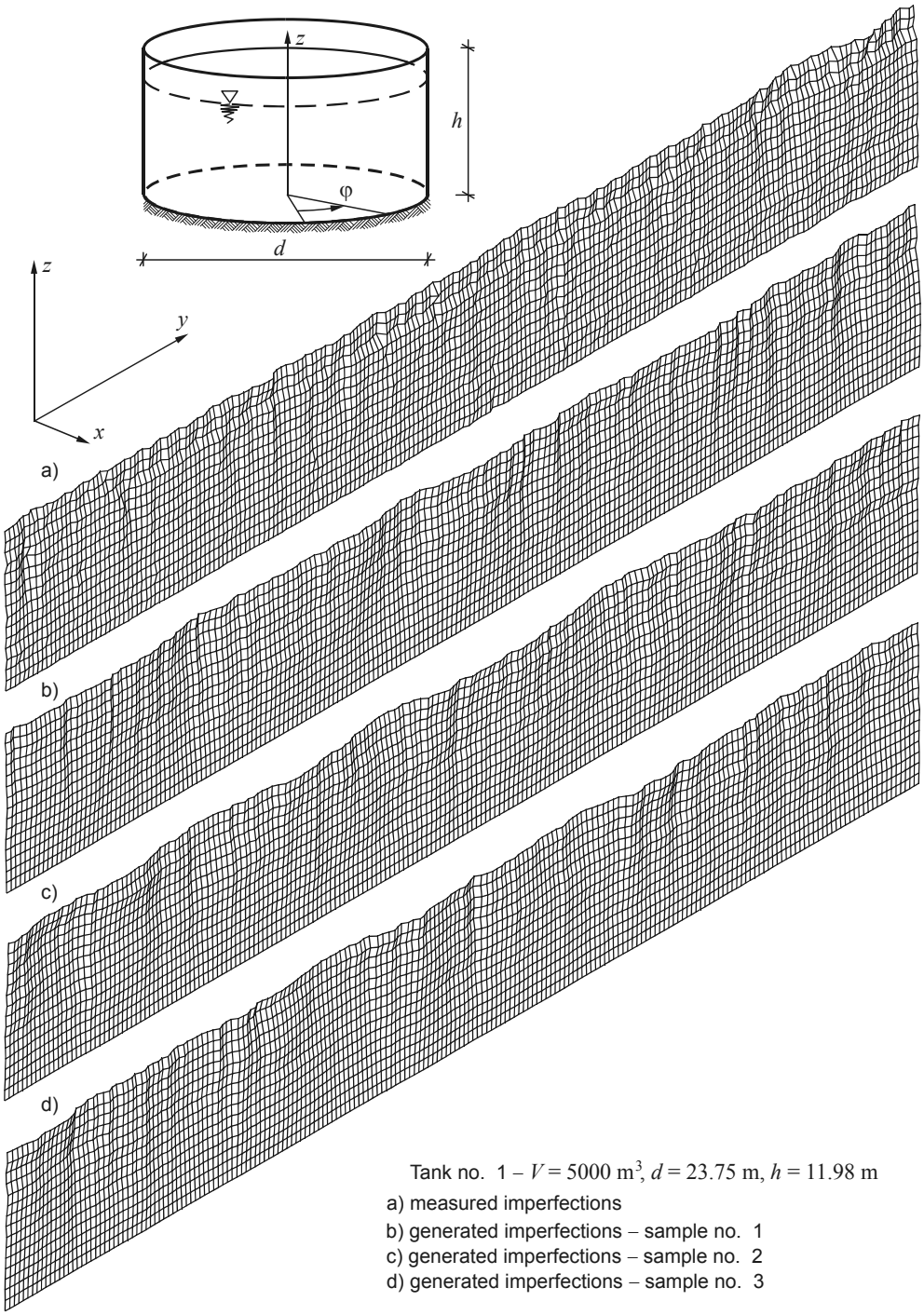

Fig. 6.6. Vertical cylindrical tank: measured geometric initial imperfections (Orlik 1976) and three samples of generated random fields.

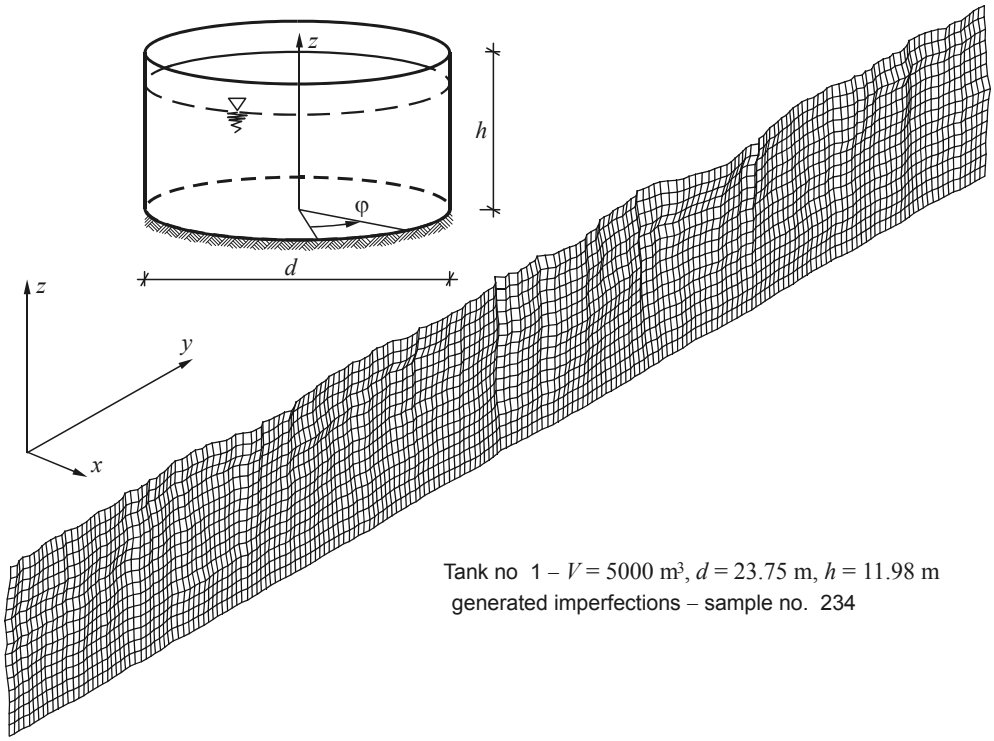

Fig. 6.7. Extreme generated initial geometric imperfections of vertical cylindrical tank

6.1.5. Numerical calculation of vertical petrol tank

The preliminary numerical calculations include three cases of tank no. 1 (5000 m^3).

The first case refers to an ideal cylindrical shell whose data are presented in Fig. 6.8 (Orlik 1976). The tank is made of 6 strakes of plates, each ca. 2000 mm height, and of thicknesses t = 11, 10, 8, 7, 7, and 7 mm, starting from the bottom. Steel St3VY is used for the lower side plates and the first row of the bottom plates, and steel St3SY for other plates. The steel yield stress has been assumed to be R = 255 MPa. Other data of the tank, for example, the foundation parameters k = 50 MN/m^3, are taken from Ziółko (1986). 15646 finite elements were used for the tank model mesh (Górski and Milulski 2005). Some of results, obtained with the help MSC NASTRAN (2001), are presented in Table 6.7.

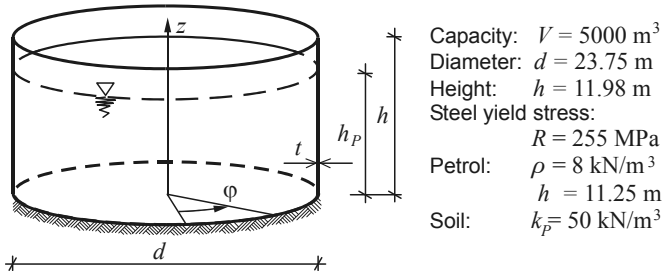

Fig. 6.8. Petrol tank (cylindrical shell) data

Table 6.7

Extreme stresses, bending moments and axial forces in tank with and without initial geometric imperfections

Internal forces	Tank surface		
	ideal	with imperfections	with imperfections
Maximal stresses σ_R MPa	92.24	255	255
Bending moments m_z kNm/m	–0.67 ÷ 0.98	–2.51 ÷ 4.19	–1.38 ÷ 3.76
Bending moments m_φ kNm/m	–0.20 ÷ 0.29	–4.11 ÷ 2.68	–3.42 ÷ 2.40
Axial force n_z kN/m	–7.97 ÷ 20.56	–516.1 ÷ 335.7	–712.7 ÷ 448.2
Axial force n_φ kN/m	–1.23 ÷ 1025.0	–433.6 ÷ 1319.0	–945.2 ÷ 1227.0

The tank data for the second case include the measured initial geometric imperfections presented in Fig. 6.1a (Orlik 1976). As the imperfections have been obtained only for 16 horizontal and 202 vertical lines (3232 points) the missing mesh values are determined by linear interpolation using the neighbouring data. The basis for the numerical calculation is the deformed shape of the cylindrical tank assumed as stress free. The petrol level is raised in every incremental step. The results are presented in Table 6.7 and in Fig. 6.9.

The third calculation are performed for the generated extreme imperfections presented in Fig. 6.7.

The results of the nonlinear calculations, presented in Fig. 6.9 and in Table 6.3 indicate that the tank initial discrepancies can cause significant variations in stress fields in comparison with the solution related to an ideal surface. The steel of the tank with imperfections has yielded at a point connecting the bottom with the side plates, and in the areas where extreme discrepancies appear.

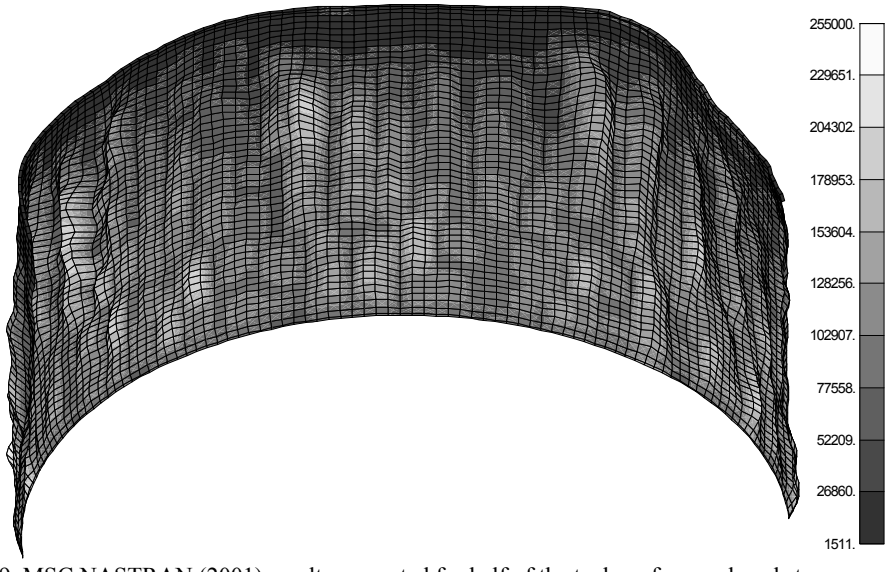

Fig. 6.9. MSC NASTRAN (2001) results presented for half of the tank surface: reduced stresses according to the Huber-Mises-Hencky hypothesis in [kPa] and displacement in magnified scale

It should be noted that the yielding process has occurred despite the fact that the initial field of imperfections is rather a typical one (see Fig. 6.1a).

The results (Fig. 6.9 and Table 6.7) reveal that there is a need for a precise description of the initial geometric imperfections to help in the estimation of their influence on the mechanical behaviour of the cylindrical steel tanks. The formulation of a methodology for the identification, classification and description of the tank imperfections can ensure a better and much safer design. The presented analysis and the numerical calculations have shown that the imperfections should be taken into consideration in the design process of cylindrical tanks, and in general in thin walled structures.

The following comments and suggestions having reference to the future improvements of the identification and modelling of the random fields of imperfections can be made:

1. The result of the identification of the correlation function from limited data measured in situ (see Eq. (6.1) and Fig. 6.6) need further investigation. It is obvious that the use of more data obtained from analyses of similar tanks can significantly improve the calculations.
2. A method of collecting the data of tank geometric imperfections should be formulated. It is essential to define the minimal mesh of the measuring points. The mesh depends on the tank diameter and the characteristics and the magnitude of the imperfections.
3. The achieved results, aided by the statistical analysis have proved the capability of the method to precisely simulate the tank geometric imperfections when the correlation function is known.
4. A generalized version of the correlation function should be formulated for vertical cylindrical tanks of various dimensions and methods of constructions. The primary relations (6.8) can help in future improvements when more measured data can be incorporated in the calculations.
5. The numerical model of tanks can easily be extended to the calculations, for example, by introducing random variability of soil foundations. Also the scattering in the boundary conditions can have a degrading effect on the loading carrying capacity of shells (Arbocz 2000).
6. Assuming that the initial imperfection distribution is given, how should one apply this knowledge to a design procedure? One of the possibilities is the assessment of the cylindrical tank reliability. For example, Arbocz and Starnes (2002) propose the following simple formula based on deterministic design procedure

$$P_a \leq \frac{\lambda_a}{F.S.} P_c \tag{6.16}$$

where P_a is the allowable applied load, P_c stands for the lowest buckling load of the perfect structure, λ_a is the reliability based knockdown factor, and *F.S.* is the safety factor.

6.2. Random imperfections of ship's hull panels

The report by Kmiecik (1970) gives the results and a detailed description of a series of tests, the purpose of which is to investigate the effect of initial deformations on the load-carrying capacity of axially and laterally loaded longitudinally stiffened ship plate panels (see Fig. 6.10). Six specimens are subjected to tests. The specimens were prepared as half-scale models of plates with stiffeners. The initial geometric vertical imperfections of $3 \times 5 = 15$ plate points and some vertical and horizontal displacements of the stiffener points ($3 \times 8 + 3 \times 4 = 24$) were measured. Their maximal values are presented in Fig. 6.11.

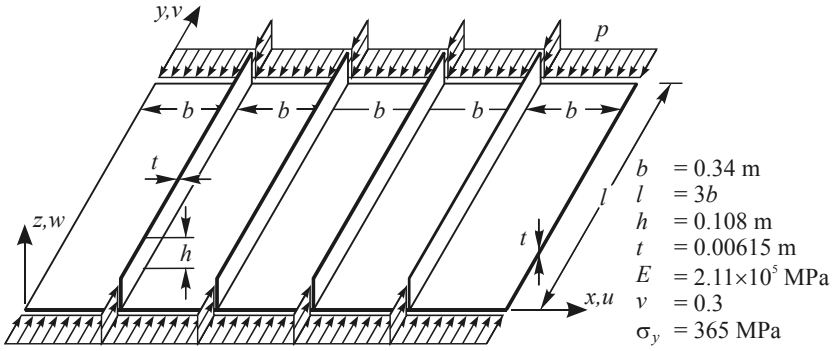

Fig. 6.10. Model of the ship's panel plate with stiffeners

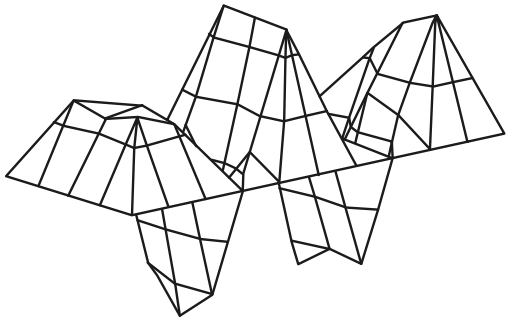

Fig. 6.11. Plate with ribs – the maximal measured value of initial geometric imperfections

Two plates were loaded axially while the others both axially and horizontally. The tests proved that the plate maximal capacity did not depend on the loading direction. The most important factor which affected the plate limit load were the initial geometric imperfections. In all cases the obtained limit load was less than its theoretical value calculated for an ideal plate with ideal boundary conditions (Kmiecik, 1970). For this reason an additional analysis of the initial geometric imperfections and their effect on the mechanical behaviour of the plate seems to be important.

As only six plate specimens were tested in the laboratory a simulation analysis could provide some additional data. Preliminary probabilistic calculations of this problem can be found in Górski and Jasina (2001a and 2001b).

The following covariance function describing the homogeneous random field is adopted:

$$R(x,y) = \sigma^2 \left(1+\lambda_x \cdot |x|\right) \quad e^{-\lambda_x |x|} \left(1+\lambda_y \cdot |y|\right) \quad e^{-\lambda_y |y|} \tag{6.17}$$

where: $|x|$ and $|y|$ denote the field point distances, λ_x and λ_y are correlation decay coefficients characterising the variability of the plate geometric imperfections, and the standard deviation σ represents their scattering. The choice of the correlation function and its parameters are the most important part in the simulation approach. An appropriate assumption of the theoretical model can significantly make the calculations easier.

In the model the distance between the measuring points is equal to $|x| = 0.17\,\text{m}$ and $|y| = 0.255\,\text{m}$ respectively. To assume the correlation coefficients, numerous tests were carried out, and the following parameters were adopted $\lambda_x = \lambda_y = 2.0$. The values confirm that the correlation between the points reach the neighbouring plates separated by the stiffeners. The standard deviations were calculated in the following way

$$\sigma = \frac{1}{3}\left|a_{extr}\right| = \frac{1}{3}2.90 \cdot 10^{-3} \approx 0.97 \cdot 10^{-3}\ \text{m} \tag{6.18}$$

where a_{extr} is the extreme measured imperfection value. It was assumed that according to the normal distribution characteristics, 99.73% of the random values were generated at the interval of $(\overline{x} - 3\sigma,\ \overline{x} + 3\sigma)$. In the calculations only the initial displacement perpendicular to the plate surface was taken into account.

The random field envelope was determined on the basis of the measured imperfection data. Appropriate averaged values were taken into consideration. The double symmetry of the plate allows for considering $6 \times 4 = 24$ (6 plates of double symmetry) sets of the measured realizations.

The upper and lower envelopes are constructed as sinusoid-like surfaces. The amplitudes of the envelopes are assumed to be the maximal and minimal values of the measured imperfections of the plate centres. The stiffener initial deformations are also modelled by appropriate sinusoids. The upper envelope is presented in Fig. 6.12 and the results of the calculations are given in Table 6.8. In the simulation algorithm the intervals $(a_i,\ b_i)$ of the random values are calculated according to the following formulas:

$$a_i = \overline{w}_i + s\left(a_i^* - \overline{w}_i\right), \qquad b_i = \overline{w}_i - s\left(\overline{w}_i - b_i^*\right) \tag{6.19}$$

where s is the truncation constant. Here, the parameter is $s = 1$, a_i^* and b_i^* are shown in Table 6.8.

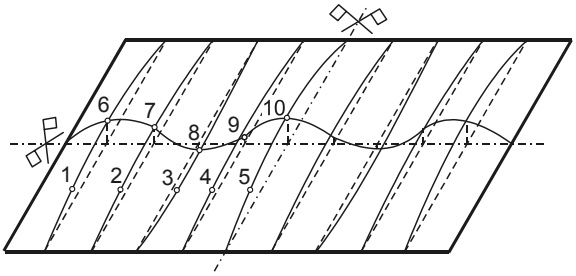

Fig. 6.12. The upper envelope of the random field of the initial geometric imperfections

Making use of the simulation program, 2000 realizations of the initial imperfection field have been generated. With their help the estimators of covariance matrix $\hat{\mathbf{K}}_w$ are determined (see Eq. (6.2)). The results are compared with the test data. The global error of the covariance matrix $\mathbf{K}_w$ is calculated (see Eq. (6.3)):

$$G_{er}\left(\mathbf{K}_w,\ \hat{\mathbf{K}}_w\right) = 19.0\% \tag{6.20}$$

In this case the error value depends not only on the choice of the algorithm parameters but also on the limited experimental data.

The presented approach leads to the nonlinear stochastic problem of compressed plates with ribs. Geometric and material nonlinear solutions have been obtained with the help of BOX program (Chróścielewski 1996). A convergence analysis of calculations of plates with initial geometric imperfection using the BOX program can be found, for example, in Chróścielewski et al. (1998). The boundary conditions are assumed as clamped with possibility of displacements in the load directions. Geometric imperfections in the finite elements nodes are introduced as stress-free kinematic constraints.

Table 6.8

The average values and the envelopes of the initial geometric imperfections

Point No.	Measured values [mm]			Calculated values [mm]		
	Mean values	Maximal values	Minimal values	Mean values $\bar{w}_i$	Maximal values a_i^*	Minimal values b_i^*
1	0.736	2.000	–0.323	0.437	1.418	–0.544
2	0.103	1.190	–0.640	0.244	0.940	–0.453
3	–1.930	–1.300	–2.650	–1.430	–0.810	–2.051
4	0.046	0.540	–0.450	0.007	0.382	–0.368
5	1.670	2.420	1.050	1.298	1.853	0.742
6	0.501	1.360	–0.773	0.617	2.005	–0.770
7	0.131	1.330	–0.600	0.345	1.330	–0.640
8	–2.060	–1.140	–2.900	–2.023	–1.145	–2.900
9	0.059	0.530	–0.520	0.010	0.540	–0.520
10	1.740	2.620	1.000	1.835	2.620	1.050

In order to determine the most unsafe (extreme) discrepancies the method of selection of the extreme input realizations presented in Chapter 5.1.2 is implemented. To this end some characteristic random variable vectors are selected from the generated realization set. These vectors are characterized by:

— maximal or minimal number of positive or negative random values,
— maximal or minimal norms of the random vectors,
— components which are close to an eigen-form of the model.

Two example of the generated realizations are presented in Fig. 6.13.

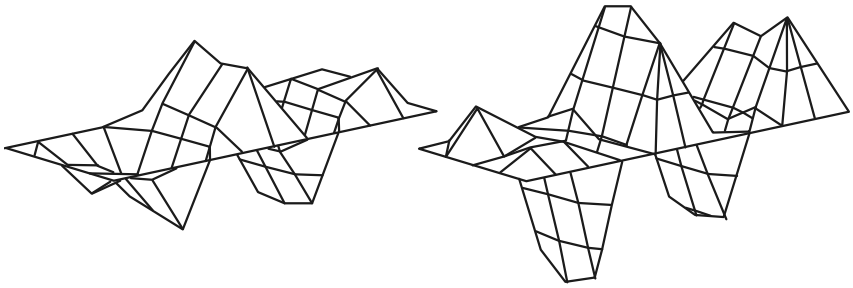

Fig. 6.13. Generated realizations of plates with geometric imperfections

In the calculation the generated imperfections of shape and magnitude close to the envelope of the measured values has been chosen (see Table 6.8). On their bases, using the BOX program the following extreme critical stresses σ_{cr}^{ext} of the plate are calculated

$$\sigma_{cr}^{ext} = 273.0 \text{ MPa} \qquad (\sigma_{cr}^{ext} / \sigma_y = 0.748) \tag{6.21}$$

Additionally, the plate critical stresses calculated for the mean imperfection $\bar{w}_i$ (Table 6.8) has been obtained

$$\sigma_{cr}^{mean} = 312.4 \text{ MPa} \qquad (\sigma_{cr}^{mean} / \sigma_y = 0.856). \tag{6.22}$$

The critical stresses calculated for the extreme values of imperfection is 12.6% less than the stresses related to the mean plate imperfection. The load paths in the two calculated cases are presented in Fig. 6.14.

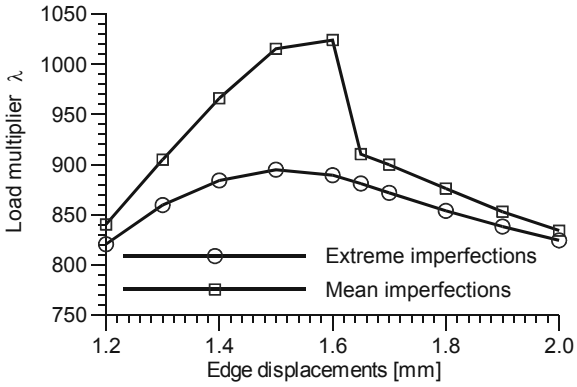

Fig. 6.14. Equilibrium paths for plates with geometric imperfections

It should be pointed out that the presented calculations are preliminary ones. The obtained geometric imperfection fields are described in terms of a set of generated realisations and the resulting statistic estimators. This can lead to a solution of a set of deterministic problems and to obtaining probabilistic distributions of the limit loads for the structure models (Monte Carlo method). Then, the reliability of the models can be computed by use of the exact formula (level-3 method).

The results of the proposed approach can be considered to be useful in modelling the random fields of engineering structures.

Chapter 7

FINAL REMARKS

The work presents the capabilities of the simulation based approach when stochastic nonlinear models of structure are considered. The following comments can be made:

1. Since exact solutions of geometrically and/or materially nonlinear random imperfect structures are not available, the simulation based approach with the Monte Carlo method and the finite element procedures is proposed.
2. This approach provides facilities for probabilistic distribution of limit loads of randomly imperfect structures, and as a result the quality of the structure stochastic responses can be specified. It has been proved that the type of random initial imperfection field, for example the degenerate type or the Wiener type, has influence on the obtained results.
3. Two methods of structure reliability estimation have been used:
   – level-3 reliability calculations,
   – determination of limit state histograms on the basis of loading multipliers calculated at every simulation step.

   The level-3 calculations have proved to be the most efficient in the case of reliability estimation of nonlinear models. But, it should be pointed out that when the theoretical load distribution is not known, the loading multipliers method presents definite advantages.
4. With the help of the limit state histogram a sensitivity analysis of random parameters describing the structure load capacity is possible.
5. Using simple nonlinear models with one and two degrees of freedom the application of direct and stratified Monte Carlo method to the reliability calculations has been examined. It has been proved that the stratified procedure combined with the level-3 reliability method characterises a faster convergence to an expected solution.
6. With respect to two dimensional structures the simulation techniques of random fields play the most important role in the analysis. The statistical analysis of the simulated nonhomogeneous, second-order random fields has proved a high accuracy of the proposed simulation method. The method will be especially useful in modelling nonlinear stochastic boundary value problems encountered in engineering.
7. The accuracy of numerical calculations can be studied at the input level (simulations of the imperfections) and/or at the output level (numerically obtained results). Advantage has been taken of the following strategies:
   – The reduction procedure of the initial number of random samples enables to minimize the calculations without losing the result estimators accuracy.
   – Progressive calculations of some measures of the output Monte Carlo results are presented. The estimators stabilize as the number of samples increases, and in this way a sufficient degree of the calculation accuracy can be obtained. The procedure effectively reduces the initial data set.

   The numerical examples show that for practical purposes the accuracy investigations can be restricted only to the output level.

– A procedure of choosing some characteristic initial realizations of the random fields has been proposed. The extreme geometrical and/or material samples can be utilized for the description of the limit response of the structure under consideration.

8. A concept of choosing a specific type of favourable and unfavourable probability distributions of random variables is proposed. Their analysis leads to the estimation of two reliability values to assess the structure reliability interval.
9. The main open question is the determination of the type of random field which should be applied to analyse the structural response. Two examples of defining the correlation function type taking into consideration the existing experimental data are given. It has been proved that the initial geometric imperfections have an evident influence on the numerical calculation results, and can reduce the structure load capacity.
10. The simulation-based approach can play an important role in the nonlinear analysis of imperfect structures. Such analyses are extremely time consuming but the power of computers is continuously growing.
11. The design processes of the imperfection-sensitivity structures such as columns, shells, plates and others, should be preceded not only by numerical calculations but also by theoretical considerations and experimental measurements. Engineering knowledge and experience play an essential role in the analysis.

REFERENCES

[1] Aczél J., Daróczy Z.: On measures of information and their characterizations. New York, San Francisco, London: Academic Press 1975.

[2] Adler R. J.: *The geometry of random fields.* Chichester, New York, Brisbane, Toronto: John Wiley & Sons 1981.

[3] Adomian G.: *Stochastic systems.* New York: Academic Press 1983.

[4] Ambartzumian R., Der Kiureghuan A., Ohanian V., Sukiasian H.: Multinormal probabilty by sequential conditional importance sampling: theory and application. *Prob. Engng. Mech.* 13, 1998, 298–308.

[5] Anders M., Hori M.: Development of stochastic finite element method for simulation of surface earthquake fault. *Journal of Applied Mechanics ASCE* 3, 2000, 595–600.

[6] Anders M., Hori M.: Stochastic finite element method for elasto-plastic body. *Int. J. Numer. Meth. Engng.* 46, 1999, 1897–1916.

[7] Ang G. L., Ang A. H. S., Tang W. H.: Optimal importance sampling density estimators. *J. Eng. Mech. ASCE* 118, 6, 1991, 1146–1163.

[8] Araújo J. M.: Probabilistic analysis of reinforced concrete columns. *Advances in Engineering Software* 32, 2001, 871–879.

[9] Arbocz J.: On accuracy of numerical buckling load predictions. *Proc. of the 6th Conference „Shell Structures. Theory and Applications".* General lectures (Eds. J. Chróścielewski, W. Pietraszkiewicz). Gdańsk, Poland 1998, 19–23.

[10] Arbocz J.: The effect of imperfect boundary conditions on the collapse behaviour of anisotropic shells. *International Journal of Solids and Structures* 37, 2000, 6891–6915.

[11] Arbocz J., Hol M. A. M.: Collapse of axially compressed cylindrical shells with random imperfections. *AIAA Journal* 29, 12, 1991, 2247–2256.

[12] Arbocz J., Hol M. A. M.: Collapse of axially compressed cylindrical shells with random imperfections. *Thin-Walled Structures* 23, 1995, 131–158.

[13] Arbocz J., Starnes J. H. Jr.: Future directions and challenges in shell stability analysis. *Thin-Walled Structures* 40, 2002, 729–754.

[14] Au S. K., Beck J. L.: First excursion probabilities for linear systems by very efficient importance sampling. *Prob. Engng. Mech.* 16, 2001, 193–207.

[15] Augusti G., Baratta A., Casciati F.: *Probabilistic methods in structural engineering.* London, New York: Chapman & Hall 1984.

[16] Augusti G., Ciampoli M. Zanobi S.: Bound to the probability of collapse monumental building. *Structural Safety* 24, 2002, 89–105.

[17] Ayyab B. M., Haldar A.: Practical structural reliability techniques. *J. Structural Engineering ASCE* 110, 8, 1984, 1707–1724.

[18] Bargiela A., Pedrycz W.: *Granular computing: an introduction.* Boston, Dordrecht, London: Kluwer Academic Publishers 2001.

[19] Bayer V., Bucher Ch.: Importance sampling for first passage problems of nonlinear structures. *Prob. Engng. Mech.* 14, 1999, 27–32.

[20] Bazant Z. P., Liu K. L.: Random creep and shrinkage in structures: sampling. *Journal of Structural Engineering ASCE* 111, 5, 1985, 1113–1134.

[21] Ben Haim Y.: A non probabilistic measure of reliability of linear system based on expansion of convex models. *Structural Safety* 17, 1995, 91–109.

[22] Ben Haim Y.: Design certification with information-gap uncertainty. *Structural Safety* 21, 1999, 269–289.

[23] Ben Haim Y.: *Robust reliability in the mechanical sciences*. Berlin, Heidelberg, New York, Barcelona, Budapest, Hong Kong, London, Milan, Paris, Santa Clara, Singapore, Tokyo: Springer-Verlag 1996.

[24] Bendat J. S.: *Nonlinear system analysis and identification from random data*. New York, Chichester, Brisbane, Toronto, Singapore: John Wiley & Sons 1990.
[25] Bendat J. S., Piersol A. G.: *Engineering applications of correlation and spectral analysis*. New York, Chichester, Brisbane, Toronto, Singapore: John Wiley & Sons 1993.
[26] Bendat J. S., Piersol A. G.: *Random data: analysis and measurement procedures*. New York, London, Sydney, Toronto: Wiley-Interscience 1971.
[27] Beniamin J. R., Cornell C. A.: *Rachunek prawdopodobieństwa, statystyka matematyczna i teoria decyzji dla inżynierów*. Warszawa: WNT 1977.
[28] Bethea R. M., Duran B. S., Boulion T. L.: *Statistical methods for engineers and scientists.* New York: Marcel Derker Inc. 1984.
[29] Bhattacharyya B., Chakraborty S.: NE-MCS technique for stochastic structural response sensitivity. *Comput. Methods Appl. Mech. Engrg.* 191, 2002, 5631–5645.
[30] Biegus A.: *Probabilistyczna analiza konstrukcji stalowych*. Warszawa, Wrocław: Wydawnictwo Naukowe PWN 1999.
[31] Bielewicz E., Górski J.: Reliability of imperfect structures – simple nonlinear models. *Journal of Civil Engineering and Management* 8, 2, 2002a, 83–87.
[32] Bielewicz E., Górski J.: Shell with random geometric imperfections. Simulation-based approach. *International Journal of Non-linear Mechanics* 37, 4–5, 2002b, 777–784.
[33] Bielewicz E., Górski J., Skowronek M.: Program generacji dwuwymiarowych, dyskretnych pól losowych. *II Konferencja – Problemy Losowe w Mechanice Konstrukcji.* Gdańsk 1985a, 23–30.
[34] Bielewicz E., Górski J., Skowronek M.: Program na EMC dla powłok obrotowych z uwzględnieniem losowego charakteru geometrii. *6 Konferencja „Metody Komputerowe w Mechanice Konstrukcji"*. Białystok 1983, 43–50.
[35] Bielewicz E., Górski J., Skowronek M.: Redukcja zbioru realizacji w symulacji dwuwymiarowego pola losowego. *Zesz. Nauk. Pol. Gdańskiej*, nr 408, *Budownictwo Lądowe* 44, 408, 1987, 7–15.
[36] Bielewicz E., Górski J., Walukiewicz H.: Computer simulation in structural mechanics and in environmental problems. *Proc. of the 6th International Conference on Civil and Structural Engineering. CIVIL-COMP95 „Developments in Computer Aided Design and Modelling for Structural Engineering"* (Ed. B. H. V. Topping). Cambridge, England 1995a, 245–252.
[37] Bielewicz E., Górski J., Walukiewicz H.: Digital simulation of random fields for structural applications. *Proc. of the 2nd Conference on Computational Structures Technology „Advances in Computational Mechanics"* (Eds. M. Papadrakakis, B. H. V. Topping). Greece 1994. Edinburgh, Scotland 1994a, 353–359.
[38] Bielewicz E., Górski J., Walukiewicz H.: *Dyskretne dwu-wymiarowe pola losowe. Symulacja i klasyfikacja*. Centralny Program Badań Podstawowych, Instytut Podstawowych Problemów Techniki PAN, Problem Węzłowy 05.12, Temat 11.2, Gdańsk 1988.
[39] Bielewicz E., Górski J., Walukiewicz H.: Monte Carlo method in nonlinear structural analysis. *Zesz. Nauk. Pol. Gdańskiej*, nr 520, *Budownictwo Lądowe* 50, 1995b, 11–25.
[40] Bielewicz E., Górski J., Walukiewicz H.: Random fields. Digital simulation and applications in structural mechanics. *Proc. of the 1st International Conference „Computational Stochastic Methods"* (Eds. P. D. Spanos, C. A Brebia). Corfu, Greece 1991, 559–568.
[41] Bielewicz E., Skowronek M., Górski J.: *Algorytmy i programy na EMC symulacji pól losowych w powłokach*. Centralny Program Badań Podstawowych, Instytut Podstawowych Problemów Techniki PAN, Problem Węzłowy 05.12, Temat 11.2, Gdańsk 1985b.
[42] Bielewicz E., Skowronek M., Górski J.: *Obliczenia statystyczne i dynamiczne powłok o losowej nieliniowości materiałowej i losowej geometrii.* Centralny Program Badań Podstawowych, Instytut Podstawowych Problemów Techniki PAN, Problem Węzłowy 05.12, Temat 11.2, Gdańsk 1984.
[43] Bielewicz E., Skowronek M., Górski J.: *Zastosowanie metody perturbacji w analizie powłok obrotowych z geometrycznymi imperfekcjami*. Centralny Program Badań Podstawowych, Instytut Podstawowych Problemów Techniki PAN, Problem Węzłowy 05.12, Temat 11.2, 1981–1982, Gdańsk 1982.

[44] Bielewicz E., Dobrowolski K., Skowronek M., Górski J.: *Analiza statyczna powłok z losowymi parametrami*. Centralny Program Badań Podstawowych, Instytut Podstawowych Problemów Techniki, Problem Węzłowy Nr 05.12, Temat 11.2, Gdańsk 1980.
[45] Bielewicz, E., Górski, J., Schmidt, R., Walukiewicz, H.: Random fields in the limit analysis of elastic-plastic shell structures. *Computers and Structures* 51, 3, 1994b, 267–275.
[46] Bielewicz E., Chróścielewski J., Górski J., Jankowski R., Jasina M., Smoleński W. Walukiewicz H., Jagiełło J.: *Pola losowe i ich zastosowanie w mechanice*. Komitet Badań Naukowych. Projekt badawczy 3 P40405505, 1993–1995, Gdańsk 1995c.
[47] Biondini F., Bontempi F., Frangopol D. M., Malerba P. G.: Reliability of material and geometrically non-linear reinforced and prestressed concrete structures. *Computers and Structures* 82, 2004, 1021–1031.
[48] Bjerager P.: Probability integration by directional simulation. *J. Eng. Mech. ASCE* 114, 8, 1988, 1285–1302.
[49] Bołotin W. W.: *Metody statystyczne w mechanice budowli.* Warszawa: Arkady 1968.
[50] Borowkow A. A.: *Rachunek prawdopodobieństwa.* Warszawa: PWN 1977.
[51] Brandt S.: *Analiza danych. Metody statystyczne i obliczeniowe.* Warszawa: Wydawnictwo Naukowe PWN 1998.
[52] Breitung K.: Asymptotic approximation for multinormal integrals. *J. Eng. Mech. ASCE* 110, 3, 1984, 357–366.
[53] Brenner C., Bucher C.: A contribution to the SFE-based reliability assessment of non linear structures under dynamic loading. *Prob. Eng. Mech.* 10, 4, 1995, 265–273.
[54] Brinkmann G., et al.: *Leicht und Weit. Zur Konstruktion Weitgespannter Flächentragwerke.* Weinheim: VCH 1990.
[55] Brząkała W., Puła W.: A probabilistic analysis of foundation settlements. *Computers and Geotechnics* 18, 4, 1996, 291–309.
[56] Bucher C.: Adaptive sampling – an iterative fast Monte Carlo procedure. *Structural Safety* 5, 2, 1988, 119–126.
[57] Bucher C.: Some recent software developments for stochastic structural analysis. *Proc. of the 5th International Conference, Modern Building, Materials, Structures and Techniques.* Vilnius, Lithuania, 2, 112, 1997.
[58] Bucher C., Bourgund U.: A fast and efficient response surface approach for structural reliability problem. *Structural Safety* 7, 2, 1990, 57–66.
[59] Bucher C., Brenner C. E.: Stochastic response of uncertain systems. *Archive of Applied Mechanics* 62, 1992, 507–516.
[60] Bucher C., Schuëller G. I.: Software for reliability-based analysis. *Structural Safety* 16, 1/2, 1994, 13–22.
[61] Burczyński T.: *Metoda elementów brzegowych w mechanice*. Warszawa: WNT 1995.
[62] Burczyński T., Skrzypczyk J.: Theoretical and computational aspects of the stochastic boundary element methods. *Comp. Methods Appl. Mech. Eng.* 168, 1999, 321–344.
[63] Carmeliet J., Hens H.: Probabilistic nonlocal damage model for continua with random field properties. *J. Eng. Mech. ASCE* 120, 10, 1994, 2013–2026.
[64] Cederbaum G., Arbocz J.: On the reliability of imperfection-sensitive long isotropic cylindrical shells. *Structural Safety* 18, 1, 1996a, 1–9.
[65] Cederbaum G., Arbocz J.: Reliability of imperfection-sensitive composite shells via the Koiter-Cohen criterion. *Reliability Engineering and System Safety* 56, 1997, 257–263.
[66] Cederbaum G., Arbocz J.: Reliability of shells via Koiter formulas. *Thin-Walled Structures* 24, 1996b, 173–187.
[67] Chakraborty S., Bhattacharyya B.: An efficient 3D stochastic finite element method. *Inernational Journal of Solids and Sructures* 39, 2002, 2465–2475.
[68] Chakraborty S., Dey S. S.: An efficient stochastic finite element method for random field problems. *Applied Mechanic and Engineering* 4, 1, 1999, 45–71.
[69] Cheng A. H.-D., Yang C. Y. (Eds.): *Computational stochastic mechanics*. London, New York: Elsevier 1993.

[70] Cornell C. A.: Bounds on reliability of structural systems. *J. Structural Div. ACSE* 93, 1, 1967, 171–200.
[71] Chróścielewski J.: *Analiza numeryczna płyt użebrowanych w zakresie nieliniowości geometrycznej i materiałowej metodą elementów skończonych*. Rozprawa doktorska. Politechnika Gdańska, Wydz. Budownictwa Lądowego 1983.
[72] Chróścielewski J.: Rodzina elementów skończonych klasy C^0 w nieliniowej sześcioparametrowych teorii powłok. *Zesz. Nauk. Pol. Gdańskiej*, nr 540, *Budownictwo Lądowe* 53, 1996.
[73] Chróścielewski J., Górski J., Schmidt R.: Stochastic model of material uncertainties in structural analysis. *Proc. of the International Scientific Conference „Models, Numerical Methods and Applications". Numerical Methods in Continuum Mechanics*. Stara Lesna, Slovakia 1994, 322–329.
[74] Chróścielewski J., Janczewski D., Jasina M.: Sprężysto-plastyczna analiza stateczności konstrukcji cienkościennych za pomocą elementów DCT. *Konferencja „Stateczność konstrukcji cienkościennych"*. Zielona Góra 1998, 19–22.
[75] Chróścielewski J., Makowski J., Stumpf H.: Finite element analysis of smooth, folded and multi-shell structures. *Comput. Methods Appl. Mech. Engng.* 141, 1997, 1–46,
[76] Chryssanthopoulos M. K., Poggi C.: Probabilistic imperfection sensitivity analysis of axially compressed composite cylinders. *Eng. Struct.* 17, 1995, 398–406.
[77] Das P. K., Zheng Y.: Cumulative formulation of response surface and its use in reliability analysis. *Prob. Engng. Mech.* 15, 2000, 309–315.
[78] De Lima B. S. L. P., Ebecken N. F. F.: A comparison of models for uncertainty analysis by the finite element method. *Finite Element in Analysis and Design* 34, 2000, 211–232.
[79] Deml M., Wunderlich W.: Direct evaluation of the „worst" imperfection shape in shell buckling. *Compu. Methods Appl. Mech. Eng.* 149, 1997, 201–222.
[80] Deodatis G.: Bounds on response variability of stochastic finite element systems. *J. Eng. Mech. ASCE* 116, 3, 1990, 556–587.
[81] Deodatis G.: The weighted integral method, I: stochastic stiffness matrix. *J. Eng. Mech. ASCE* 117, 8, 1991, 1851–1864.
[82] Deodatis G., Shinozuka M.: The weighted integral method, II: response variability and reliability. *J. Eng. Mech. ASCE* 117, 8, 1991, 1865–1877.
[83] Der Kiureghian A., Dakessian T.: Multiple design points in first and second-order reliability. *Structural Safety* 20, 1, 1998, 37–50.
[84] Der Kiureghian A., Ke J.-B.: The stochastic finite element method in structural reliability. *Prob. Engng. Mech.* 3, 2, 1988, 83–91.
[85] Der Kiureghian A., Liu P.L.: Structural reliability under incomplete probability information. *J. Eng. Mech. ASCE* 112, 1, 1986, 85–104.
[86] Devroye L.: *Non-uniform random variate generation.* New York, Berlin, Heidelberg, Tokyo: Springer-Verlag 1986.
[87] Devroye L., Györfi L., Lugosi G.: *A probabilistic theory of pattern recognition.* New York, Berlin, Heidelberg, Barcelona, Budapest, Hong Kong, London, Milan, Paris, Santa Clara, Singapore, Tokyo: Springer-Verlag 1996.
[88] Ditlevsen O.: Narrow reliability bounds for structural systems. *J. Structural Mechanics* 7, 4, 1979, 453–472.
[89] Ditlevsen O., Madsen H. O.: *Structural reliability method.* Chichester, New York, Brisbane, Toronto, Singapore: John Wiley & Sons 1996.
[90] Ditlevsen O., Olesen R. Mohr G.: Solution of class of load combination problems by directional simulation. *Structural Safety* 4, 2, 1987, 95–109.
[91] Dolinski K.: First-Order Second Moment approximation in reliability of structural systems: critical review and alternative approach. *Structural Safety* 41, 1983, 211–213.
[92] Doob J. L.: *Measure theory*. New York, Berlin, Heidelberg, London, Paris, Tokyo, Hong Kong, Barcelona, Budapest: Springer-Verlag 1994.
[93] Elishakoff I.: Impact buckling of thin bar via Monte Carlo method. *Journal of Applied Mechanics* 45, 3, 1978, 586–590.

[94] Elishakoff I.: *Probabilistic methods in the theory of structures.* New York, Chichester, Brisbane, Toronto, Singapore: John Wiley & Sons 1983.
[95] Elseifi M. A., Gürdal Z., Nikolaidis E.: Convex/probabilistic models of uncertainties in geometric imperfections of stiffened compositie panels. *AIAA Journal* 37, 4, 1999, 468–474.
[96] Enevoldsen I., Faber M. H., Sorensen J. D.: Adaptive Response Surface Techniques in reliability estimation. In: *Structural Safety and reliability. Proc. of ICOSSAR'93.* Insbruck, Austria, 9–13 August 1993 (Eds. G. I. Schuëller, M. Schinozuka, J. T. P. Yao), II, 1994, 1257–1265.
[97] Engelund S., Rackwitz R.: A benchmark study on importance sampling techniques in structural reliability. *Structural Safety* 12, 4, 1993, 255–276.
[98] Er G.-K.: A method for multi-parameter PDF estimation of random variables. *Structural Safety* 20, 1998, 25–36.
[99] Falsone G., Impollonia N.: About the accuracy of a novel response surface method for the analysis of finite element modelled uncertain structures. *Prob. Engng. Mech.* 19, 2004, 53–63.
[100] Faravelli L.: Response-surface approach for reliability analysis. *J. Eng. Mech. ASCE* 115, 12, 1989, 2763–2781.
[101] Fenton G. A., Vanmarcke E. H.: Simulation of random fields via local average subdivision. *J. Eng. Mech. ASCE* 116, 8, 1990, 1733–1749.
[102] Ferson S., Ginzburg L. R.: Different methods are needed to propagate ignorance and variability. *Reliability Engineering and System Safety* 54, 1996, 133–144.
[103] Fisher N. I.: *Statistical analysis of circular data.* Great Britain, Cambridge University Press 1993.
[104] Florian A.: An efficient sampling scheme: Updating Latin Hypercube Sampling. *Prob. Engng. Mech.* 7, 1992, 123–130.
[105] Frangopol D. M., Yutake I., Spacone E., Iwaki I.: A new look at reliability of reinforced concrete columns. *Structural Safety* 18, 2/3, 1996, 123–150.
[106] Freudenthal A. M.: Safety, reliability and structural design. *J. Structural Div.* ASCE 87, ST3, 1961, 1–16.
[107] Freudenthal A. M., Garrelts J. M., Shinozuka M.: The analysis of structural safety. *J. Structural Div.* ASCE 92, ST1, 1966, 267–325.
[108] Fu M., Hu J.-Q.: *Conditional Monte Carlo. Gradient estimation and optimization application.* Boston, London, Dordrecht: Kluwer Academic Publishers 1997.
[109] Fujita M., Rackwitz R.: Updating first and second order reliability estimation by Importance Sampling. *Structural Engineering and Earthquake Engineering* AJSCE 5, 1, 1988, 31–37.
[110] Giannini R., Pagnoni T., Pinto P. E., Vanzi I.: Risk analysis of a medieval tower before and after strengthening. *Structural Safety* 18, 2/3, 1996, 81–100.
[111] Gomes H. M, Awruch A. M.: Comparison of response surface and neural network with other methods for structural reliability analysis. *Structural Safety* 26, 7, 2004, 49–67.
[112] Gomes H. M, Awruch A. M.: Reliability of reinforced concrete structures using stochastic finite elements. *Engineering Computations* 19, 7, 2002, 764–786.
[113] Górski J.: Geometric imperfections of cylindrical shell-identification and simulation. *Proc. of the 7th International Conference „Modern Building Materials, Structures and Techniques"*. Vilnius, Lithuania 2001a, CDROM Proceedings, 6.
[114] Górski J.: Identification and simulation of geometric imperfections in plates and shells. *Proc. of the 2nd European Conference on Computational Mechanics „Solid, Structures and Coupled Problems in Engineering"*. Cracow, Poland, Abstract Vol. 1, 2001b, 318–319.
[115] Górski J.: Simulation-based nonlinear analysis of imperfect structures. *Archives of Civil Engineering* 47, 1, 2001c, 3–18.
[116] Górski J., Jasina M.: Identyfikacja i symulacja imperfekcji geometrycznych płyt z żebrami. *Zesz. Nauk. Pol. Gdańskiej*, nr 585, *Budownictwo Lądowe* 56, 2001a, 79–86.
[117] Górski J., Jasina M.: Symulacja imperfekcji geometrycznych na podstawie danych doświadczalnych. *VII Warsztaty Naukowe PTSK „Symulacja w Badaniach i Rozwoju"* (Eds. L. Bobrowski, R. Bogacz). Zakopane 2000. Warszawa 2001b, 75–84.

[118] Górski J., Mikulski T.: Statistical description and numerical calculations of cylindrical vertical tanks with initial geometric imperfections. *The 8th Conference „Shell Structures. Theory and Applicatios"* (Eds. C. Szymczak, W. Pietraszkiewicz). Gdańsk, Poland 2005.
[119] Górski J., Walukiewicz H.: Symulacja i analiza pól loswych z osobliwą macierzą kowariancyjną. *VI Warsztaty Naukowe PTSK „Symulacja w Badaniach i Rozwoju"* (Eds. L. Bobrowski, R. Bogacz). Białystok, Białowieża 1999. Warszawa 2000, 55–63.
[120] Graham L. L., Gurley K., Masters F.: Non-Gaussian simulation of local material properties based on a moving-window technique. *Prob. Engng. Mech.* 18, 2003, 223–234.
[121] Griannini R., Pagnoni T., Pinto P. E., Vanzi I.: Risk analysis of a medieval tower before and after strengthening. *Structural Safety* 18, 2/3, 1996, 81–100.
[122] Grigoriu M.: Crossing of non-Gaussian translation processes. *J. Engineering Mechanics Div. ASCE* 110, 6, 1983, 610–620.
[123] Grigoriu M., Balopoulou S.: A simulation method for stationary Gaussian random function based on the sampling theorem, *Prob. Engng. Mech.* 8, 1993, 239–254.
[124] Grimmelt M. J., Shuëller G. I.: Benchmark study on methods to determine collapse failure probabilities of random structures. *Structural Safety* 1, 1982, 93–106.
[125] Hall P.: *The Bootstrap and the Edgeworth Expansion*. New York: Springer-Verlag 1992.
[126] Hammersley J. M., Handscomb D. C.: *Monte Carlo methods*. London: Methuen & Co Ltd 1964.
[127] Haugen E. B.: *Probabilistic approach to design*. London, New York, Sydney: John Wiley & Sons 1968.
[128] Helton J. C., Davis F. J.: Latin hypercube sampling and the propagation of uncertainty in analyses of complex system. *Reliability Engineering and System Safety* 81, 2003, 23–69.
[129] Henriques A. A. R., Calheiros F., Figueiras J. A.: Latin hypercube sampling and the propagation of uncertainty in analyses of complex system. *Engineering Computations* 19, 3, 2002, 346–363.
[130] Hong H. P., Lind N. C.: Approximate reliability analysis using normal polynomial and simulation results. *Structural Safety* 18, 1996, 329–339.
[131] Hong H. P., Zhou W.: Reliability evaluation of RC columns. *Journal of Structural Engineering* 125, 7, 1999, 784–790.
[132] Hora S. C., Helton J. C.: A distribution-free test for the relationship between model input and output when using Latin hypercube sampling. *Reliability Engineering and System Safety* 79, 2003, 333–339.
[133] Hoshiya M.: Conditional simulation of a stochastic field. In: *Structural Safety and reliability. Proceeding of ICOSSAR'93*, Insbruck, Austria, 9–13 August 1993 (Eds. G. I. Schuëller, M. Schinozuka, J. T. P. Yao) 1994, 349–354.
[134] Hou Z., Hera A., Noori M.: A stochastic model for localized disturbances and its applications. *Prob. Engng. Mech.* 19, 2004, 211–218.
[135] Huntington D. E., Lyrintzis C. S.: Improvements to and limitations of Latin hypercube sampling. *Prob. Engng. Mech.* 13, 4, 1998, 245–253.
[136] Hurtado J. E.: Analysis of one-dimensional stochastic finite element using neural network. *Prob. Engng. Mech.* 17, 2002, 35–44.
[137] Hurtado J. E., Alvarez D. A.: Classification approach for reliability analysis with stochastic finite-element modelling. *Journal of Structural Engineering* 129, 8, 1999, 1141–1149.
[138] Hurtado J. E., Alvarez D. A.: Neural-network-base reliability analysis: a comparative study. *Computer Methods in Applied Mechanical Engineering* 191, 2001, 113–132.
[139] Hurtado J. E., Barbat A. H.: Monte Carlo techniques in computational stochastic mechanics, *Archives of Computational Method in Engineering* 5, 1, 1998, 3–30.
[140] Huseyin, K.: *Nonlinear Theory of Elastic Stability.* Leyden: Noordhoff International Publishing 1975.
[141] Ikeda K., Murota K.: Random initial imperfections of structures. *Int. J. Solids and Structures* 28, 8, 1991, 1003–1021.
[142] Jankowski R., Walukiewicz H.: Modeling of two-dimensional random fields. *Prob. Engng. Mech.* 12, 2, 1997, 115–121.

[143] Jeong H. K., Shenoi R. A.: Probabilistic strength analysis of rectangular FRP plates using Monte Carlo simulation. *Computers and Structures* 76, 2000, 219–235.
[144] Johnson N. L. S., Kotz S., Balakrishnan N.: *Continuous Univariate Distribution*. 2nd edition, New York: John Wiley 1994.
[145] Kamada H., Morikawa H.: Conditional stochastic processes for conditional random fields. *J. Eng. Mech. ASCE* 120, 4, 1994, 855–875.
[146] Khamlichi A., Bezzazi M., Limam A.: Buckling of elastic cylindrical shells considering the effect of localized axisymmetric imperfections. *Thin-Walled Structures* 42, 2004, 1035–1047.
[147] Kim S.-H., Na S.-W.: Response surface method using vector projected sampling points. *Structural Safety* 19, 1, 1997, 3–19.
[148] Kleiber M., Hien T. D.: *The stochastic finite element method.* Chichester, New York, Brisbane, Toronto, Singapore: John Wiley & Sons 1992.
[149] Kleiber M., Rojek J., Stoicki R.: Reliability assessment for sheet metal forming operations. *Comput. Methods Appl. Mech. Engrg.* 191, 2002, 4511–4532.
[150] Kleiber M., Woźniak C.: *Nonlinear mechanics of structures.* Warszawa: PWN, Dordrecht: Kluwer Academic Publishers 1991.
[151] Kmiecik M.: *The load-carrying capacity of axially loaded longitudinally stiffened plate panels having initial deformations.* Report No. R-80. The Ship Research Institute of Norway. Trondheim 1970.
[152] Kmiecik M., Soares C. G.: Response surface approach to the probability distribution of the strength of compressed plates. *Marine Structures* 15, 2002, 139–156.
[153] Knabe W., Przewłócki J., Różyński G.: Spatial averages for linear elements for two-parameter random field. *Prob. Engng. Mech.* 13, 3, 1998, 147–167.
[154] Kolassa J.: *Series Approximation Methods in Statistics.* 2nd. Edition. New York, Berlin, Heidelberg, Tokyo: Springer-Verlag 1997.
[155] Koutsourelakis P. S., Pradlwarter H. J., Schuëller G. I.: Reliability of structures in high dimensions, part I: algorithms and applications. *Prob. Engng. Mech.* 19, 2002, 409–417.
[156] Kowalski D.: *Wpływ imperfekcji wykonawczych na stan naprężeń w płaszczu stalowego zbiornika o osi pinowej*. Rozprawa doktorska. Politechnika Gdańska, Wydz. Inżynierii Lądowej i Środowiska 2004.
[157] Krajcinovic D.: *Damage mechanics.* Amsterdam, Lausanne, New York, Oxford, Shannon, Tokyo: Elsevier 1996.
[158] Krätzig W. B.: Eine einheitliche statische und dynamische Stabilitätstheorie für Pfadverfolgungs-algorithmen in der numerischen Festkörpermechanik. *Z. Angew. Math. Mech.* 69, 7, 1989, 203–213.
[159] Krishnaiah P. R. (Ed.): *Handbook of statistics*, Vol. 1 *Analysis of variance.* Amsterdam: North-Holland 1994.
[160] Li C. C., Der Kiureghian A.: Optimal discretization of random fields. *J. Eng. Mech*. 119, 6, 1993, 1136–1154.
[161] Li G.-Q., Li J.-J.: A semi-analitical simulation method for reliability assessments of structural systems. *Reliability Engineering and System Safety* 78, 2002, 275–281.
[162] Lin S. C.: Reliability predictions of laminated composite plates with random system parameters. *Prob. Engng. Mech.* 15, 2000, 327–338.
[163] Lind N. C. (Ed.): *Structural reliability and codified design.* University of Waterloo 1970.
[164] Liu J. S.: *Monte Carlo strategies in scientific computing*. New York, Berlin, Heidelberg: Springer-Verlag 2001.
[165] Liu W. K., Belytschko T., Mani A.: Random field finite elements. *Int. J. Num. Meth. Eng.* 23, 10, 1986, 1831–1845.
[166] Liu P. L., Der Kiureghian A.: Finite element reliability of geometrically non linear uncertain structures. *J. Eng. Mech. ASCE* 117, 8, 1991, 1806–1825.
[167] Liu P., Liu K.: Selection of random field mesh in finite element reliability analysis. *J. Eng. Mech. ASCE* 119, 4, 1993, 667–680.
[168] Liu Y. W., Moses F.: A sequential response surface method and its application in the reliability analysis of aircraft structural systems. *Structural Safety* 16, 1/2, 1994, 39–46.

[169] Low B. K., Tang W. H.: Reliability analysis using object-oriented constrained optimization. *Structural Safety* 26, 2004, 69–89.
[170] Lutes L. D., Sarkani S., Jin S.: Efficiency and accuracy in simulation of random fields. *Prob. Engng. Mech.* 11, 1996, 73–86.
[171] Mahadevan S., Haldar A.: Practical random field discretization in stochastic finite element analysis. *Structural Safety* 9, 1991, 283–304.
[172] Mahadevan S., Raghothamachar P.: Adaptive simulation for system reliability analysis of large structures. *Computers and Structures* 77, 2000, 725–734.
[173] Mann M. R., Schafer R. E., Singpurwalla N. D.: *Methods for statistical analysis of reliability and life data.* New York: John Wiley 1974.
[174] Marek P., Guštar M., Anagnos T.: Codified design of steel structures using Monte Carlo techniques. *Journal of Constructional Steel Research* 52, 1999a, 69–82.
[175] Marek P., Guštar M., Anagnos T.: *Simulation-based reliability assessment for structural engineers.* Boca Raton, New York, London, Tokyo: CRC Press 1996.
[176] Marek P., Guštar M., Krejsa M.: Simulation-based reliability assessment: tool for efficient steel design. *J. Construct. Steel Res.*74, 1–3, 1998, 156–158.
[177] Marek P., Guštar M., Permaul K.: Transition from partial factor method to Simulation-Based Reliability Assessment in structural design. *Prob. Engng. Mech.* 14, 1999b, 105–118.
[178] Matheron G.: *Random sets and integral geometry.* New York, Sydney, Toronto: John Wiley & Sons 1975.
[179] Matthies H. G., Brenner C. E., Bucher C. G., Soares C. G.: Uncertainties in probabilistic numerical analysis of structures and solids – stochastic finite elements. *Structural Safety* 19, 3, 1997, 283–336.
[180] Maymon G.: Probability of failure of structures without a closed-form failure function. *Computers and Structures* 49, 2, 1993, 301–313.
[181] Melchers R. E.: Radial importance sampling for structural reliability. *J. Eng. Mech. ASCE* 116, 1, 1990, 189–203.
[182] Melchers R. E.: *Structural reliability analysis and prediction*. Chichester, New York, Brisbane, Toronto: John Wiley & Sons 1999.
[183] Melchers R. E, Ahammed M.: A fast approximate method for parameter sensitivity estimation in Monte Carlo structural reliability. *Computer and Structures* 82, 2004, 55–61.
[184] Melchers R. E, Ahammed M.: Estimation of failure probabilities for intersections of non-linear limit states. *Structural Safety* 23, 2001, 123–135.
[185] Melchers R. E, Ahammed M.: Gradient estimation for applied Monte Carlo analyses. *Reliability Engineering and System Safety* 78, 2002, 283–288.
[186] Melnik-Melnikov P. G., Dekhtyaruk E. S.: Rare events probabilities estimation by "Russian Roulette and Splitting" simulation technique. *Prob. Engng. Mech.* 15, 2000, 125–129.
[187] Mignolet M. P., Spanos P. D.: Simulation of homogeneous two-dimensional random fields: Part I – AR and ARMA models. *Journal of Applied Mechanics ASME* 59, 2, 1992, 260–269.
[188] Mirza S. A.: Monte Carlo simulation of dispersion in composite steel-concrete column strength interaction. *Engineering Structures* 20, 1/2, 1998, 97–104.
[189] Moore R.: *Methods and application of interval analysis*. Philadelphia: SIAM 1979.
[190] Moses F., Kinser D. E.: Analysis of structural reliability. *J. Structural Div. ASCE* 93, ST5, 1967, 147–164.
[191] *MSC Nastran for Windows*. *Version 2001*. Los Angeles, USA: MSC Software Corporation.
[192] Murzewski, J.: *Niezawodność konstrukcji inżynierskich.* Warszawa: Arkady 1989.
[193] Náprstek J.: Strongly non-linear stochastic response of a system with random initial imperfections. *Prob. Engng. Mech.* 14, 1999, 141–148.
[194] Niczyj J.: Reliability-based multicriterion optimization and assessments of technical states of truss structures with fuzzy sets. *Prace Nauk. Pol. Szczecińskiej*, nr 581, Szczecin 2003.
[195] Nie J., Ellingwood R.: A new directional simulation method for system reliability. Part I: application of deterministic point sets. *Prob. Engng. Mech.* 19, 2004a, 425–436.
[196] Nie J., Ellingwood R.: A new directional simulation method for system reliability. Part II: application of neural networks. *Prob. Engng. Mech.* 19, 2004b, 437–447.

[197] Nie J., Ellingwood R.: Directional methods for structural reliability analysis. *Structural Safety* 22, 2000, 233–249.
[198] Niezgoda T.: Material database optimization using Monte Carlo method in engineering application. *Prob. Engng. Mech.* 16, 2001, 349–354.
[199] Nordgren R. P., Conte J. P.: On one-dimensional random fields with fixed end values. *Prob. Engng. Mech.* 14, 1999, 301–310.
[200] Olsson A., Sandberg G., Dahlblom O.: On Latin hypercube sampling for structural reliability analysis. *Structural Safety* 25, 2003, 47–68.
[201] Orlik G.: *Deformacje kształtu stalowych zbiorników cylindrycznych, ich statystyczne własności oraz symulacja numeryczna*. Rozprawa doktorska. Politechnika Gdańska, Wydz. Budownictwa Lądowego 1976.
[202] Papadimitriou C., Beck J. L., Katafygiotis L. S.: Updating robust reliability using structural test data. *Prob. Engng. Mech.* 16, 2001, 103–113.
[203] Papadopoulos V., Papadrakakis M.: Finite-element analysis of cylindrical panels with random initial imperfections. *J. Eng. Mech. ASCE* 130, 8, 2004, 867–876.
[204] Papadopoulos V., Papadrakakis M.: Stochastic finite element-based reliability analysis of space frames. *Prob. Engng. Mech.* 13, 1, 1998, 53–65.
[205] Papadrakakis M., Lagaros N. D.: Reliability-based structural optimization using neural networks and Monte Carlo simulation. *Comput. Methods Appl. Mech. Engrg.* 191, 2002, 3491–3507.
[206] Papadrakakis M., Papadopoulos V.: Robust and efficient methods for stochastic finite element analysis using Monte Carlo simulation. *Comput. Methods Appl. Mech. Engrg.* 134, 1996, 325–340.
[207] Papadrakakis M., Papadopoulos V., Lagaros N. D.: Structural reliability analysis of elastic-plastic structures using neural networks and Monte Carlo simulation. *Comput. Methods Appl. Mech. Engrg.* 136, 1996, 145–163.
[208] Penmetsa R. C., Grandhi R. V.: Adaptation of fast Fourier transformations to estimate structural failure probability. *Finite Elements in Analysis and Design* 39, 2003, 473–485.
[209] Popescu R., Deodatis G., Prevost J. H.: Simulation of homogeneous nonGaussian stochastic vector fields. *Probab. Eng. Mech.* 13, 1998, 1–13.
[210] Pradlwarter H. J., Schuëller G. I.: On advanced Monte Carlo simulation procedures in stochastic structural dynamics. *J. Nonlinear Mechanics* 32, 4, 1997, 735–744.
[211] Pradlwarter H. J., Schuëller G. I., Melnik-Melnikov P. G.: Reliability of MDOF-Systems. *Prob. Engng. Mech.* 9, 1994, 235–243.
[212] Przewłócki J., Górski J.: Strip foundation on 2-D and 3-D random subsoil. *Prob. Engng. Mech.* 16, 2, 2001, 121–136.
[213] Puig B., Poirion F., Soize C.: Non-Gaussian simulation using Hermite polynomial expansion: convergences and algorithm. *Prob. Engng. Mech.* 17, 2002, 253–264.
[214] Putresza J., Jendo S.: Review of probabilistic methods for the calculation of structural reliability. *Archives of Civil Engineering* 41, 2, 1995, 153–175.
[215] Rahman S., Rao B. N.: An element-free Galerkin method for probabilistic mechanics and reliability. *International Journal of Solids and Structures* 38, 2001, 9313–9330.
[216] Raizer V.: Theory of reliability in structural design. *Appl. Mech. Rev.* 57, 1, 2004, 1–21.
[217] Rajashekhar M. R., Ellimgwood B. R.: A new look at the response surface approach for reliability analysis. *Structural Safety* 12, 3, 1993, 227–230.
[218] Rajashekhar M. R., Ellingwood B. R.: Reliability of reinforced-concrete cylindrical shells. *Journal of Structural Engineering* 121, 2, 1995, 336–347.
[219] Royset J. O., Polak E.: Reliability-based optimal design using sample average approximations. *Prob. Engng. Mech.* 19, 2004, 331–343.
[220] Rozmarynowski B.: Numerical techniques in structural reliability. *Proc. of the 5th International Conference „Modern Buildings materials, Structures and Techniques"* 21–24 May, 1997, Vilnius, Lithuania 1997, 130–135.
[221] Rubinstein R. Y.: *Simulation and the Monte Carlo method.* New York: J. Wiley & Sons 1981.

[222] Schaefer R. L., Anderson R. B.: *The students edition of MINITAB Statistical software adapted for education*. Addison-Weslley Publishing Company Inc. 1989.
[223] Schenk C. A., Schuëller G. I.: Buckling analysis of cylindrical shells with random geometric imperfection. *International Journal of Non-Linear Mechanics* 38, 2003, 1119–1132.
[224] Schuëller G. I. (Ed.): A state-of-the-art report on computational stochastic mechanics, *Prob. Engng. Mech.* 12, 4 1997, IASSAE Report.
[225] Schuëller G. I.: Computational stochastic mechanics – recent advances. *Computers and Srucutres* 79, 2001, 2225–2234.
[226] Schuëller G. I., Bucher C. G.: Computational stochastic structural analysis – a contribution to the software development for the reliability assessment of structures under dynamic loading. *Prob. Engng. Mech.* 6, 3–4, 1991, 134–138.
[227] Schuëller G. I., Pradlwarter H. J., Bucher C. G.: Efficient computational procedures for reliability estimates of MDOF systems. *J. Nonlinear Mechanics* 26, 6, 1991, 961–974.
[228] Shao S., Murotsu Y.: Reliability of complex structural systems using an efficient directional simulation. In: *Structural Safety and reliability*. *Proc. of ICOSSAR'93.* Insbruck, Austria, 9–13 August 1993 (Eds. G. I. Schuëller, M. Schinozuka, J. T. P. Yao), III, 1994, 1529–1534.
[229] Shia D., Hui C. Y.: A Monte Carlo solution method for linear elasticity. *International Journal of Solids and Structures* 37, 2000, 6085–6105.
[230] Shinozuka M.: Computational stochastic mechanics: recent and future developments. In: *Structural Safety and Reliability* (Eds. G. I. Schuëller, M. Shinozuka, J. T. P. Yao). Rotterdam: A. A. Balkema 1994, 1747–1754.
[231] Shinozuka M. (Ed.): *Stochastic mechanics* Vol. I, Columbia University 1987. Vol. II, Columbia University 1988. Vol. III, Princeton University 1987a.
[232] Shinozuka M.: Structural response variability. *Journal of Engineering Mechanisc ASCE* 113, 6, 1987b, 825–842.
[233] Shinozuka M., Deodatis G.: Simulation of multidimensional Gaussian stochastic fields by spectral representation. *Appl. Mech. Rev*. 49, 1996, 29–53.
[234] Shinozuka M., Leone R.: A probabilistic model for spatial distribution of material properties. *Engineering Fracture Mechanics* 8, 1976, 217–227.
[235] Shooman M. L.: *Probabilistic Reliability: An Engineering Approach*. New York: McGraw-Hill 1968.
[236] Simonnet M.: *Measures and probabilities.* New York, Berlin, Heidelberg: Springer-Verlag 1996.
[237] Skalmierski B., Tylikowski A.: *Stochastic processes in dynamics.* Warszawa: PWN, The Hague, Boston, London: Martinus Nijhoff Publishers 1982.
[238] Śniady P.: *Podstawy stochastycznej dynamiki konstrukcji.* Wrocław: Oficyna Wydawnicza Politechniki Wrocławskiej 2001.
[239] Sobczyk K.: *Metody dynamiki statystycznej*. Warszawa: PWN 1973.
[240] Sobczyk K.: *Stochastyczne równania różniczkowe.* Warszawa: WNT 1991.
[241] Sobczyk K.: Spencer B. *Stochastyczne modele zmęczenia materiałów.* Warszawa: WNT 1996.
[242] Soh Y. C., Lam Y. C., Wu Z.: Efficient algorithm for probabilistic analysis of complex function in engineering applications. *Engineering Computation* 21, 5, 2004, 540–558.
[243] Sólnes J.: *Stochastic processes and random vibrations. Theory and practice.* Chichester, New York, Weinheim, Brisbane, Singapore, Toronto: John Wiley & Sons 1997.
[244] Spanos P. D., Mignolet M. P.: Simulation of homogeneous two-dimensional random fields: Part II – MA and ARMA models, *Journal of Applied Mechanics ASME* 59, 2, 1992, 270–277.
[245] Spanos P. D., Zeldin B. A.: Effective iterative ARMA approximation of multivariate random process for structural dynamics applications. *Earthquake Engineering and Structural Dynamics* 25, 1996, 497–507.
[246] Srivastava M. S., Carter E. M.: *An introduction to applied multivariate statistics.* New York, Amsterdam, Oxford: North-Holland 1983.
[247] Stefanou G., Papadrakakis M.: Stochastic finite element analysis of shells with combined random material and geometric properties. *Comput. Methods Appl. Mech. Engrg.* 193, 2004, 139–160.

[248] Surdet B., Der Kiureghian A.: Comparison of finite element reliability methods. *Prob. Engng. Mech.* 17, 2002, 337–348.
[249] Surdet B., Der Kiureghian A.: *Stochastic finite element methods and reliability. A state-of-the art-report*. Department of Civil and Environmental Engineering, University of California, Berkeley 2000.
[250] Takeda T.: Weighted integral method in multidimensional stochastic finite element analysis, *Prob. Engng. Mech.* 5, 4, 1990a, 158–166.
[251] Takeda T.: Weighted integral method in stochastic finite element analysis. *Prob. Engng. Mech.* 5, 3, 1990b, 146–156.
[252] Thoft-Christensen P., Baker M.J.: *Structural reliability theory and its applications*, Berlin, Heidelberg, New York, Tokyo: Springer-Verlag 1982.
[253] Thoft-Christensen P., Murotsu Y.: *Application of structural systems reliability theory.* Berlin, Heidelberg, New York, Tokyo: Springer-Verlag 1986.
[254] Thompson J. M. T., Hunt G. N.: *A general theory of elastic stability.* London, New York, Sydney, Toronto: John Wiley & Sons 1973.
[255] Tylikowski A.: *Stochastyczna stateczność układów ciągłych.* Warszawa PWN 1991.
[256] Val D., Bljuger F., Yankelevsky D.: Reliability evaluation in nonlinear analysis of reinforced concrete structures. *Structural Safety* 19, 2, 1997, 203–217.
[257] Vanmarcke E.-H.: Matrix formulation of reliability and reliability-based design. *Computers and Structures* 3, 1973, 757–770.
[258] Vanmarcke E. -H.: *Random Fields: Analysis and Synthesis.* Cambridge: MIT Press 1983.
[259] Vanmarcke E.-H.: Stochastic finite elements and experimental measurements. *Prob. Engng. Mech.* 9, 1994, 103–114.
[260] Vanmarcke E.-H., Grigoriu M.: Stochastic finite element analysis of simple beams. *J. Eng. Mech. ASCE* 109, 5, 1983, 1203–1214.
[261] Vanmarcke E., Shinozuka M., Nakagiri S., Schuëller G. I., Grigoriu M.: Random fields and stochastic finite elements. *Structural Safety* 3, 1986, 143–166.
[262] Walukiewicz H.: Information entropy in modeling of civil engineering problems. *Proc. of 5th International Conference „Modern Building Materials, Structures and Techniques"*. Vilnius, Lithuania, May 21–24, 1997. Vilnius Gediminas Technical University: Vilnius 1997 Vol. II, 1997b, 125–129
[263] Walukiewicz H.: Information entropy of random fields in modeling of structures. *Proc. of Euromech 372 Colloquium of the European Mechanics Society „Reliability in nonlinear structural mechanics"* 21–24 October 1997, Clermont-Ferrand, France, (Eds. O. D. Ditlesven, J. C. Mitteau). Clermont-Ferrand, Universitate Blaise Pascal: 1997a, 165–170.
[264] Walukiewicz H., Bielewicz E., Górski J.: Discrete spatial simulations in structural mechanics and in environmental problems. *Advances in Engineering Software* 29, 7–9, 1998, 723–731.
[265] Walukiewicz, H., Bielewicz, E., Górski, J.: Simulation of nonhomogeneous random fields for structural applications. *Computers and Structures* 64, 1–4, 1997, 491–498.
[266] Walukiewicz H., Bielewicz E., Górski J.: Statistical analysis of simulated random fields. *Proc. of the ICASP7 Conference. Applications of Statistics and Probability*, Vol. 2, Rotterdam, Brookfield: A. A. Balkema 1995, 1267–127.
[267] Wang Z. M.: Mesoscopic study of concrete. I: generation of random aggregate structure and finite element mesh. *Computers and Structures* 70, 1999, 533–544.
[268] Wang G. S., Ang A. H. S.: Adaptive Kernel method for evaluating structural system reliability. In: *Structural Safety and reliability. Proc. of ICOSSAR'93.* Insbruck, Austria, 9–13 August 1993 (Eds. G. I. Schuëller, M. Schinozuka, J. T. P. Yao) III, 1994, 1495–1500.
[269] Warner R. F., Kabaila A. P.: Monte Carlo study of structural safety. *J. Structural Div. ASCE*, 94, ST12, 1968, 2847–2859.
[270] Waszczyszyn Z., Cichoń Cz., Radwańska M.: *Metoda elementów skończonych w stateczności konstrukcji.* Warszawa: Arkady 1990.
[271] Watson G. S.: *Statistic on spheres.* New York, Chichester, Brisbane, Toronto, Singapore: John Wiley & Sons 1983.
[272] Went Y. K.: Reliability and performance-based design. *Structural Safety* 23, 2001, 407–428.

[273] Wilde P.: *Dyskretyzacja pól losowych w obliczeniach inżynierskich*. Warszawa, Poznań: PWN 1981.
[274] Winkler G.: *Image analysis, random fields and dynamic Monte Carlo methods. A mathematical introduction.* Berlin, Heidelberg, New York: Springer-Verlag 1995.
[275] Wu Y.-T., Milwater H. R., Cruse T. A.: Advanced probabilistic structural analysis method for implicit performance function. *AIAA Journal* 28, 9, 1990, 1663–1669.
[276] Yamazaki F., Shinozuka M.: Digital generation of non-Gaussian stochastic fields. *J. Eng. Mech. ASCE* 114, 7, 1988, 1183–1197.
[277] Yamazaki F., Shinozuka M.: Simulation of stochastic fields by statistical preconditioning. *J. Eng. Mech. ASCE* 116, 2, 1990, 268–287.
[278] Yonezewa M., Okuda S.: An improved Importance Sampling density estimation for structural reliability assessment. In: *Structural Safety and reliability*. *Proc. of ICOSSAR'93*. Insbruck, Austria, 9–13 August 1993 (Eds. G. I. Schuëller, M. Schinozuka, J. T. P. Yao) III, 1994, 1501–1508.
[279] Zadeh J.: The role of fuzzy logic in the management of uncertainty in expert systems. *Fuzzy Sets and Systems* 11, 1983, 199–228.
[280] Zhang J., Ellinwood B.: Error measure for reliability studies using reduced variable set. *J. Eng. Mech. ASCE* 121, 8 1995, 935–937.
[281] Zhang J., Ellinwood B.: Orthogonal series expansion of random fields in reliability analysis. *J. Eng. Mech. ASCE* 120, 12, 1994, 2660–2678.
[282] Zhao Y.-G., Ono T., Kato M.: Second-order third-moment reliability method *Journal of Structural Engineering* 128, 8, 2002, 1087–1090.
[283] Žiha K.: Descriptive sampling in structural safety. *Structural Safety* 17, 1995, 33–41.
[284] Ziółko, J.: *Zbiorniki metalowe na ciecze i gazy*. Warszawa: Arkady 1986.
[285] Zubrzycki S.: *Wykłady z rachunku prawdopodobieństwa i statystyki matematycznej*. Warszawa: PWT 1966.

NON-LINEAR MODELS OF STRUCTURES WITH RANDOM GEOMETRIC AND MATERIAL IMPERFECTIONS
SIMULATION-BASED APPROACH

Assessment of reliability, safety and stability of structures with initial material and geometric imperfections belong to the most complex problems in applied mechanics. The random nature of the imperfections has evoked the use of probabilistic methods. Exact analytical solutions of the stochastic problems exist only for simple models of structures and uncomplicated cases of loading. To obtain approximate results a great variety of perturbation techniques and stochastic finite element methods have been developed. To estimate the structure reliability the following techniques are in use: Monte Carlo, first and second order reliability methods, response surface, artificial neural networks and others. When nonlinear geometric and material effects are taken into consideration the structures reliability can be evaluated only numerically.

In this work some general nonlinear stochastic models for static analysis of physically and geometrically nonlinear models of structures with random geometric and material imperfections are implemented. The Monte Carlo simulation seems to be the only method to solve such a class of nonlinear problems. The proposed methodology can be described as a simulation-based approach.

Digital simulations of random variables and random fields on two-dimensional meshes are applied. The simulation process is based on the original conditional, rejection method of generation. An important role in the calculations is played by the propagation base scheme covering sequentially the mesh points and the random field envelope which allows to fulfil the geometric and boundary conditions of the structure model. Any homogeneous or non-homogeneous field of practically unlimited sizes can be generated.

The Monte Carlo method combined with the finite element program analysis is employed. Structural initial imperfections are assumed as random fields described in terms of a set of generated realizations and the resulting statistic estimators. This leads to solutions of a set of deterministic problems for the assessment of the structure model responses. The critical load histograms obtained numerically make it possible to estimate the structure reliability. An alternative procedure for the reliability estimation is also proposed. Random imperfections of the structure and the applied loads are simultaneously generated and an appropriate loading multiplier responsible for the structure failure is calculated. A set of the loading multipliers defines the histogram of the limit state of the structure and on its basis the factor describing the structures reliability is estimated.

Special attention is paid to the discussion of reduction methods concerning the number of the Monte Carlo realizations. Two methods are considered: the reduction of the initial sets of data, and the accuracy analysis of the output results. An assessment of the structure reliability interval is also proposed.

A comprehensive analysis of simple models (rigid bars with inclined springs) makes provision for an examination of efficiency and accuracy of the direct and stratified Monte Carlo methods. Most examples presented in the work concern compressed shallow cylindrical shell structures.

Two examples of identification and simulation of the real structure geometric discrepancies are also presented. The implemented method enables the reproduction of the measured imperfection maps of vertical petrol tanks and longitudinally stiffened ship's hull panels. The numerical analysis indicates that the initial geometrical imperfections decrease the nominal load carrying capacities of the structure models.

The application of the simulation-based approach can result in lowering the laborious and high cost of the experiments. The formulation of a methodology for the identification, classification and description of the initial imperfections can ensure a better and much safer design.

NIELINIOWE MODELE KONSTRUKCJI Z GEOMETRYCZNYMI I MATERIAŁOWYMI IMPERFEKCJAMI
ROZWIĄZANIE SYMULACYJNE

Problemy określenia niezawodności, bezpieczeństwa, a także stateczności konstrukcji z materiałowymi i geometrycznymi imperfekcjami należą do najbardziej złożonych zagadnień mechaniki. Ponieważ wstępne odchyłki mają charakter losowy, do ich opisu zazwyczaj stosuje się metody probabilistyczne. Problem ten może być opisany równaniem

$$L_{\omega}(\omega)\left[\mathbf{u}(\mathbf{r},\omega)\right]=\mathbf{P}(\mathbf{r},\omega)$$

gdzie ω jest symbolem zdarzenia elementarnego, $\mathbf{u}(\mathbf{r},\omega)$, $\mathbf{P}(\mathbf{r},\omega)$ są wektorowymi polami losowymi przemieszczenia i obciążenia, $L_{\omega}(\omega)$ oznacza nieliniowy operator stochastyczny zależny od parametrów losowych, a $\mathbf{r}$ jest wektorem pozycyjnym.

Ścisłe rozwiązania analityczne tego typu stochastycznych zagadnień nie są możliwe nawet w prostych przypadkach konstrukcji oraz nieskomplikowanego obciążenia. Rozwiązanie przybliżone można uzyskać, wykorzystując różne warianty metod perturbacyjnych, stochastycznych elementów skończonych (SFEM) i stochastycznych elementów brzegowych (SBEM). Wynikami obliczeń są zazwyczaj wartości oczekiwane obciążenia niszczącego oraz jego odchylenie standardowe. Wygodnym parametrem pozwalającym na stochastyczny opis konstrukcji jest niezawodność. Można ją wyznaczyć za pomocą metody Monte Carlo, metod pierwszego i drugiego rzędu (FORM i SORM), poszukiwania powierzchni odpowiedzi (response surface), a także wykorzystując sieci neuronowe i inne techniki. W przypadku, gdy analizowane są zagadnienia materiałowo i geometrycznie nieliniowe, niezawodność można określić jedynie na drodze numerycznej.

W pracy przedstawiono ogólne stochastycznie nieliniowe rozwiązania materiałowo i geometrycznie nieliniowych modeli konstrukcji z losowymi imperfekcjami. Obciążenie jest także definiowane jako losowe, ale w pracy nie przeprowadzono jego szczegółowej analizy. Przyjęto, że stan graniczny konstrukcji jest funkcją pewnej liczby zmiennych losowych. Metoda Monte Carlo wydaje się jedynym podejściem umożliwiającym rozwiązanie tego typu nieliniowych problemów. Zaproponowane algorytmy obliczeniowe można określić jako rozwiązanie symulacyjne.

Zastosowano numeryczną symulację dyskretnych pól losowych. Podstawę generacji stanowi dowolna teoretyczna funkcja korelacyjna, dobrana zgodnie z typem analizowanego pola, lub macierz kowariancyjna określona na podstawie danych doświadczalnych. Danymi metody są także wartości oczekiwane określone w każdym punkcie pola. Oryginalny algorytm symulacji wykorzystuje warunkową metodę akceptacji i odrzucania. W obliczeniach istotną rolę odgrywa bazowy schemat propagacji, za pomocą którego są pokrywane w sposób sekwencyjny wszystkie punkty dyskretnego pola. W standardowym kroku obliczeniowym, wykorzystując wcześniej wygenerowane wartości pola, obliczana jest kolejna, nowa, pojedyncza zmienna losowa (punkt pola). Definiowany jest także maksymalny rozmiar bazowego schematu stosowanego w obliczeniach.

Algorytm generacji wykorzystuje także obwiednię pola losowego określającą minimalne i maksymalne wartości zmiennych losowych, uzależnione od wartości oczekiwanej określonej w każdym punkcie pola. Obwiednie zazwyczaj definiowane są jako wielokrotność odchylenia standardowego. W ogólnym przypadku mogą to być dowolne funkcje umożliwiające modelowanie imperfekcji wstępnych uwzględniających warunki brzegowe oraz specyfikę geometrii konstrukcji.

Za pomocą zaproponowanej metody można wygenerować dowolne jedno- dwu- lub trójwymiarowe, jednorodne lub niejednorodne pola losowe, o regularnej lub nieregularnej, dyskretnej siatce i praktycznie nieograniczonych wymiarach. Przeprowadzona analiza dowiodła poprawności i efektywności algorytmu.

W pracy za pomocą metody Monte Carlo w połączeniu z metodą elementów skończonych wykonywana jest stochastyczna analiza nieliniowych modeli konstrukcji inżynierskich. Takie podejście,

z uwagi na stale rosnące możliwości obliczeń komputerowych, wydaje się możliwe i celowe. Wstępne imperfekcje geometryczne i/lub materiałowe konstrukcji zostały opisane za pomocą pól losowych danych w postaci zbioru wygenerowanych realizacji i opisujących ich estymatorów. Następnie, zgodnie z ideą metody Monte Carlo, rozwiązywany jest zbiór problemów deterministycznych – modeli konstrukcji z wstępnymi imperfekcjami. Na tej podstawie wyznacza się rozkład obciążenia krytycznego. Przyjęcie rozkładu obciążenia rzeczywistego jako danego umożliwia zastosowanie dokładnego wzoru opisującego niezawodność (metody poziomu 3.).

Zaproponowano także alternatywną procedurę umożliwiającą estymację niezawodności konstrukcji. W każdym kroku metody Monte Carlo generowane są jednocześnie losowe imperfekcje oraz obciążenie zewnętrzne. Przyjmując imperfekcje jako stałe w danym kroku obliczeniowym, określa się mnożnik opisujący zniszczenie modelu. Zbiór mnożników definiuje bezwymiarowy histogram stanu granicznego konstrukcji i na jego podstawie wyznacza się jej niezawodność określoną przez liczbę mnożników większych od jedności.

Wykazano, że rozkłady opisujące stany graniczne umożliwiają badanie wrażliwości konstrukcji na poszczególne losowe imperfekcje wstępne. Wynika to z faktu, że dodatkowym generowanym parametrem może być zarówno zewnętrzne losowe obciążenie, jak i inna dowolna zmienna opisująca materiał lub geometrię konstrukcji. Takie alternatywne obliczenia pozwalają na wyznaczenie tej samej niezawodności modelu, ale uzyskane rozkłady znacznie się różnią. Porównanie rozkładów stanów granicznych i ich estymatorów otrzymanych w wyniki działania różnych losowych parametrów umożliwia określenie ich wpływu na mechaniczną odpowiedź konstrukcji.

Numeryczne obliczenia za pomocą programu wykorzystującego elementy skończone wymagają stosowania rozwiązania przyrostowego z iteracjami na każdym przyroście. Analiza nieliniowa połączona z metodą Monte Carlo jest więc bardzo czasochłonna. W pracy podjęto próby sformułowania efektywnego algorytmu obliczeń. Istotne jest określenie minimalnej liczby realizacji potrzebnej do uzyskania dostatecznie dokładnych rozwiązań. Zagadnienie to można rozwiązywać, analizując dane wejściowe lub wyniki końcowe.

W pierwszym przypadku określa się liczbę realizacji opisujących dostatecznie dokładnie wygenerowane pola imperfekcji geometrycznych lub materiałowych. W tym celu wykorzystywane są standardowe metody analizy statystycznej. Analiza tego typu podejścia prowadzi do wniosku, że minimalna liczba realizacji wykorzystanych w obliczeniach powinna wynosić 2000. Nieliniowe rozwiązanie takiej liczby deterministycznych problemów za pomocą metody elementów skończonych jest praktycznie niemożliwe.

Bardziej efektywny sposób redukcji czasu obliczeń jest związany z analizą zbieżności rozwiązania. W tym celu w każdym kroku obliczeniowym metody Monte Carlo wyznacza się wartość średnią obciążenia krytycznego, jego odchylenie standardowe oraz inne statystyczne estymatory. Badana jest zmienność tych parametrów w funkcji liczby realizacji. Przeprowadzone obliczenia wykazały, że w przypadku analizowanych modeli konstrukcji wystarczy 150 do 200 próbek, aby uzyskane wyniki uznać za wystarczająco dokładne.

Radykalne ograniczenie liczby badanych próbek losowych polega na wyborze z wygenerowanego zbioru kilku lub kilkunastu charakterystycznych realizacji, których wpływ na rozwiązanie konstrukcji będzie miał ekstremalny charakter. Parametrami decydującymi o wyborze takich pól losowych są, np.: minimalne i maksymalne wartości zmiennych losowych w zbiorze, ekstremalne wartości średnie lub normy poszczególnych realizacji, a także liczba zmian znaku pola lub wektory własne odpowiadające charakterystycznym wartościom własnym. Należy podkreślić, że wybór realizacji ekstremalnych ma charakter subiektywny i może prowadzić jedynie do wstępnego oszacowania losowej nośności konstrukcji. Inżynierska wiedza i doświadczenie odgrywają istotną role w tego typu analizach.

Inną analizowaną w pracy przybliżoną metodą redukcji liczby realizacji jest poszukiwanie przedziału niezawodności modelu. W tym celu imperfekcje są opisane minimalnymi lub maksymalnymi wartościami wybranymi z wygenerowanego zbioru n realizacji (np. $n = 3$). Obliczenia niezawodności wykonuje się niezależnie dla obu zbiorów. W ten sposób można uzyskać dwie wartości definiujące przedział niezawodności. Metoda pozwala więc na szacunkowe określenie bezpieczeństwa układu.

Wszystkie omawiane problemy przedstawiono za pomocą kilku numerycznych przykładów.

W analizie dokładności i efektywności różnych wariantów metody Monte Carlo zastosowano prosty model sztywnego pręta podpartego sprężynami opisanymi sprężystymi i sprężysto-plastycznymi

równaniami konstytutywnymi, z jednym lub dwoma stopniami swobody. Wykazano, że zastosowanie próbkowania uwarstwionego (stratified sampling) umożliwia przeprowadzenie efektywnych obliczeń niezawodności nieliniowych modeli konstrukcji. Metoda bezpośrednia (direct) Monte Carlo wymaga znacznie większej liczby analizowanych realizacji. Dodatkowo zbadano transformację losowych danych wejściowych w probabilistyczne rozkłady rozwiązań. Stwierdzono, że nieliniowy operator odgrywa zasadniczą rolę w uzyskanych rozwiązaniach.

Kilka przykładów prezentowanych w pracy dotyczy małowyniosłych ściskanych powłok cylindrycznych, w przypadku których obciążenie niszczące można wyznaczyć jedynie uwzględniając w obliczeniach wstępne imperfekcje geometryczne lub/i materiałowe. Należy podkreślić, że rozkład siły krytycznej prostego modelu sztywnego pręta mają charakter podobny do wyników obliczeń małowyniosłej ściskanej powłoki. A więc wnioski uzyskane na podstawie wstępnych analiz prętów można wykorzystać bezpośrednio w obliczeniach powłok. Wykonano numeryczne obliczenia, stosując jako dane zdegenerowane pola losowe opisane pojedynczą zmienną losową. Przeprowadzono także obliczenia powłoki z imperfekcjami opisanymi polem dwuwymiarowym.

Zaprezentowano dwa przykłady identyfikacji i symulacji rzeczywistych imperfekcji geometrycznych konstrukcji inżynierskich. Wykorzystano dostępne w literaturze, pomierzone odchyłki geometryczne pionowych zbiorników cylindrycznych i ściskanych modeli użebrowanych płyt poszycia statków. Zastosowane metody pozwalają na odwzorowanie podstawowych cech pomierzonych pól imperfekcji. Analiza numeryczna wykazała, że wstępne geometryczne odchyłki wpływają na wyniki numerycznych obliczeń i zmniejszają wartość obciążenia niszczącego.

Zastosowanie metod symulacyjnych może ograniczyć pracochłonne i kosztowne badania doświadczalne. Sformułowanie metod identyfikacji i opisu wstępnych imperfekcji oraz badanie ich wpływu na nośność konstrukcji, prowadzi do lepszego i bezpieczniejszego projektowania.

Pracę podzielono na siedem rozdziałów.

W pierwszym rozdziale opisano zakres i cel pracy. W rozdziale drugim dokonano przeglądu metod mechaniki stochastycznej. Przedstawiono procedury dyskretyzacji pól losowych, techniki perturbacji, stochastyczną metodę elementów skończonych, metody analizy niezawodności konstrukcji, metody FORM i SORM, powierzchni odpowiedzi i inne. Z uwagi na zastosowane w pracy podejście, przede wszystkim omówiono różne wersje metody Monte Carlo. Rozdział trzeci zawiera opis metody generacji dyskretnych pól losowych. Przedstawiono podstawy teoretyczne, algorytm programu oraz zaprezentowano generację kilku teoretycznych jednorodnych i niejedorodnych pól losowych (biały szum, pole jednorodne, Wienera i Brauna). W rozdziale czwartym analizowane są proste nieliniowe modele o jednym i dwóch stopniach swobody. Wnioski sformułowane w tym rozdziale zostały bezpośrednio wykorzystane w obliczeniach zagadnień dwuwymiarowych. I tak, w rozdziale piątym przedstawiono przykłady stochastycznej analizy małowyniosłych ściskanych powłok. Rozdział szósty poświęcono identyfikacji i generacji imperfekcji geometrycznych na podstawie dostępnych w literaturze wyników pomiarów cylindrycznych zbiorników na paliwa płynne oraz użebrowanych płyt. Sformułowane ogólne wnioski przedstawiono w rozdziale szóstym. Pracę kończy obszerna bibliografia.

Podstawowe elementy pracy zostały sformułowane w projektach Ministerstwa Nauki i Szkolnictwa Wyższego „Nieliniowe problemy w stochastycznej teorii powłok" 1980–1985, 1988–1991 i dwóch projektach Komitetu Badań Naukowych „Pola losowe i ich zastosowanie w mechanice" 1991–1992 (nr 304259101) oraz 1991–1993 (nr 3P40405505). Kierownikiem projektów był prof. dr hab. inż. Eugeniusz Bielewicz, a głównym wykonawcą dr hab. inż. Henryk Walukiewicz. W latach 1995–2002 w wyniku kontynuowania rozpoczętych tematów opublikowano szereg dodatkowych prac. Tytuły wszystkich ważniejszych publikacji zostały ujęte w spisie literatury, a w tekście umieszczono odpowiednie odwołania.

Oryginalnymi elementami badań naukowych autora monografii, oprócz udziału w badaniach zespołowych, które mają odzwierciedlenia we wspólnych opublikowanych pracach, są: ulepszenie algorytmu generacji pól losowych, które umożliwiło analizę pól o dowolnych rozmiarach (odpowiedni fragment rozdziału 3.), weryfikacja różnych wersji metody Monte Carlo i ich przydatności w obliczeniach nieliniowych modeli konstrukcji (rozdział 4.1) oraz identyfikacja i generacja rzeczywistych odchyłek pionowych zbiorników cylindrycznych (rozdział 6.1). Elementem nowym w stosunku do opracowań przedstawionych przez współautorów projektów jest także obszerny przegląd literatury dotyczącej zastosowania metod stochastycznych w zagadnieniach teorii konstrukcji (rozdział 2).